AD-A190 498 THEORETICAL INVESTIGATIONS OF NITROCUBANE DECOMPOSITION 1/2
(U) CHEMICAL DYNAMICS CORP UPPER MARLBORO MD
B C GARRETT ET AL. 29 FEB 88 N00014-87-C-0746
UNCLASSIFIED F/G 7/4 NL

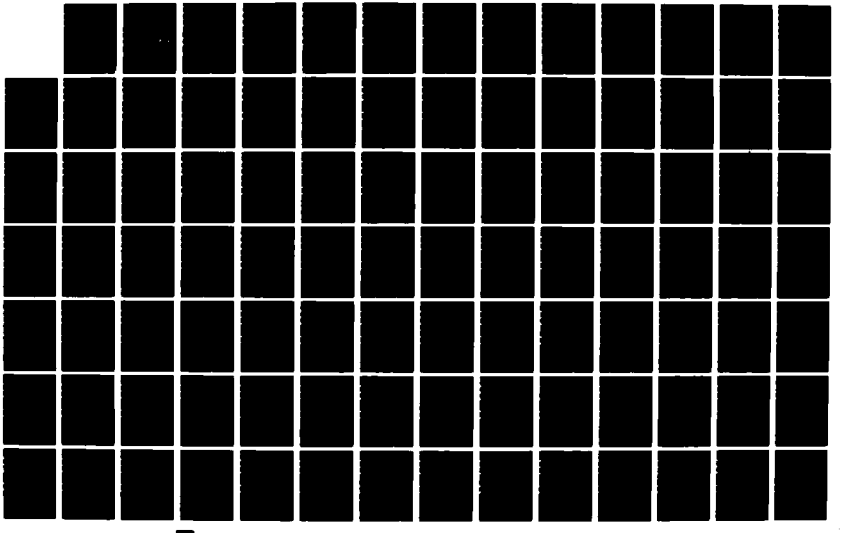

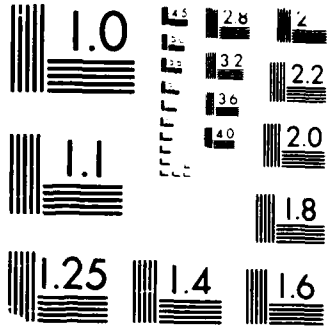

MICROCOPY RESOLUTION TEST CHART

UNCLASSIFIED

SECURITY CLASSIFICATION OF THIS PAGE (When Data Entered)

(9)

AD-A190 498

REPORT DOCUMENTATION PAGE

READ INSTRUCTIONS BEFORE COMPLETING FORM

1. REPORT NUMBER	2. GOVT ACCESSION NO. / 3. RECIPIENT'S CATALOG NUMBER
4. TITLE (and Subtitle): Theoretical Investigations of Nitrocubane Decomposition	5. TYPE OF REPORT & PERIOD COVERED: FINAL, 870CT01-88FEB29
	6. PERFORMING ORG. REPORT NUMBER
7. AUTHOR(s): Bruce C. Garrett and Michael J. Redmon	8. CONTRACT OR GRANT NUMBER(s): N00014-87-C-0746
PERFORMING ORGANIZATION NAME AND ADDRESS: Chemical Dynamics Corporation, 9560 Pennsylvania Avenue, Suite 106, Upper Marlboro, MD 20772	10. PROGRAM ELEMENT, PROJECT, TASK AREA & WORK UNIT NUMBERS
CONTROLLING OFFICE NAME AND ADDRESS: Office of Naval Research, Department of the Navy, 800 N. Quincy St., Arlington, VA 22217	12. REPORT DATE: 88Feb29 13. NUMBER OF PAGES: 109
MONITORING AGENCY NAME & ADDRESS (if different from Controlling Office)	15. SECURITY CLASS. (of this report): Unclassified 15a. DECLASSIFICATION/DOWNGRADING SCHEDULE

DISTRIBUTION STATEMENT (of this Report)

Unlimited distribution

17. DISTRIBUTION STATEMENT (of the abstract entered in Block 20, if different from Report)

Unlimmited distribution

18. SUPPLEMENTARY NOTES

19. KEY WORDS (Continue on reverse side if necessary and identify by block number)

Propellant decomposition, theoretical methods, gas-phase reactions, thermochemistry, reaction rates, nitrocubane decomposition, ab initio electronic structure, variational transition state theory

20 ABSTRACT (Continue on reverse side if necessary and identify by block number)

See reverse side

DD FORM 1 JAN 73 1473 EDITION OF 1 NOV 65 IS OBSOLETE

UNCLASSIFIED

SECURITY CLASSIFICATION OF THIS PAGE (When Data Entered)

20. Abstract

Gas-phase chemical reactions play an important role in determining the power and sensitivity of energetic materials which are used as fuels in military propulsion systems. Theoretical methods can provide detailed dynamical information about the important chemical reactions, thereby aiding in the design of new propellants. High order electronic structure calculations with empirical bond additivity corrections have been applied to prototype reactions and validated by comparisons of different levels of theory and by comparison with experiment. These methods provide the most cost effective means of obtaining thermal rate data and show promise of being applicable to reactions involving large polyatomic molecules important in nitrocubane decomposition.

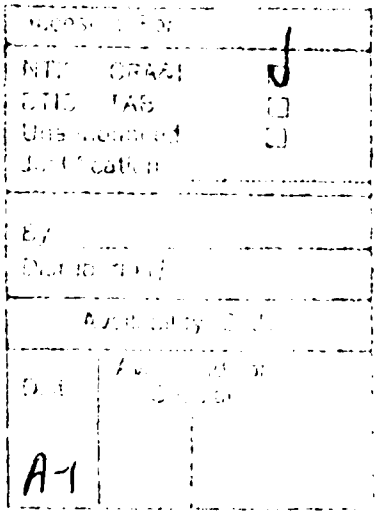

EXECUTIVE SUMMARY

This document reports the results of a six-month Phase I small business innovative research program through the strategic defense initiative. The main objective of this program was to establish the feasibility of using theoretical methods for obtaining kinetic data important in nitrocubane decomposition. The potential utility of theoretical methods for the aid in the design of new propellants is unquestionable; what remains in question is whether the methods are of sufficient accuracy and capable of treating large enough molecules to be of use. The present report outlines the first successful steps taken in answering these questions.

The research preformed on this program entailed a collaborative effort of electronic structure and dynamics calculations. The electronic structure calculations provide information about the potential energy surface which is then used in dynamics calculations of the rate constants. The sensitivity of the computed rate constants to the level of theory was studied for a relatively small reaction (involving five atoms) for which high levels of theory could be afforded. Comparison was also made between the computed and experimental rates as further validation of the methods. These studies indicate that accurate rate constants (to within about 50%) can be obtained for a modest computational effort – several hours of Cray 1s computer time were required to obtain rates for temperatures from 200 to 2400 K.

In order to treat reactions involving very large molecules (such as the initial unimolecular decomposition step in nitrocubane combustion) approximate methods for estimating kinetic parameters are needed. As a first step in this direction we have carried out a systematic study of hydrogen attack on a series of nitro containing molecules to examine the effects of substituents on the computed reaction rates. In addition, a new thermochemical kinetic analysis has been presented which includes important dynamical effects that are crucial for reliable predictions of thermal rates. This new analysis will be the basis for methods of estimating kinetic parameters for large polyatomic systems from bond and group additivity relationships, but using information about potential energy surfaces for smaller analogous reactions.

TABLE OF CONTENTS

1. Introduction

Propulsion requirements for the strategic defense initiative require the development of new fuels that are lightweight yet highly energetic. Fuels based upon combining beryllium with an oxidizer show promise of meeting this criteria of a high specific impulse. The ideal oxidizing agent is one which is highly energetic yet stable and, therefore, detonates in a well characterized, predictable manner. An example of a highly energetic yet stable molecule is the cage compound cubane[1]

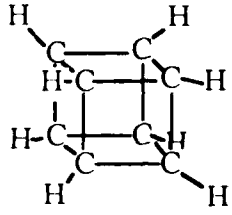

with much of its energy arising from the ring strain imposed by the cubic geometry of the carbon skeleton. There is currently a large effort within SDI to develop high-density oxidizers by substituting cubanes with nitro (NO_2) or nitro-containing groups. The explosive nature of nitrocubanes derives from the ring strain and the energy-rich oxidizing nitro substituents. Nitrocubanes containing many nitro groups are more energetic and more effective oxidizers, but also tend to to be more unstable. Some stability can be regained by placing the nitro groups onto substituents that move them further away from the cube. Examples of recent compounds along this line are the ammonium nitronate salts, e.g.,

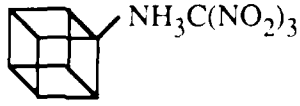

The synthesis and characterization of nitrocubanes such as these is currently of great interest and is being pursued in several laboratories.

One of the factors controlling the stability of nitrocubanes is the rate of the unimolecular decomposition of the parent molecule in the condensed phase. This is controlled largely by the bond strength of the weakest bond in the molecule. To fully realize the power stored in these molecules they must be converted into more thermodynamically stable molecules such as H_2O,

CO_2, and N_2. This conversion is controlled by chemistry occurring in the gas phase. Gas-phase chemical reactions play an important role in the sensitivity as well as the energetics of the propellants. The exothermicity of the gas-phase reactions determine their energy output and the kinetics of the gas-phase reactions control the burn rate, and together they determine the power of the propellant.[2] Also, radicals which are products of the gas-phase reactions can attack the parent molecules and affect the sensitivity of the nitrocubane. The effect of substituent groups on the sensitivity of nitrocubanes is twofold. Firstly, the substituent can affect the sensitivity by changing the strength of the weakest bond in the parent molecule, and secondly, the substituent can control the sensitivity by altering the mix of H/C/N/O which affects the gas-phase kinetics. An understanding of the kinetically important reaction pathways which are operative in the complex decomposition mechanism is crucial to developing energetic yet stable oxidizers.

Theoretical methods can make a contribution to the understanding of the decomposition of propellants. To date, great strides have been made in computer modeling of the ignition and flames of propellants such as RDX.[3] Studies of ignition solve the nonlinear coupled differential equations for temperature and species mass fraction as a function of time. Comparison with experimental observations of gross features of the ignition (such as ignition time or observed formation rates of specific molecules) tests the underlying reaction mechanism and kinetic data used as input into the computer model. The level of detailed species concentration as a function of time that is afforded by these simulations is currently not available in experimental studies. This detail enables identification of important reaction pathways – the important elementary reaction steps – and sensitivity analysis identifies crucial kinetic data that must be determined accurately.

Great strides have also been made in the theoretical methods for describing the kinetics of elementary reactions. We are currently on the threshold of attaining the necessary capabilities to enable routine calculations of gas-phase chemical reaction rates. With this capability in hand, it will be easy to test the influence of substituents on the bond strengths and, thereby, unimolecular decomposition rates, and also to test their influence on the subsequent gas-phase kinetics. Theoretical calculations provide an important complementary tool to experimental gas kinetic

studies. Elementary reaction steps can be studied theoretically for reactant species that are very short lived and hard to prepare experimentally. Furthermore, the theoretical calculations can be used to extend experimental data to physical conditions which are not attainable in the laboratory. In collaboration with computer modeling efforts, these theoretical studies can provide physical insight into the reaction pathways and detailed dynamics of the chemical reactions. For systems which are not too large the theoretical methods are capable of quantitative predictions of the gas-phase reaction rates and for very large systems these methods will give qualitative rate data which will allow the assessment of the most important reaction pathways. These studies are crucial to the detailed understanding of substituent effects upon the energetics and sensitivity of the oxidizers.

One objective of the Phase I research has been to extend and validate the theoretical methods used for computing rate constants for elementary gas-phase reactions and to demonstrate the feasibility of a theoretical approach for describing the dynamics of these gas-phase reactions. The theoretical calculation of the chemical reaction rate is a two step process: first, the interaction energies between the atoms are obtained from an electronic structure (quantum chemistry) calculation, followed by a dynamical calculation of the rate. Although the electronic structure calculations do provide vital insight into the energetically accessible reaction pathways, they provide only structural information which is often not enough; dynamical constraints can make energetically accessible reaction pathways so slow that they become unimportant in the kinetic mechanism. A collaborative effort which successfully interfaces the quantum chemistry and dynamics calculations is needed to accurately determine the dynamics of elementary gas-phase reactions.

The dynamics calculations are based upon variational transition state theory with quantum mechanical tunneling effects included by semiclassical adiabatic ground-state transmission coefficients.[4] The use of variational transition state theory in these calculations is mandated for several reasons: (1) it includes the factors most important in controlling the rate of chemical reactions and is currently the most cost effective method for obtaining reliable predictions of rates for a variety of gas-phase reactions; (2) it is capable of utilizing limited information about the

potential along the minimum energy path without requiring a global potential energy surface; (3) because of the nature of the semiempirical potential information utilized in this work, the dynamical bottleneck for the reaction does not occur at the saddle point for the reaction and a variational procedure to locate the dynamical bottleneck is needed; and (4) it provides a consistent method for incorporating quantum mechanical tunneling effects which are crucial for accurate predictions of the rates, especially for reactions which actively involve hydrogen atoms at temperatures below 600 K.

Rigorous *ab initio* electronic structure calculations are currently incapable of predicting the energetics of a polyatomic reaction accurately enough to allow even a qualitative estimate of the rate constant. The most successful electronic structure methods incorporate some type of correction, justified either on a theoretical or empirical basis. One such approach is the BAC-MP4 method[5] developed by Dr. Carl Melius at Sandia National Laboratories, Livermore, California (SNLL). The present research was performed in collaboration with Dr. Melius and Dr. M. L. Koszykowski at SNLL. The BAC-MP4 method has been successfully applied to the calculation of the thermochemistry of bound species and is currently the foremost method for prediction of thermochemical data for transient species. In the present application the BAC-MP4 method is extended to calculations of potential information in the interaction region of the potential rather than at equilibrium geometries. A major goal of this work is the validation of this method for obtaining the potential information needed for the dynamics calculations.

Another objective of this research was to treat chemical reactions of current interest and importance in propellant chemistry. In this direction it was proposed to validate the theoretical methods in a study of the simplest prototype of a radical attack on a nitro group

$$H + RNO_2 \rightarrow RN\langle^{O}_{OH} \quad \text{(R1)}$$

$$RN\langle^{O}_{OH} \rightarrow R + HONO \quad \text{(R2)}$$

$$\rightarrow RNO + OH \quad \text{(R3)}$$

where R is replace by a hydrogen atom. Towards this end, we examined the prototypical reactions

$$H + NH_3 \rightarrow H_2 + NH_2 \quad \text{(R4)}$$

$$H_2 + NH_2 \rightarrow H + NH_3 \quad \text{(R5)}$$

and

$$D + ND_3 \rightarrow D_2 + ND_2 \quad \text{(R6)}$$

These reactions provide a wealth of experimental data for a critical test of the theoretical methods and the reactions are small enough (have a small enough number of electrons) to afford relatively large electronic structure calculations for the validation. Subsequently reactions (R1)-(R3) were studied for R = H, CH_3, OH, NH_2, and CH_3NH but no validation of the theoretical methods was attempted for these reactions.

The Phase I objectives have been surpassed in the six month research effort. The feasibility of the theoretical methods have been established in critical comparisons of different levels of theory, as well as comparisons to experiment for reactions (R4)-(R6). In addition, comparisons between the BAC-MP4 method and multireference configuration self consistent field (MCSCF) theory has been made for the unimolecular hydrogen migration reaction

$$HONO \rightarrow HNO_2 \quad \text{(R7)}$$

The multivalent nature of the nitro groups makes them hard to treat accurately by quantum chemical methods and reactions involving nitro groups generally require a multireference electronic wavefunction or a configuration interaction (CI) calculation for an adequate description of the electronic structure. A real concern with the BAC-MP4 method has been that it is based upon a single reference (HF) wavefunction and may give such a poor zeroth order description of the electronic structure that the empirical bond additivity correction cannot make up for the errors. The

comparisons of the BAC-MP4 and MCSCF calculations for reaction (R7) show excellent agreement in geometries, frequencies, and qualitative agreement in the energetics. This give encouragement for the use of the BAC-MP4 method for treating nitro groups which are very important in propellant chemistry.

Another interest that has developed during the course of this research has been the estimation of kinetic parameters for gas-phase reactions. The ability to provide reasonable estimates of reaction rates for large polyatomic systems is vital in the accurate modeling of the complex gas-phase reaction mechanisms. Benson[6] has developed methods for estimating kinetic data from bond or group additivity relationships based on conventional transition state theory. These estimates are obtained from statistical mechanical evaluations of quasithermodynamic parameters based upon the geometry and structure of the saddle point for the reaction. This approach lacks important dynamical effects: (1) the fact that the dynamical bottleneck controlling the reaction rate may be at a location different from the saddle point, and (2) that quantum mechanical tunneling makes sizeable contributions to the thermal rates. These deficiencies have been addressed by basing a thermochemical kinetic analysis on variational transition state theory with semiclassical adiabatic ground-state transmission coefficients. The importance of these effects has been demonstrated and the development of a new database which incorporates these effects has been initiated in Phase I.

The remainder of this report is organized as follows. Section 2 gives a brief review of the theoretical methods used in this research. Section 3 presents the results and provides a discussion of their significance. Section 4 summarizes our conclusions and outlines the future directions of this research. Two appendices of papers which are ready for submission for publication are also included. Appendix A is a detailed description of our calculations on reactions (R4)-(R6). Appendix B is a presentation of the new thermochemical kinetic analysis. These papers include more details of both the theory and results for the interested reader.

2. Theoretical Background

2.1 Variational transition state theory

Transition state theory (TST)[7] provides one of the most practical approximation schemes for calculating equilibrium rate constants for thermally activated gas-phase reactions. The popularity of TST over the last 50 years is largely due to its success - it incorporates the factors most crucial in determining the rates - and its simplicity - the rates are obtained from equilibrium statistical mechanical calculations and use only limited PES information. However, the utility of conventional TST for predicting reaction rates is limited by the accuracy of the approximations employed. The major deficiencies of TST are: the fundamental assumption that if the reaction gets to a critical configuration (the transition state), then it will always proceed to products; the need to incorporate further approximations to include quantum mechanical tunneling effects; and the approximate method by which anharmonic terms in the potential are treated. These approximations can lead to quantitatively inaccurate rate constants and incorrect physical interpretations.

Variational transition state theory (VTST)[4] provides a convenient framework for consistently improving upon the limitations of conventional TST. The variational procedure is a method to minimize the errors caused by the breakdown of the fundamental assumption of TST. Conventionally the transition state is a dividing surface separating reactants and products and located at the saddle point of the potential energy surface. Significant improvement over conventional TST can be obtained by locating the dividing surface by a variational criterion.[8] Consistent methods of included quantum mechanical effects and anharmonicity have been developed and extensively tested, and it has been found that the theory is capable of giving quantitative accuracy in the calculation of thermal rate constants for atom-diatom reactions.[9-15] More recently, application of VTST has been made to a four-atom system (OH + H2)[16] and a general computer program is now available for calculating thermal rate constants for reactions involving a large number of atoms.[17]

The emphasis of this research has been the effective use of PES information within the framework of VTST. Therefore, the remainder of the technical discussion is a brief review of some of the details of the theory and a description of the type of PES information that is needed for the calculations. More details of the theory are provided in ref. 4.

Conventional transition state theory[7] reduces the calculation of the rate constant to one of quasiequilibrium statistical mechanics: the equilibrium rate is approximated as the equilibrium flux headed towards reactants through a dividing surface located at the saddle point. With this approximation, the rate constant $k^{\ddagger}(T)$ for temperature T takes on the simple textbook form

$$k^{\ddagger}(T) = \frac{k_B T}{h} \frac{Q^{\ddagger}(T)}{\Phi^R(T)} \exp\left(V^{\ddagger} / k_B T \right) \tag{1}$$

where k_B is Boltzmann's constant, h is Planck's constant, $Q^{\ddagger}(T)$ is the partition function for the bound degrees of freedom at the saddle point, $\Phi^R(T)$ is the reactants partition function, and $V^{\ddagger}$ is the value of the potential at the saddle point. Thus conventional transition state theory requires information about the potential energy surface only in the saddle point and reactant regions. If the partition functions are computed using a harmonic approximation then the matrix of second derivatives (the Hessian matrix) suffices.

In variational transition state theory the dividing surface is viewed as a tentative dynamical bottleneck to flux, and the best bottleneck (the dividing surface allowing the least flow of flux) is located by a variational procedure. The generalized expression for the thermal rate constant is given as a function of the location s of the dynamical bottleneck along the reaction coordinate

$$k^{GT}(T, s) = \frac{k_B T}{h} \frac{Q^{GT}(T, s)}{\Phi^R(T)} \exp\left(V_{MEP}(s) / k_B T \right) \tag{2}$$

where $Q^{GT}(T,s)$ is the generalized partition function for the bound degrees of freedom orthogonal to the reaction path at s, and $V_{MEP}(s)$ is the value of the potential along the reaction path at s. One

version of variational transition state theory, the canonical variational theory (CVT),[8] results from minimizing eq. (2) with respect to s

$$k^{CVT}(T) = \min_{s} k^{GT}(T, s) \tag{3}$$

The improved canonical variational theory (ICVT)[12] also variationally optimizes the location of the transition state dividing surface for a given temperature, but provides an improved treatment of threshold energies by using an ensemble which removes energies below the ground-state adiabatic threshold. To compute the rate constant using either the canonical or improved canonical variational theory more information about the potential energy surface is required than for a conventional transition state theory calculation; information about the potential in a region around the reaction path is required.

For most chemical reactions of interest, especially those involving hydrogen atoms, it is imperative to include quantum mechanical effects in the theory. Quantum mechanical effects are included in VTST in an ad hoc manner: bound modes are quantized by using quantum mechanical partition functions in eq. (2) and quantum mechanical effects on the reaction coordinate motion are included by a multiplicative factor, the transmission coefficient $\kappa^X(T)$. The quantized rate constant is given by

$$k^{ICVT/X}(T) = \kappa^X(T)\, k^{ICVT}(T) \tag{4}$$

where the superscript X specifies the yet undefined method used in calculating the transmission coefficient. The transmission factor includes the effect of nonclassical reflection for energies above the classical barrier as well as the effect of quantum mechanical tunneling. The Wigner correction factor[18] has been very popular for estimating quantum mechanical tunneling effects because it requires knowledge of the shape of the classical barrier near the saddle point; this type of information can be obtained from the negative eigenvalue of the Hessian at the saddle point.

Unfortunately, the approximations of this method are rarely valid for chemical reactions, i.e., when tunneling is important it occurs over distances much longer than that represented by a quadratic representation of the potential near the saddle point, and a more global description of tunneling is required.

More successful transmission coefficients are based upon the vibrationally and rotationally adiabatic approximation.[19,20] In this approximation the difficult multidimensional scattering problem is transformed into the much easier problem of scattering on a one-dimensional effective potential. The vibrationally-rotationally adiabatic potential is given by

$$V_a(s, \alpha) = V_{MEP}(s) + \varepsilon_\alpha^{GT}(s) \tag{5}$$

where α is a collective index of the quantum numbers for the bound modes and $\varepsilon_\alpha^{GT}(s)$ is the bound energy level for state α at the generalized transition state located at s along the reaction path. The adiabatic approximation is made in a curvilinear coordinate system and although the potential term is very simple, the kinetic energy term is complicated by factors dependent upon the curvature of the reaction path (the MEP). The method of treating the reaction-path-curvature terms is ambiguous and several approaches have been tried. The best methods treat tunneling along a path which depends upon the reaction path curvature. An example is the small-curvature semiclassical ground state (SCSAG) tunneling method which is based upon the ground-state adiabatic potential and in which the tunneling probabilities are computed by the WKB method.[20] This method works well for systems in which the reaction path curvature is not too large. Note that for this tunneling method the type of PES information needed is nearly identical to that needed for the variational calculation; the only additional piece of information necessary is the curvature of the reaction path which can be obtained from the first and second derivatives of the potential along the reaction path.

In the present work the ICVT/SCSAG method is applied using limited information about the potential energy surface; the information necessary to carry out these calculations is the potential along the minimum energy path (MEP; the minimum energy path is the path of steepest

decents in a mass scaled coordinate system from the saddle point to both reactants and products), the matrix of force constants along the minimum energy path, and the curvature of the reaction path. The method directly uses the results of quantum chemistry calculations of information about the potential energy in the form of the energy and its derivatives. The development of quantum chemistry methods to analytically evaluate the derivatives[21] has greatly reduced the computational effort and such methods are used when available. Typically the potential information is obtained on a sparse grid along the minimum energy path and methods have been developed to interpolate the necessary parameters of the reaction-path Hamiltonian (RPH).[17,22]

2.2 Quantum chemistry

Today, most quantitative theoretical studies of intermolecular forces and their related potential energy surfaces are based on *ab initio* methods, which can be pursued to increasing levels of accuracy, thereby providing useful estimates of the errors at preceding levels. Historically, the majority of calculations have determined the ground electronic states of atomic and molecular systems. The most well-known *ab initio* method is the LCAO-SCF or Hartree-Fock (HF) method.[23] In this procedure the wavefunction for the system is expressed as a determinant of one-electron orbitals formed from linear combinations of orbitals centered on each of the nuclei. The Hartree-Fock solution is a "variational" one; i.e., for a given set of atomic orbitals ("basis set"), it yields the lowest energy possible for a single-determinant wavefunction. In this type of calculation there can be two sources of error: that from the use of a finite basis set and that from the neglect of correlation. Experience has shown that the accurate determination of properties, particularly bond strengths, even for singly bonded substituents, requires that both types of errors be eliminated to the maximum extent possible.

Theoretically, the correlation energy is defined to be the difference between the Hartree-Fock energy and the exact (nonrelativistic) energy within the basis.[24] When a method corrects for the approximations in the independent particle model by including components from other electron configurations in the wavefunction, correlation is accounted for and the total electronic energy

obtained will be lower than the HF energy. The conventional method of obtaining a correlated wavefunction is the configuration interaction (CI) method.[25] When increasing numbers of determinants of orbitals representing states excited relative to the SCF determinant are included in the description of the wavefunction, the CI method converges monotonically (from above) to the basis-set-limited exact electronic energy (i.e., the "full CI" limit). The convergence with respect to the basis set can be assessed by examining the changes in calculated properties as basis functions are added. It is particularly important that the errors in different regions of a potential energy surface remain fairly constant; otherwise, spurious barriers or other features may appear.

Electron correlation may be classified as dynamical or nondynamical.[26] Nondynamical correlation errors are large for systems which are inadequately described by a single determinant. This case arises when two or more configurations are nearly degenerate in energy or when alternative arrangements of electrons in partially filled subshells are required for proper dissociation. One method particularly appropriate for obtaining nondynamical correlation is the multiconfiguration-SCF (MCSCF) method.[27] In this procedure, both the orbital coefficients and *the correlation coefficients within a limited CI space are varied and iterated to convergence.* For a given configuration space, the MCSCF orbitals are the optimal ones. Dynamical correlation is obtained in this procedure by a CI using the optimized orbitals to give the MCSCF-CI[28] method.

An alternate to the CI method is based upon perturbation theory such as diagrammatic many-body perturbation theory (MBPT)[29] or Møller-Plesset perturbation theory.[30] As higher-order perturbations are included, the energy (for systems for which a single determinantal starting point is adequate) converges to the full CI limit, although not usually monotonically since the MBPT energy does not include certain spurious positive terms present in nonfull CI energies that are cancelled as the full CI is reached and are responsible for the monotonic convergence. However, recognition of these terms makes it possible to approximately correct and improve the nonfull CI energies.[31] For ground state thermochemistry and properties at equilibrium geometries and transition states, the perturbation based codes (e.g., GAUSSIAN 82[32]) offer superior performance over MCSCF-CI calculations in many instances.

In the present work we attempt to keep the computational effort affordable by using moderate sized basis sets and partial descriptions of the electron correlation. These give results of modest accuracy which are improved by empirical corrections using the bond additivity correction (BAC) method.[5] This approach begins with a Hartree-Fock (HF) optimization of critical geometries (such as equilibrium geometries and transition states), followed by higher quality calculations of the energy using full fourth-order Møller-Plesset perturbation theory (MP4), and finally applying an empirical bond additivity correction. This method is denoted HF/BAC-MP4 to distinguish it from other possibilities discussed below. The correction is given in terms of an adjustment to the total energy for each bond in the molecule. The bond correction dies off exponentially with the bond length. The parameters of the BAC-MP4 method are fitted to a database of experimental heats of formation of atomic and molecular species in a least squares sense. These parameters will change with the level of the *ab initio* calculation and in the limit of a complete basis set and full CI the correction goes to zero. The strengths of the BAC-MP4 method are: (1) it is based upon *ab initio* methods and therefore incorporates a qualitatively correct picture of the multicenter nature of the molecular bonding, (2) it can be systematically improved by improving the level of the underlying *ab initio* calculation, and (3) the corrections are estimated from a large database of experimental heats of formation. For corrections to energies at equilibrium geometries the BAC method can be viewed as an interpolation technique, whereas for transition states and other geometries in the strong interaction region for which experimental data is not available the method is more an extrapolation technique and must be more critically tested.

A major concern in using the HF/BAC-MP4 method is the accuracy of the computed potential energy surface information. One test is to improve the quality in the underlying *ab initio* calculation to decrease the magnitude of the empirical bond additivity correction and test the effect on the computed rate constant. As a first step in this direction, we have reevaluated the potential information using the MP2/BAC-MP4 method. In this method the geometry of the equilibrium structure or transition state is determined using a full second-order Møller-Plesset perturbation theory (MP2) calculation. The matrix of second derivatives is also calculated at the MP2 level at

the same geometry. The minimum energy path is located by following the path of steepest descents using the gradient vectors and Hessian matrices computed at the MP2 level. For each point along the minimum energy, the energy is then computed by the MP4 method followed by a bond additive correction. Because the geometries and vibrational frequencies are different at the HF and MP2 levels, the BAC correction is also different and the parameters are refitted to experimental heats of formation as was done for the HF/BAC-MP4 method.

One further step that has been considered is the MP4/BAC-MP4 method in which the energy and first and second derivatives along the entire minimum energy path are calculated by the MP4 method. The bond additivity correction is then made to the MP4 energy at each point along the minimum energy path. This method has not been fully implemented, but by observing the change of the geometries and frequencies in going from the MP2/BAC-MP4 method to the MP4/BAC-MP4 method, we obtain an estimate of the sensitivity of the calculations to even higher levels of the underlying *ab initio* electronic structure calculations. Similar comparisons have been made between the HF/BAC-MP4 method and MCSCF calculations for which a bond additivity correction is not available. These comparisons give an estimate of the importance of using a multireference wavefunction for optimizing geometries and obtaining frequencies, and provide a good measure of the accuracy of the HF-based pertubative approaches.

2.3 Thermochemical kinetic analysis

Our ability to address reactions involving large polyatomic molecules such as found in the initial stages of nitrocubane decomposition will rely to a great extent on developing methods to estimate Arrhenius parameters from bond additivity or group additivity relationships. Statistical mechanics provides the prescription for using information about the structure and vibrational frequencies of bound chemical species to directly calculate thermochemical data such as heats of formation of stable compounds and heat release and equilibrium constants for chemical reactions.[33] The structural and energetic information can be reduced into thermodynamic quantities, the enthalpy and entropy, which can be accurately approximated using bond additivity and group

additivity relationships. Using the quasithermodynamic formulation of conventional transition state theory[6,7] these ideas have been extended to the prediction of reaction rate constants by estimating the enthalpy and entropy of the activated complex from knowledge of the structure and vibrational frequencies at the saddle point of the reaction. This approach neglects important contributions to the thermal rate from variational optimization of the transition state and quantum mechanical tunneling. Recently, a new partitioning of the thermal rate constant has been produced which allows analysis of the rates in terms of quasithermodynamic quantities which include these important dynamical effects.[34]

In traditional thermochemical kinetic analysis the enthalpy and entropy of activation are estimated from properties at a single location along the minimum energy path – the saddle point. Basing the thermochemical kinetic analysis upon variational transition state theory presents a problem because the role of the saddle point is replaced by that of the dynamical bottleneck which moves with temperature. At 0 K it occurs at the maximum of the ground-state adiabatic potential curve s_*^{AG} and past experience has shown that the dynamical bottleneck for temperatures up to about 600-1000 K tend to be in the vicinity of this adiabatic maximum. Therefore, it is more reasonable to base the thermochemical kinetic analysis upon the generalized transition state rate constant given by eq. (2) evaluated at s_*^{AG} instead of the saddle point location of s=0. This takes into account most of the variational effects but still neglects thermal fluctuations of the dynamical bottleneck from s_*^{AG} which become more important at higher temperatures, and also neglects quantum mechanical tunneling effects which are important at low temperatures. These effects are also included by partitioning the rate constant [eq.(4)] as follows

$$k^{ICVT/X}(T) = \kappa^{X}(T)\ \kappa_{therm}(T)\ k^{GT}(T, s_*^{AG}) \qquad (6)$$

where $\kappa_{therm}(T)$ accounts for finite-temperature deviations due to the temperature dependence of the improved canonical variational transition state and is given by the expression

$$k^{ICVT}(T) = \kappa_{therm}(T)\ k^{GT}(T,s_*^{AG}) \tag{7}$$

The generalized transition state theory rate constant $k^{GT}(T,s_*^{AG})$ is obtained from the properties of a single generalized transition state, "a substance", and is factored in the usual manner in terms of substantial activation parameters, $\Delta_s S_T^o$ and $\Delta_s H_T^o$,

$$k^{GT}(T, s) = \frac{k_B T}{h}(C^o)^{\Delta n^{\neq}} \exp\left(\Delta_s S_T^o / R\right) \exp\left(-\Delta_s H_T^o / RT\right) \tag{8}$$

where C^o is the concentration in the standard state and $\Delta n^{\neq}$ is the stoichiometric change in the number of moles in passing from the reactants to the transition state ($\Delta n^{\neq}$=-1 for reactions studied here). For an ideal gas at a standard state of P^o = 1 atm, the concentration of the standard state is given by P^o/RT, and the substantial enthalpy and entropy of activation can be expressed in terms of the reaction rate constant by

$$\Delta_s H_T^o = RT^2 \frac{d \ln k}{dT} - 2RT \tag{9}$$

$$\Delta_s S_T^o = \frac{\Delta_s H_T^o}{T} + R \ln\left[\frac{k(T) h P^o}{(k_B T)^2 N_A^u}\right] \tag{10}$$

where N_A is Avogadro's number, and u is one for k(T) in molar units and zero for k(T) in molecular units.

The transmission coefficients $\kappa_{therm}(T)$ and $\kappa^{SCSAG}(T)$ depend upon more extended regions of the potential energy surface rather than a single transition state location but we still factor them in a manner analogous to eq. (8), in terms of nonsubstantial activation parameters, $\Delta_n S_T^o$ and $\Delta_n H_T^o$,

$$\kappa(T) = \exp\left(\Delta_n S_T^o / R\right) \exp\left(-\Delta_n H_T^o / RT\right) \tag{11}$$

where

$$\kappa(T) = \kappa^{SCSAG}(T)\ \kappa_{therm}(T) \tag{12}$$

and the nonsubstantial enthalpy and entropy of activation are obtained from

$$\Delta_n H^o_T = RT^2 \frac{d\ \ln\ \kappa}{dT} \tag{13}$$

$$\Delta_n S^o_T = RT\ \frac{d\ \ln\ \kappa}{dT} + R\ \ln\ \kappa(T) \tag{14}$$

Since $\Delta_s S^o_T$ and $\Delta_s H^o_T$ are quasithermodynamic parameters, their temperature dependences can be obtained from a single temperature-dependent substantial heat capacity of activation $\Delta_s C^o_P$

$$\Delta_s S^o_T = \Delta_s S^o_{T_o} + \int_{T_o}^{T} \left(\Delta_s C^o_P / T \right)\ dT \tag{18}$$

and

$$\Delta_s H^o_T = \Delta_s H^o_{T_o} + \int_{T_o}^{T} \Delta_s C^o_P\ dT \tag{19}$$

The parameters $\Delta_n S^o_T$ and $\Delta_n H^o_T$ are purely phenomenological; however, because of their definition in eqs. (13) and (14), their temperature dependences can also be obtained from a single heat capacity analog $\Delta_n C^o_P$ given by expressions analogous to eqs. (15) and (16).

This new thermochemical kinetic analysis separates contributions from a single transition state structure from contributions due to thermal and quantum mechanical tunneling which depend on more global properties of the potential energy surface. The former can be estimated using bond additivity or group additivity relationships, but the new schemes are needed for estimating the latter.

3. Results and Discussion

3.1 Validation of theoretical methods

3.1.1 Application to $H + NH_3 \rightleftarrows H_2 + NH_2$ and $D + ND_3 \rightarrow D_2 + ND_2$

Greater detail and discussion of the results for these reactions as well as a prediction of the rate constants for the reverse of reaction (R6) is presented in appendix A. The results are summarized in this section with an emphasis on the validation of the HF/BAC-MP4 method and the computational effort required for these calculations.

First the saddle point geometries are compared at the HF, MP2, and MP4 levels for the reaction of H with NH_3. At the saddle point the geometry is

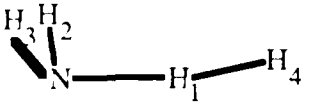

where the bond lengths and angles are given in table 1.

Table 1. Saddle point geometry for the $H + NH_3 \rightarrow H_2 + NH_2$ reaction.

	HF	MP2	MP4
R_{NH_1}(Å)	1.244	1.305	1.277
R_{NH_2}(Å)	1.010	1.023	1.026
R_{NH_3}(Å)	1.010	1.023	1.026
$R_{H_1H_4}$(Å)	0.949	0.869	0.893
$\theta_{NH_1H_4}$(degrees)	100.5	99.1	99.3
$\theta_{H_1NH_2}$(degrees)	100.5	99.1	99.3
$\theta_{H_1NH_3}$(degrees)	105.4	103.5	103.3
$\theta_{H_1NH_3}$(degrees)	166.7	158.5	158.3

geometries. The largest changes are for the NH_1 and H_1H_4 bond lengths which are most actively involved in the rearrangement. Note that the geometries do not change monotonically with improvement in the level of treatment but the HF values for R_{NH_1} and $R_{H_1H_4}$ are closer to the MP4 values than are the MP2 values. The NH_1 and H_1H_4 bond distances computed at the HF and MP2 levels are shown in figure 1 for points along the minimum energy path. The agreement between the two methods for the whole minimum energy path is as good as or better than the agreement seen at the saddle point .

The saddle point frequencies are compared at the HF, MP2, and MP4 levels for the reaction of H with NH_3 in table 2. The imaginary frequencies at the top of each column correspond to the unbound mode for motion along the reaction coordinate. Note that of all the frequencies this imaginary one changes the most as the level of theory is improved. The harmonic zero point energy given at the bottom of each column is one-half the sum of the frequencies for all bound modes. Although the frequencies for some individual modes do change by as much as 20%, the changes in zero point energy are much smaller. A change of 110 cm^{-1} in the zero point energy (a typical difference between the HF and MP2 values) will shift the adiabatic potential curve by only 0.3 kcal/mol.

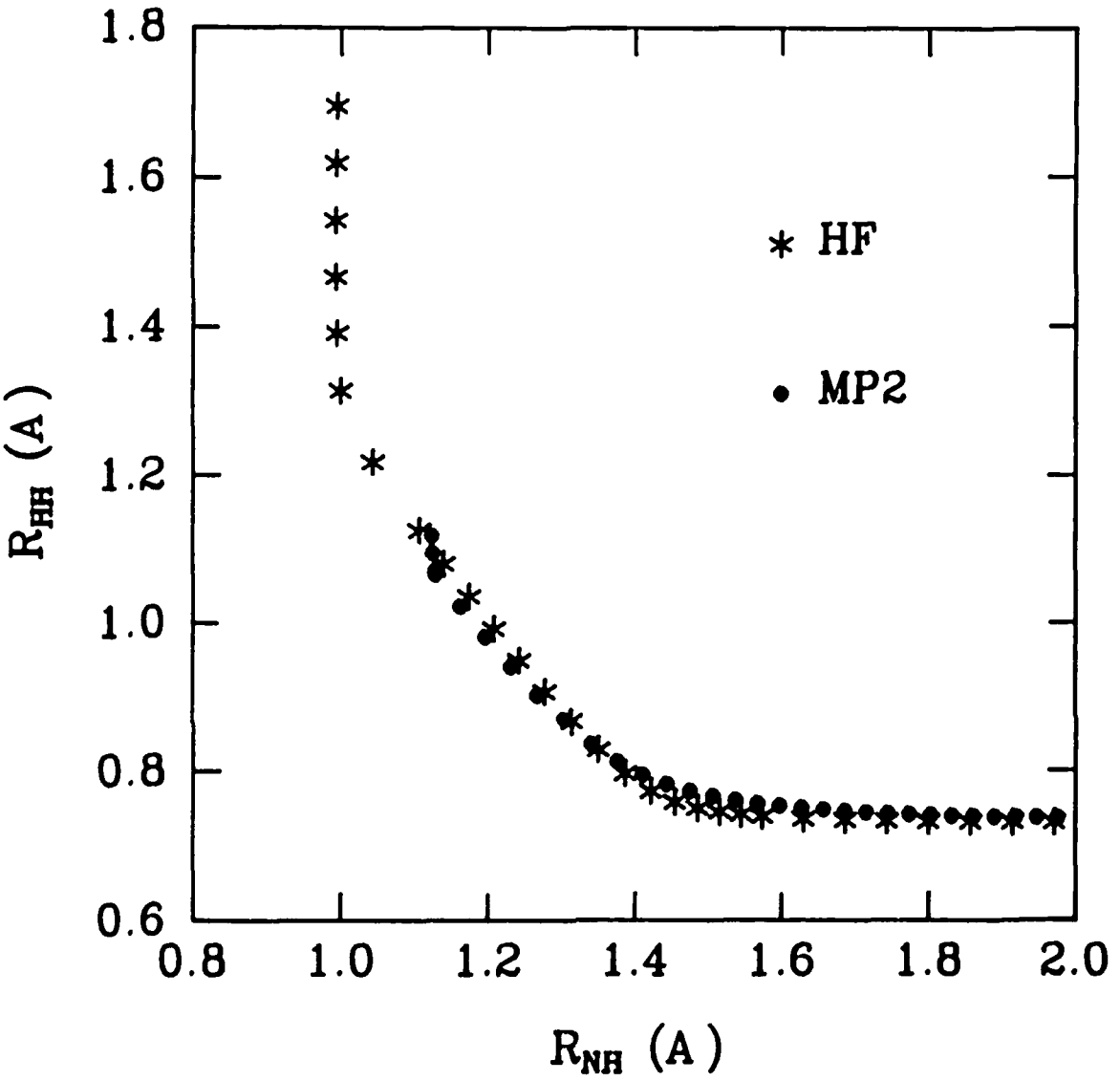

Figure 1. NH and HH bond distances along the minimum energy path for the reaction $H + NH_3 \rightarrow H_2 + NH_2$ at two levels of *ab initio* electronic structure theory – Hartree-Fock (*) and second-order Moller-Plesset perturbation theory (•)

Table 2. Saddle point harmonic frequencies zero point energy (cm^{-1}) for the $H + NH_3 \rightarrow H_2 + NH_2$ reaction.

	HF	MP2	MP4
	2833i	2021i	1905i
	723	718	726
	732	730	901
	1258	1146	1186
	1485	1315	1347
	1541	1610	1629
	1731	2077	1921
	3647	3489	3497
	3750	3606	3553
Zero point energy	7434	7345	7381

The bond additivity correction is based upon information about the potential energy surface only through quadratic terms (a harmonic treatment) but is designed to fit the experimental heats of formation of bound molecules which include the effects of anharmonicity. Therefore, the BAC method has anharmonic effects built into it in an averaged sense, not on a mode-by-mode basis. The harmonic frequencies computed at the HF level are known to be systematically high and the BAC method corrects for this discrepancy as well as including the effects of anharmonicity. The relatively small differences in the zero point energy with improved level of theory is encouraging since it means that smaller changes will have to be made in the bond additivity correction to account for these changes in frequencies.

A comparison of the potential energy curve $V_{MEP}(s)$ and the ground-state adiabatic potential curves $V^A(s)$ for reaction (R4) using the HF/BAC-MP4 and MP2/BAC-MP4 methods is

given in figure 2. Comparison of the rates for reaction (R4) computed by the ICVT/SCSAG method using the potential information obtained by the HF/BAC-MP4 and MP2/BAC-MP4 methods is given in table 3 and figure 3.

Table 3. Comparison of ICVT/SCSAG reaction rates (in units of $cm^3molecule^{-1}s^{-1}$) computed using two different sets of information about the potential energy surface.

T,K	HF/BAC-MP4	MP2/BAC-MP4
200	$9.9x10^{-24}$	$3.2x10^{-24}$
300	$1.8x10^{-20}$	$1.2x10^{-20}$
400	$2.0x10^{-18}$	$1.6x10^{-18}$
600	$4.5x10^{-16}$	$4.0x10^{-16}$
1000	$6.2x10^{-14}$	$6.2x10^{-14}$
1500	$1.1x10^{-12}$	$1.1x10^{-12}$
2400	$6.9x10^{-12}$	$8.1x10^{-12}$

Also included in figure 3 is a comparison with the experimental results of Marshall and Fontijn.[35] The potential along the minimum energy path and the adiabatic potential curves show very similar shapes for the two methods, although the MP2/BAC-MP4 results are shifted slightly to the left. The classical barrier heights are very similar, 17.1 kcal/mol for HF/BAC-MP4 compared to 16.7 kcal/mol for MP2/BAC-MP4, and the adiabatic barriers are 15.5 and 15.7 kcal/mol above the reactant zero point energies for the HF/BAC-MP4 and MP2BAC-MP4 methods, respectively.

The rate constants computed using the two sets of potential information agree well for temperatures above 300 K. At 300 K and below tunneling is very important and the rates are sensitive to finer details of the adiabatic potential curves. At 300 K, the rates computed using the two sets of potential information differ by only 50% but at 200 K the difference increases to a factor of 3.1. The overall agreement with the experimental results is also very good except at the

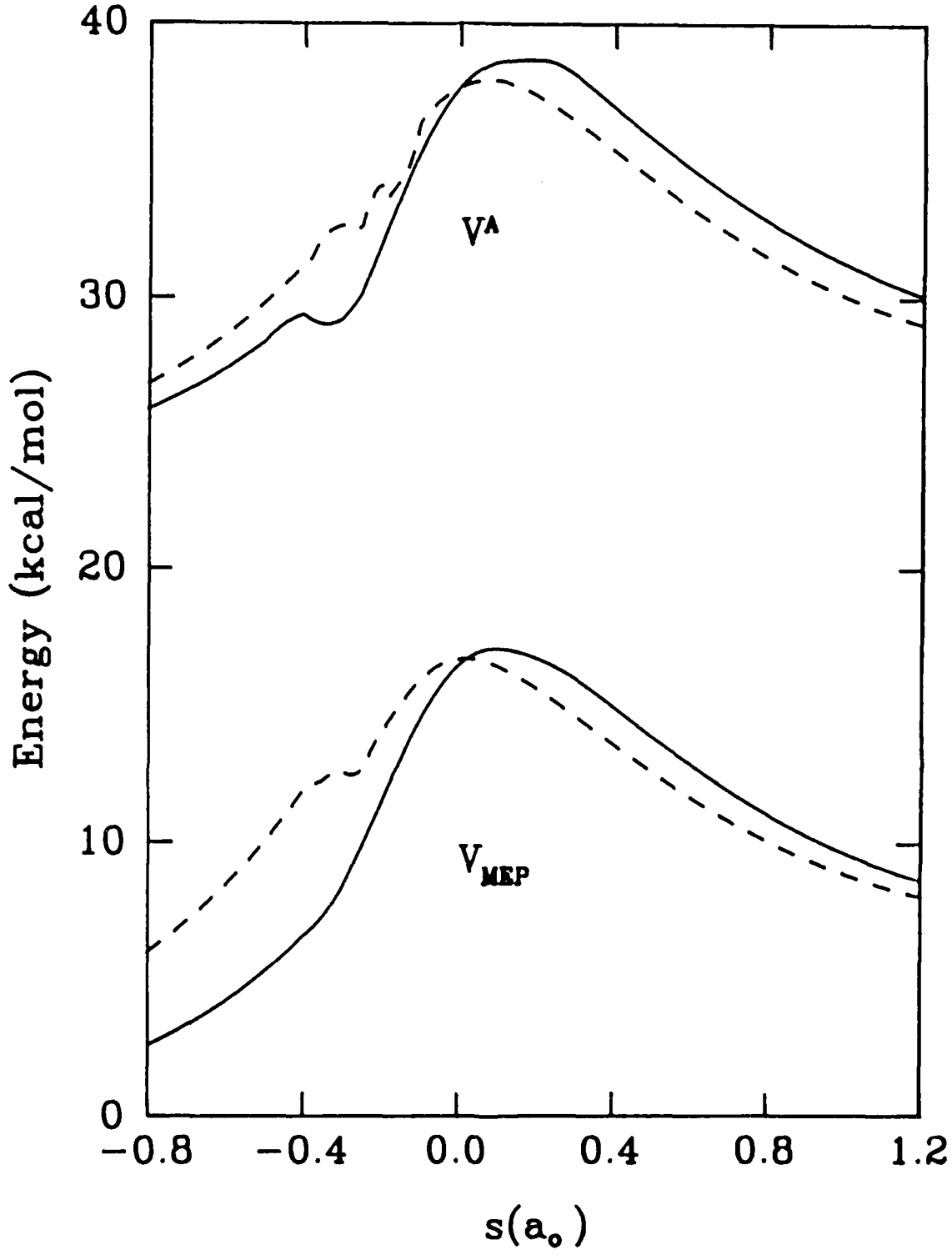

Figure 2. Comparison of potential energy along the minimum energy path [$V_{MEP}(s)$] and ground-state adiabatic potential [$V^A(s)$] as a function of reaction coordinate s computed using the HF/BAC-MP4 method (solid curves) and the MP2/BAC-MP4 method (dashed curves) for the reaction H + $NH_3 \rightarrow H_2 + NH_2$.

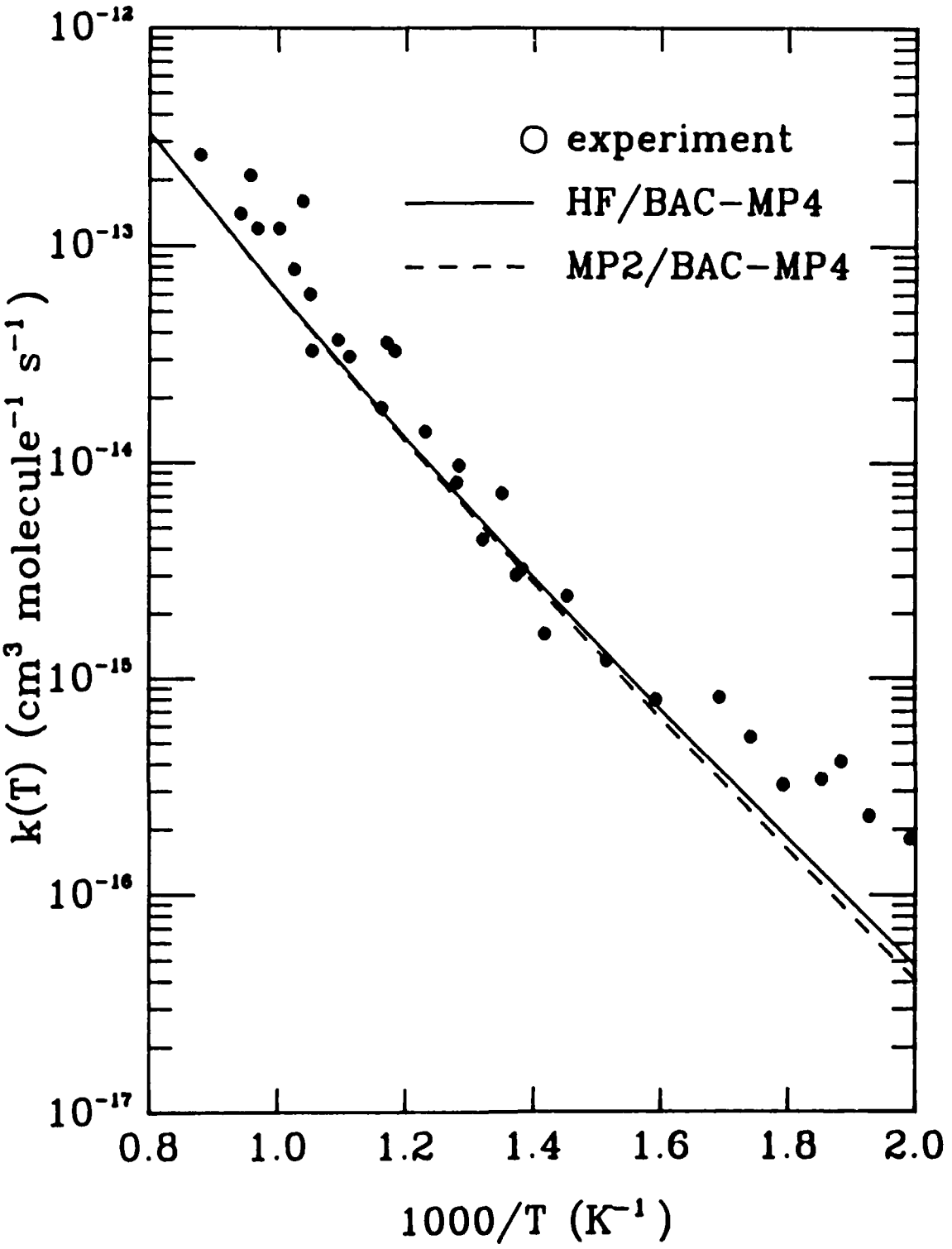

Figure 3. Rate constants as a function of temperature for the reaction $H + NH_3 \rightarrow H_2 + NH_2$ computed using the improved canonical variational theory with small-curvature semiclassical adiabatic ground-state transmission coefficient from potential information obtained using the HF/BAC-MP4 method (solid curves) and the MP2/BAC-MP4 method (dashed curves). Comparison is also made with the experimental rate constants of P. Marshall and A. Fontijn, ref. 35a, denoted MF (•).

lowest temperatures which is discussed in more detail below. Comparison can also be made to least-squares Arrhenius fits to experimental results for the temperature ranges from 500 to 1140 K,[35] 908 to 1777 K,[36] and 673 to 1003 K.[37] These fits give activation energies of 17.2±0.8, 16.0±0.2, and 14.6±1.0 kcal/mol, respectively. Activation energies derived from the computed rates show an interesting behavior of initially increasing with increasing temperature but turning around and decreasing at even higher temperature; e.g., the computed activation energies are 12.9, 14.7, 17.1, and 14.7 kcal/mol over the temperature ranges 400-600 K, 600-1000 K, 1000-1500 K, and 1500-2400 K respectively. In general the agreement between the experimental and computed activation energies is excellent; however, the theoretical results systematically underestimate the experimental reaction rate indicating a systematic overestimate in the free energy of activation. The underestimation of the rate may be attributed to a barrier height which is too large; however, lowering just the barrier will tend to decrease the activation energy which is inconsistent with the experiments. Another possibility is that the energetics are approximately correct (i.e., the ground-state adiabatic barrier is about right) and that the entropic factors controlled by the higher lying vibrational levels are not accurately described.

Reaction rates computed by the the ICVT/SCSAG method with the HF/MP4-BAC potential information for reaction (R5) are compared with the experimental ones of Hack *et. al.*[37] and Demissy and Lesclaux[38] in figure 4. The agreement with the low temperature results of Demissy and Lesclaux is excellent (differences of 18-40%) but at higher temperatures the computed rates are factors of 2.2 to 2.7 lower than the results of Hack *et. al.* The discrepancy at the higher temperatures can be attributed to uncertainties in the heat of formation of NH_2. At lower temperatures the computed heat of formation of NH_2 agrees well with the experimental values and we expect less uncertainty in the computed rate constant.

Reaction rates computed by the ICVT/SCSAG method using the HF/BAC-MP4 potential information for reaction (R6) are compared with experimental one of Marshall and Fontijn[39] in figure 5. Once again the agreement is excellent, although the theoretical results systematically underestimate the reaction rates. This underestimate is consistent with our observations for the H

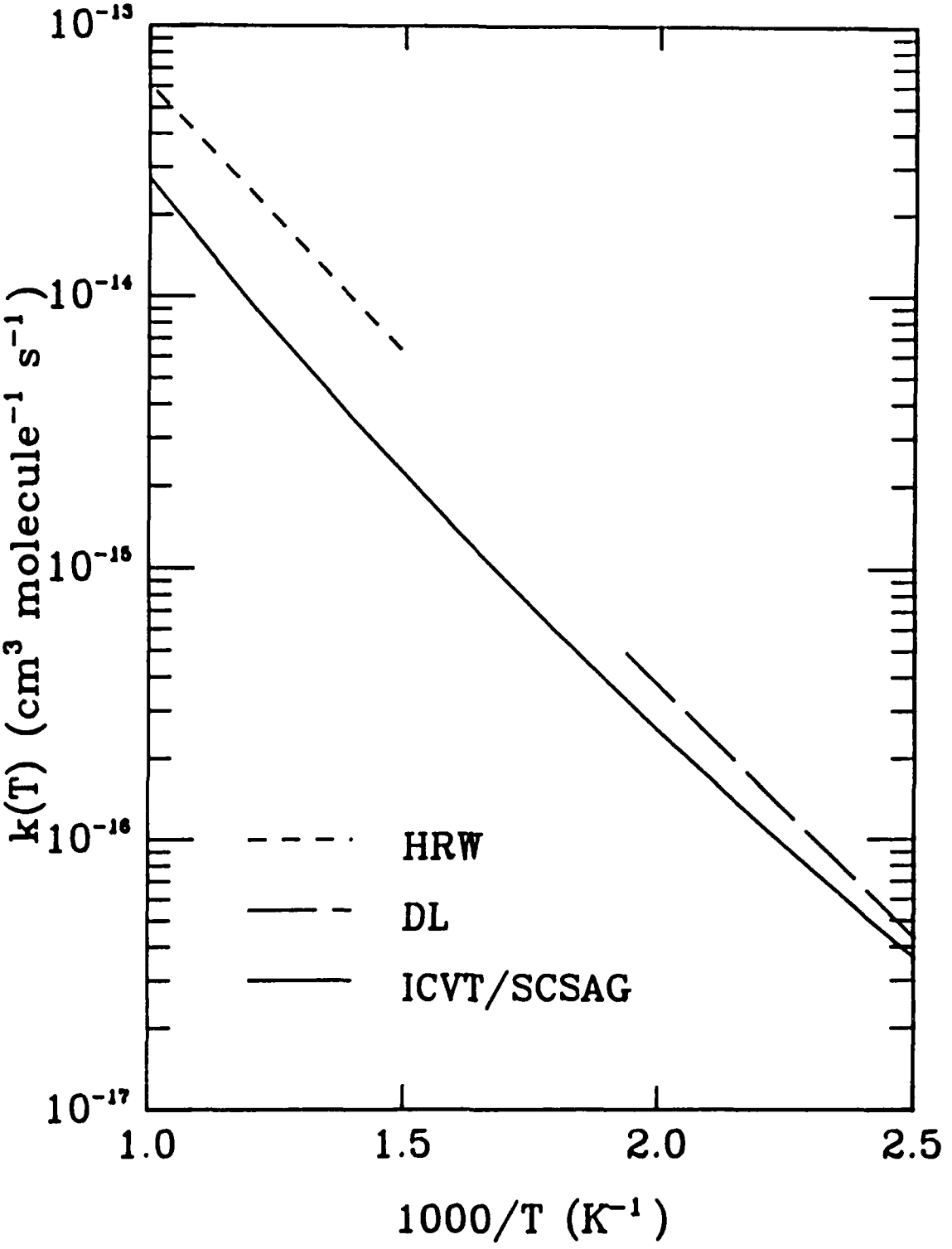

Figure 4. Comparison of computed and experimental rate constants for the reaction $H_2 + NH_2 \rightarrow H + NH_3$. The experimental results are the Arrhenius fit of W. Hack, P. Rouveirolles, and H. Gg. Wagner, ref. (36), denoted HRW (short dashed curve) and the Arrhenius fit of M. Demissy and R. Lesclaux, ref. (38), denoted DL (long dashed curve). The solid line is the result of the improved canonical variational theory with small-curvature semiclassical adiabatic ground-state transmission coefficient (ICVT/SCSAG) from potential information obtained using the HF/BAC-MP4 method.

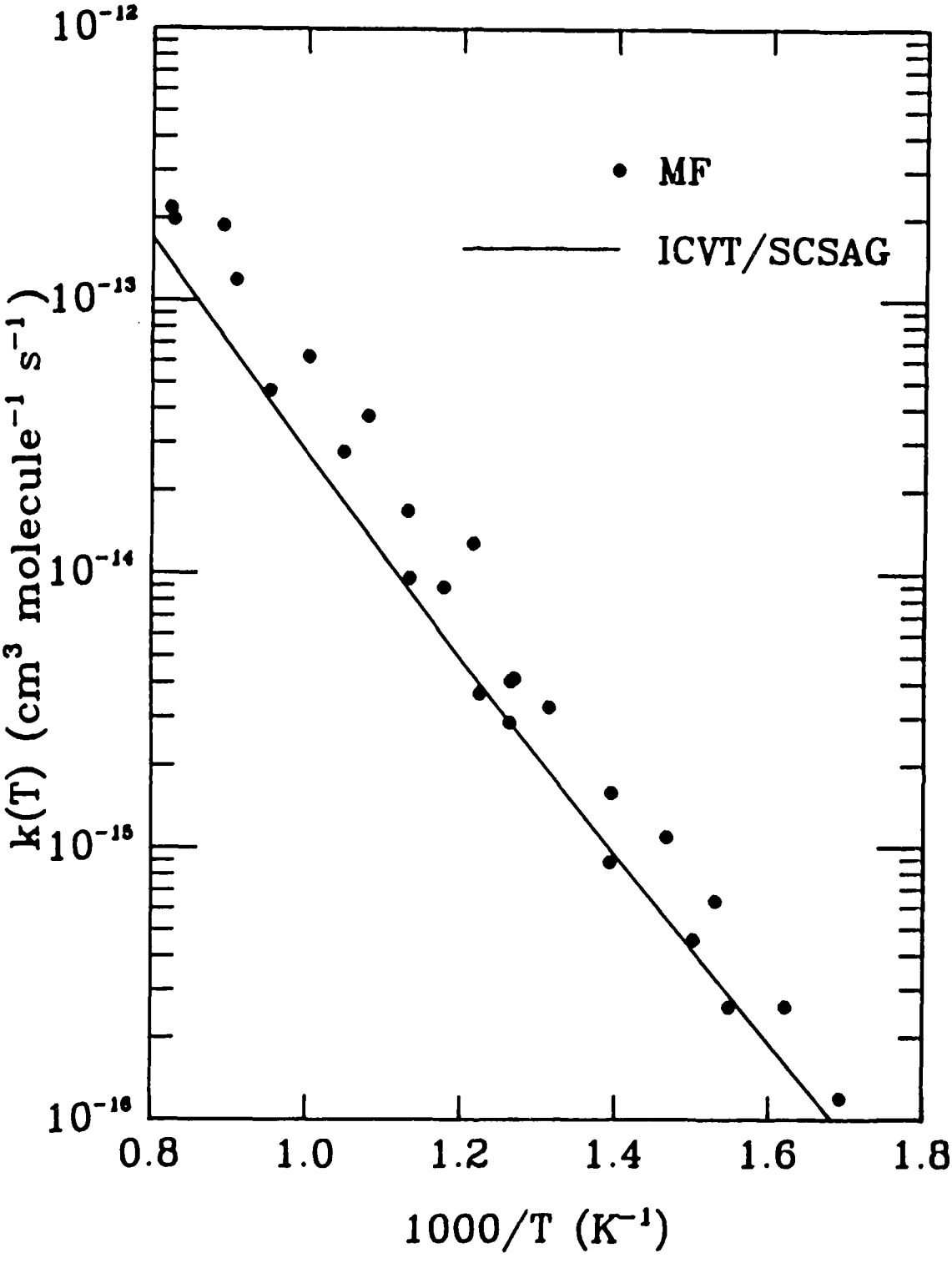

Figure 5. Comparison of computed and experimental rate constants for the reaction D + ND_3 → D_2 + ND_2. The experimental results are from P. Marshall and A. Fontijn, ref. (39), denoted MF (•). The solid line is the result of the improved canonical variational theory with small-curvature semiclassical adiabatic ground-state transmission coefficient (ICVT/SCSAG) from potential information obtained using the HF/BAC-MP4 method.

+ $NH_3 \rightarrow H_2 + NH_2$ reaction that some feature of the potential energy surface is giving rise to a free energy of activation which is too low. Compared to reaction (41), tunneling is less important for the deuterated reaction. For example, at 300 K, the ICVT/SCSAG transmission coefficient is 44.5 for reaction (R4) and only 8.5 for (R5), and at 600 K these decrease to 2.4 and 1.6, respectively. As for reaction (R4), the good agreement between the computed and experimental activation energy indicates that the reaction energetics are approximately correct but the entropic factors controlled by higher lying vibrational levels leads to the underestimate of the rates.

For the three reactions for which experimental results are available, the agreement between theory and experiment is very good except in comparison with the experimental results of Marshall and Fontijn[35] for reaction (R4) at temperatures below 660 K. Below this temperature the experimental results show much more curvature in the Arrhenius plot than the theoretical rates and at 500 K the experimental rates are higher than the theoretical ones by about a factor of 4. Such curvature in the Arrhenius plot is often attributed to quantum mechanical tunneling, but in the present calculations the large amount of tunneling necessary to reproduce the experimental curvature is inconsistent with the excellent agreement between theory and experiment for temperatures above 660 K. For example, at 660 K the SCSAG tunneling correction factor is about 2 and gives good agreement with experiment. At 500 K the SCSAG tunneling correction factor is 3.6 but would have to be about 15 to agree with experiment. To reproduce this sharp increase in tunneling over such a small change in temperature would require a radically different shape of the adiabatic potential which is inconsistent with the reliability established in previous tests and uses of the methods.

Another indication of the inconsistency of these low temperature results is given by the low temperature results for reaction (R5) which are related to those of reaction (R4) by detailed balance. Knowledge of the equilibrium constant as a function of temperature allows calculation of rates for one of the reactions from the other. At lower temperatures the heats of formation of all four species (two reactants and two products) are accurately known, thus the equilibrium constant can be accurately computed at these temperatures. Therefore, the good agreement between the

computed rates and the experimental results of Demissy and Lesclaux[38] for reaction (R5) is inconsistent with the poorer agreement observed between theory and the experimental results of Marshall and Fontijn[35] for temperatures below 660 K. This is further evidence of the inconsistency of the low temperature experimental results for reaction (R4).

The good agreement between the different levels of theory and the overall good agreement between the experimental and computed rates is encouraging for application of the HF/BAC-MP4 method to a variety of reactions. This work establishes the feasibility of this approach for providing reliable predictions of thermal rate constants and shows the utility of semiempirical corrections to *ab initio* electronic structure calculations of information about the potential energy surface. In particular, the HF/BAC-MP4 method is a cost effective means of obtaining this type of information. Calculations of the energy and its first and second derivatives at each point along the minimum energy path required only eight minutes of cpu time on a Cray 1s computer. To obtain rate constants numerically converged to about 20% at 300 K requires about 40 points along the reaction path. At higher temperatures these requirements relax so that at 1000 K only about 10 points along the reaction path are needed for the same type of convergence. Thus, for about five and one-half hours of Cray 1s computer time rates accurate to better than 50% can be obtained over the entire temperature range from 200 to 2400 K. The calculations at the MP2 and MP4 levels become much more costly in part because some or all of the analytically derivatives are not available and must be computed by numerical differentiation. For the MP2 calculations only analytic first derivatives are available and for the MP4 calculations no analytic derivatives are available. Calculation of the derivatives by finite difference greatly increases the cost of the calculations. The MP2 and MP4 calculations require over three and seventeen hours, respectively, of Cray 1s computer time per point along the minimum energy path. The reliability of the lower HF level of theory with the BAC correction makes this efficient approach feasible.

3.1.2 Application to $HONO \rightarrow HNO_2$

As a further test of the BAC-MP4 method, the hydrogen migration reaction from trans-HONO to HNO_2 was studied at several levels of electronic structure theory. Molecules containing nitro groups present a challenge to *ab initio* methods for obtaining accurate representations of the potential energy surface. The utility of a single reference wavefunction has been questioned for this type of system and it has been suggest that a multireference wavefunction such as used in the multiconfiguration SCF (MCSCF) method will be necessary to obtain reasonable estimates of the reaction energetics. Therefore, this type of reaction represents a stringent test of the BAC-MP4 method which is based on a single reference HF wavefunction.

In this section we present a comparison of BAC-MP4 and MCSCF results for reaction (R7). Two different MCSCF calculations are considered, both using double-zeta plus polarization (DZP) basis sets. A DZP basis set is comparable to the 6-31G* basis set used in the HF optimizations of the BAC-MP4 calculations and the following comparisons are a test primarily of the methods for including electron correlation and not a test of basis set effects. The first MCSCF calculation treats the σ and π spaces independently. The σ-space correlation includes selected single and double excitations from a HF reference and correlation is included for the the complete active π space; this is denoted MC(σ/π). The second MCSCF calculation considers all double excitations from the seven highest occupied orbitals into the seven lowest unoccupied orbitals; this is denoted MC14.

For the BAC-MP4 method to be useful, the location of the critical geometries (equilibrium geometries and saddle points) and minimum energy path for the reaction must be accurately reproduced. In figure 6 the HF and MC(σ/π) minimum energy paths are compared. During the entire reaction all four atoms lie in a plane; figure 6 shows the motion in this plane of the H and two O atoms relative to fixing the N atom at the origin. The excellent agreement of the two paths indicates that the BAC-MP4 method has passed the first test; the HF method is capable of placing the system in the correct location.

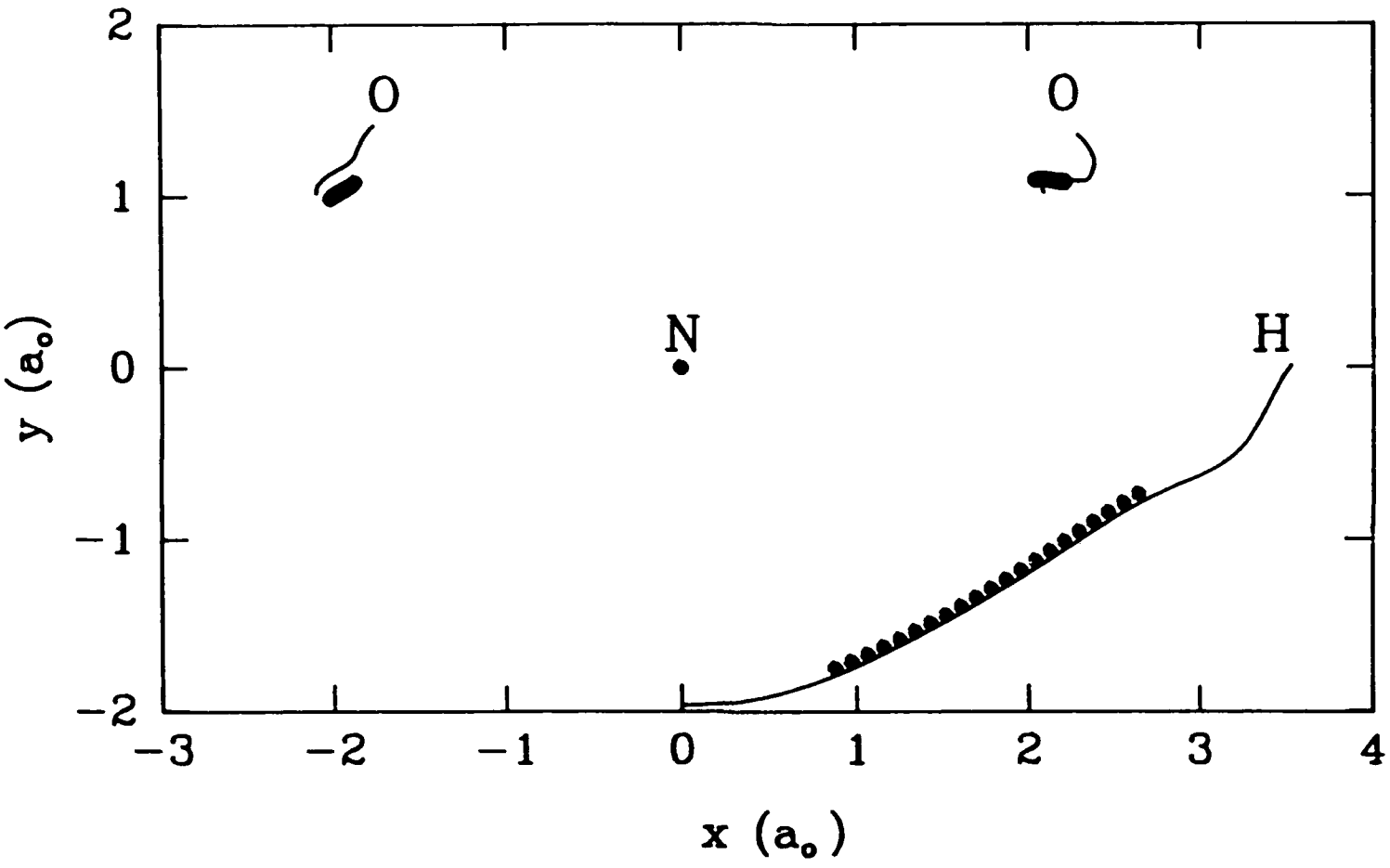

Figure 6. Minimum energy path for the unimolecular reaction HONO → HNO_2 computed using information about the potential energy surface obtained from MCSCF calculations (solid curves) and BAC-MP4 calculations (•) During the entire reaction the four atoms remain in a plane. The motion of the oxygen and hydrogen atoms in this plane, relative to the nitrogen atom at the origin, is depicted.

In the BAC-MP4 method the frequencies are also calculated at the HF level and it is interesting to see how well they compare with the MCSCF ones. A comparison of the frequencies from the two MCSCF calculations and the BAC-MP4 calculations, as well as comparison to experiment[40] is presented in table 4.

Table 4. Frequencies (in cm^{-1}) for trans HONO

	MC(σ/π)	MC14	BAC-MP4	JANAF
	632	522	604	543
	676	767	794	598
	925	1104	1104	794
	1376	1480	1520	1260
	1744	1827	2049	1696
	3828	4126	4092	3590
Zero point energy	4591	4913	5082	4241

Comparison between individual modes shows some fairly large discrepancies but the crucial quantity in determining the thermal rate is the total zero point energy given at the bottom of each column. Because of the separation of the σ and π spaces in the MC(σ/π) calculation the frequency of the lowest mode, which is an out-of-plane bend, is not accurately reproduced. Otherwise this MCSCF calculation includes the most correlation and gives the best agreement with the experimental zero point energy. The MC14 and BAC-MP4 frequencies agree well and the zero point energy for these methods is overestimated by about 18%. This is higher than the usual 12% overestimate expected from HF frequencies but of sufficient accuracy for applying the BAC correction. The theoretical frequencies at the saddle point are presented in table 5. In this case the BAC-MP4 frequencies agree better with the MC(σ/π) ones than with the MC14 frequencies but the differences in zero point energies are less than 0.3 kcal/mol.

Table 5. Frequencies (in cm^{-1}) for the migration transition state HONO $\rightarrow$ HNO_2.

MC(σ/π)	MC14	BAC-MP4
2345i	2385i	2424i
319	436	394
341	711	709
628	1344	1360
765	1680	1686
1179	2629	2434
3234	3400	3292

The reaction energetics computed from the BAC-MP4 and MC(σ/π) methods are presented in figure 7 as a comparison of the ground-state adiabatic potential curves. The MCSCF calculation has errors arising from basis set limitations and from neglect of some of the electron correlation. The uncertainties in the energetics obtained from this method are estimated to be about 10 kcal/mol. The BAC-MP4 gives the best estimate of the adiabatic barrier because it uses a bond additivity correction to compensate for the errors caused the small basis set and the limited amount of electron correlation included. The agreement in the barrier heights may be fortuitous (they differ by less than 5 kcal/mol) but the general shape of the two curves are qualitatively similar. This indicates that the BAC-MP4 method is not giving unphysical behavior as a result of the bond additivity correction over- or under-compensating for gross errors in the MP4 energies. The BAC-MP4 method gives physically reasonable results even for systems containing nitro groups.

Another encouraging feature of the BAC-MP4 calculations is the computational effort required. The calculation of the energy and first and second derivative at each point along the minimum energy required less than 20 minutes of Cray 1s computer time. This system is much

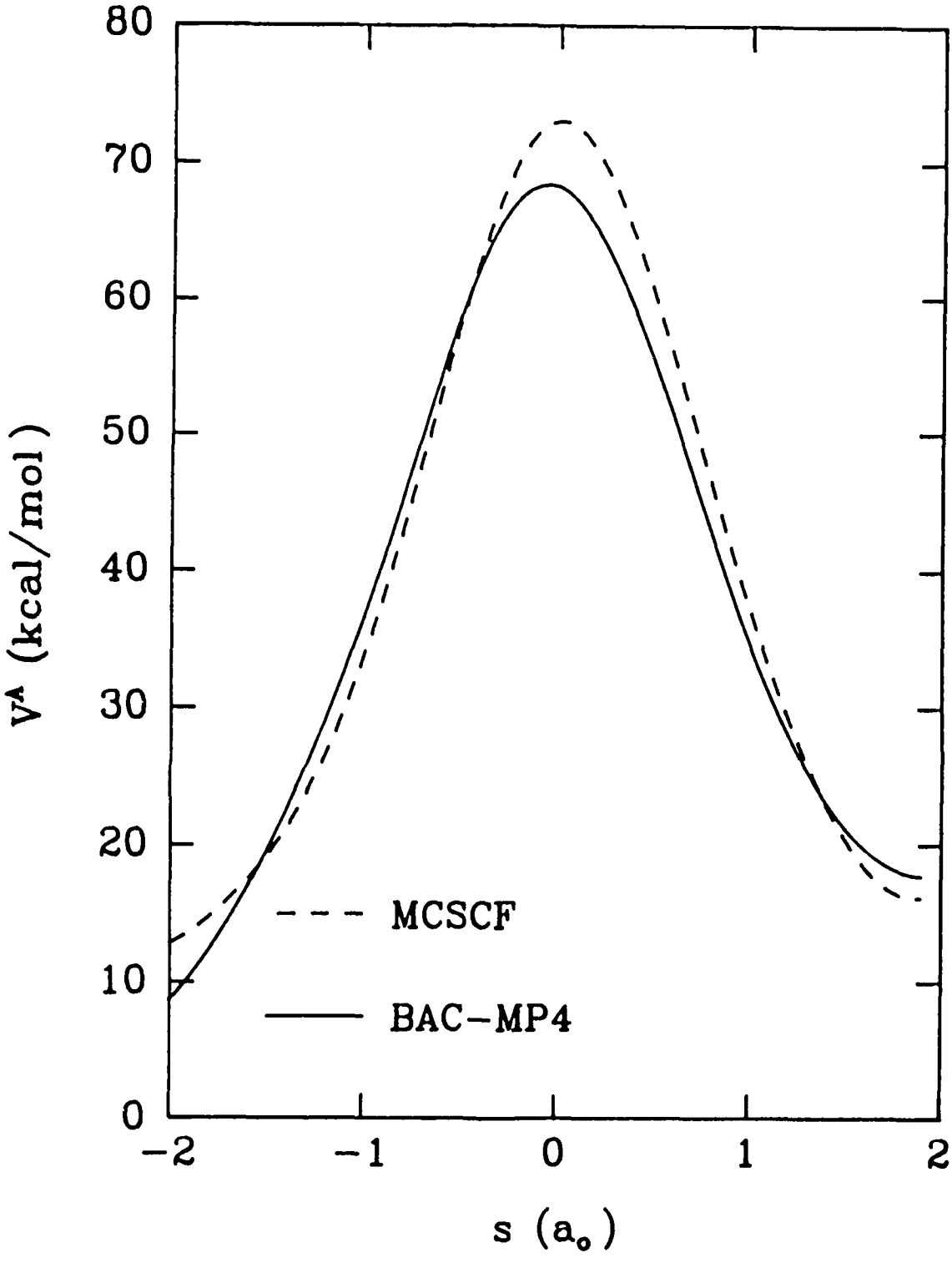

Figure 7. Ground-state adiabatic potential curves as a function of reaction coordinate s for the unimolecular reaction HONO → HNO_2 computed using information about the potential energy surface obtained from MCSCF calculations (dashed curve) and BAC-MP4 calculations (solid curve)

larger than the H + NH_3 reaction considered (24 electrons as compared to 11) but the computational effort is small enough to allow the entire reaction path from -1.0 to 1.0 a_0 to be mapped out in less than eight hours of Cray 1s computer time. Thus, we are encouraged to treat even larger polyatomic systems which should require only a moderate computational effort.

3.2 Systematic studies of the H + RNO_2 reactions for R = H, CH_3, OH, NH_2, and CH_3NH

The systematic study of a homologous set of reactions with different substituents allows for an assessment of the effect of the substituents on reaction dynamics and is the beginning of any empirical model based upon group additivities. As a first step, such a study has been performed on reactions (R1) and (R2) using conventional transition state theory with HF/BAC-MP4 information about the potential energy surface. More rigorous studies in the future will use variational transition state theory. For reactions (R3) with all substituents except OH the HF/BAC-MP4 method predicts that the saddle point energy is below the asymptotic energy for the products. This is unphysical and requires the use of variational transition state theory for a consistent evaluation of the thermal rate constants. This type of study has been carried out for one of the substituents R=NH_2 and allows a complete description of the reaction system for all three reactions (R1)-(R3) for the substituents H, CH_3, OH, NH_2, and CH_3NH.

3.2.1 H + $RNO_2 \rightarrow RN\langle^{O}_{OH}$

The enthalpy of reaction at 0 K, $\Delta_r H_0$, is the change in the ground-state adiabatic potential curve in going from reactants to products. This gives an estimate of the heat release (for a negative enthalpy) upon reaction . The free energy of reaction for a given temperature T, $\Delta_r G_T$, is a better measure of the thermodynamic driving force behind the reaction since it includes both the entropic and enthalpic terms. Negatives values for the free energy of reaction indicate that the products are more stable than reactants. The enthalpy of activation at 0 K, $\Delta_r H_0$, is the change in the ground-state adiabatic potential curve in going from reactants to the saddle point and is a measure of the energetic barrier to the reaction. Within the approximations of conventional transition state theory

the rate at which the reaction proceeds for a given temperature is governed by the free energy of activation, $\Delta_r G_T$, which includes the energetic factor $\Delta_r H_0$ and the entropic terms. The enthalpies free energies of reaction, the enthalpies free energies of activation, and the rate constant at 1000 K for reaction (R1) is summarized in table 6 for all five substituents.

Table 6. Reaction energetics and rates for the reaction $H + RNO_2 \rightarrow RN\langle^{O}_{OH}$

R	$\Delta_r H_0$ (kcal/mol)	$\Delta_r G_T$ (kcal/mol)	$\Delta_r H_0$, (kcal/mol)	$\Delta_r G_T$ (kcal/mol)	$k^+(T=1000\ K)$ (s^{-1})
H	-37.7	-18.4	8.7	28.3	1.9×10^{-12}
CH_3	-41.1	-17.4	7.8	31.1	4.6×10^{-13}
OH	-35.0	-16.2	9.3	30.0	8.1×10^{-13}
NH_2	-32.7	-12.8	9.9	29.8	4.6×10^{-13}
CH_3NH	-33.3	-13.8	9.0	30.5	6.3×10^{-13}

It is clear that the addition of a hydrogen atom to the oxygen end of RNO_2 is fairly insensitive to the substituent attached to the nitrogen. Although the enthalpy of reaction changes by as much as 8 kcal/mol in changing the substituent from CH_3 to NH_2, the enthalpy of reaction changes by less than 2.2 kcal/mol for all five substituents. Similarly changes in the free energies of reaction are as large as 5.6 kcal/mol but the free energy of activation changes by less than 3 kcal/mol. The rates change at most by about a factor of 4 and the Arrhenius parameters are all very similar at 1000 K – the activation energies are 11.2, 10.2, 11.9, 11.3 and 11.3 kcal/mol for the substituents H, CH_3, OH, NH_2, and CH_2NH, respectively and the base ten logarithms of the A factors are -9.3, -10.1, -9.5, -9.6, and -9.7, respectively.

The present calculations are presented as a qualitative guide to substituent effects. A more consistent treatment of the reaction dynamics would involve a variational transition state theory approach including tunneling effects. Since these reactions involve primarily the motion of a hydrogen atom and the barriers for reaction are high (ranging from 8 to 10 kcal/mol), tunneling is

expected to be very important at temperatures below about 600 K. At 1000 K, where the current comparisons are being made, tunneling should enhance the rate by at most 50% and the qualitative comparison made above should be valid. For meaningful comparisons at temperature below 600 K tunneling should be treated.

3.2.2 $RN\langle^{O}_{OH} \rightarrow R + HONO$

A similar comparison of reaction energetics and rates for reaction (R2) is provided in table 7.

Table 7. Reaction energetics and rates for the reaction $RN\langle^{O}_{OH} \rightarrow R + HONO$

R	$\Delta_r H_0$ (kcal/mol)	$\Delta_r G_T$ (kcal/mol)	$\Delta_{\ddagger} H_0$, (kcal/mol)	$\Delta_{\ddagger} G_T$ (kcal/mol)	$k^{\ddagger}$(T=1000 K) (s^{-1})
H	28.9	5.7	34.4	34.3	$6.6x10^5$
CH_3	20.2	-11.6	28.3	25.7	$5.0x10^7$
OH	3.0	-25.4	6.0	6.2	$9.2x10^{11}$
NH_2	4.2	-28.1	10.7	10.4	$1.1x10^{11}$
CH_3NH	4.6	-31.3	10.9	11.7	$5.7x10^{10}$

The rates reported for the unimolecular reaction are for the high pressure limit. These reactions involve the breaking of the R-N bond and the thermal rates are very sensitive to the substituent R. There is a weak correlation between the free energy of reaction and the free energy of activation and thereby the reaction rate. More important though is the comparison between the energetics and rates for the NH_2 and CH_2NH substituents. In these cases a NO bond is being broken in the course of the reaction and the energetics and rates are very similar.

3.2.3. $NH_2N\langle^{O}_{OH} \rightarrow NH_2 + HONO$ and $NH_2N\langle^{O}_{OH} \rightarrow NH_2NO + OH$

An important aspect of the reaction system (R1)-(R3) is the branching ratio between the two unimolecular reactions (R2) and (R3). This has been studied in more detail for the substituent NH_2. Rate constants for the reaction $NH_2N\langle^{O}_{OH} \rightarrow NH_2NO + OH$ were computed using variational transition state theory with semiclassical adiabatic ground-state transmission coefficients using HF/BAC-MP4 information about the potential energy surface. The potential along the minimum energy path and the ground-state adiabatic potential curve are shown in figure 8. Note that the value of the potential at the HF saddle point location (indicate by s=0) is much lower than its maximum value which occurs for s at about 0.25 a_0. This same type of behavior is seen in the ground-state adiabatic potential curve and in the free energy of activation curves show in figure 9 for 300 and 1000 K. As a result, the conventional transition theory state rates are much higher than the ones obtained from the improved canonical variational theory as seen in table 8.

Table 8. Rate constants (in units of s^{-1}) for the two reactions

	$NH_2N\langle^{O}_{OH} \rightarrow NH_2NO + OH$			$NH_2N\langle^{O}_{OH} \rightarrow NH_2 + HONO$
T,K	$k^{\dagger}(T)$	$k^{ICVT}(T)$	$k^{ICVT/SCSAG}(T)$	$k^{\dagger}(T)$
300	9.4×10^{9}	3.5×10^{6}	5.3×10^{6}	1.1×10^{5}
400	6.9×10^{10}	2.4×10^{8}	3.0×10^{8}	1.4×10^{7}
600	5.6×10^{11}	1.9×10^{10}	2.0×10^{10}	1.9×10^{9}
1000	3.4×10^{12}	7.4×10^{11}	7.6×10^{11}	1.1×10^{11}
1500	8.9×10^{12}	5.0×10^{12}	5.1×10^{12}	9.4×10^{11}
2400	1.9×10^{13}	1.7×10^{13}	1.7×10^{13}	5.2×10^{12}

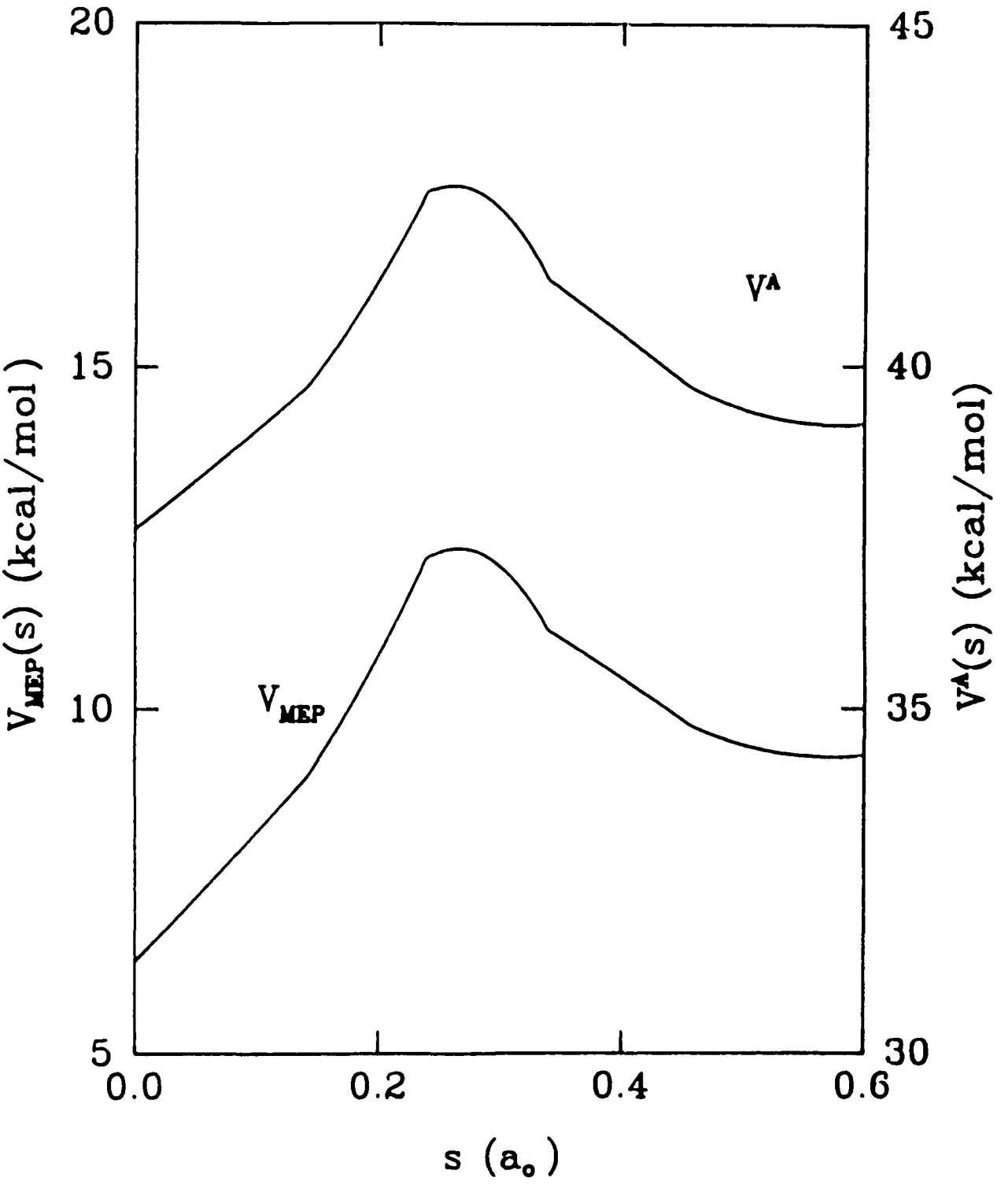

Figure 8. Potential energy along the minimum energy path [$V_{MEP}(s)$] and ground-state adiabatic potential [$V^A(s)$] as a function of reaction coordinate s computed using the HF/BAC-MP4 method for the reaction $NH_2N(O)OH \rightarrow NH_2NO + OH$.

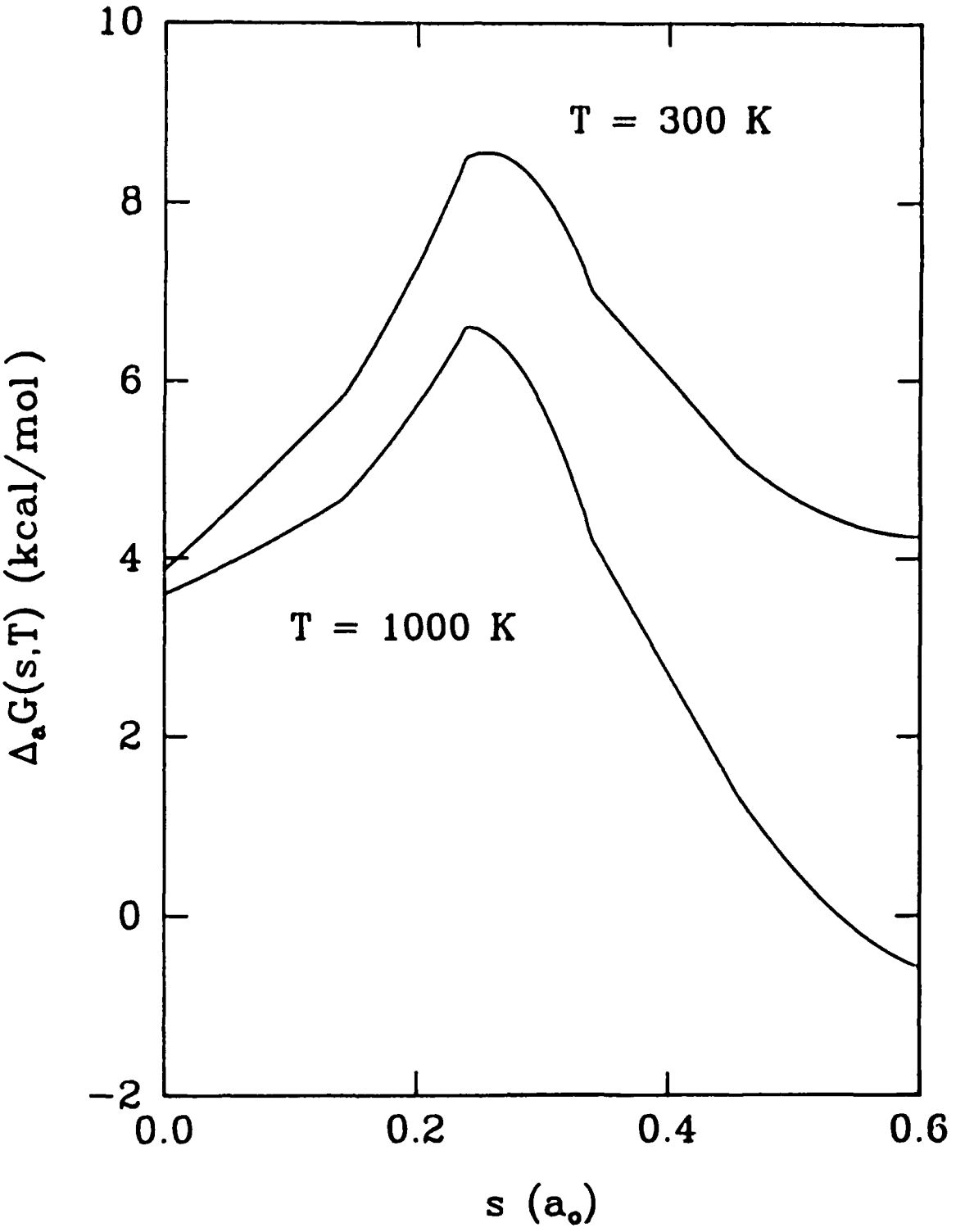

Figure 9. Free energy of activation [$\Delta G_a(T,s)$] as a function of reaction coordinate s for temperature of 300 and 1000 K computed using the HF/BAC-MP4 method for the reaction $NH_2N(O)OH \rightarrow NH_2NO + OH$.

Tunneling is relatively unimportant for this reaction and the rate obtained by the ICVT/SCSAG method are only slightly higher than those with the tunneling correction factor.

The rates for the reaction $NH_2N\langle^{O}_{OH} \rightarrow NH_2 + HONO$ are also presented in table 8 for comparison. The value of the ground-state adiabatic barrier above the reactant value is about 10.7 kcal/mol at the saddle point for the HONO channel and about 9.1 kcal/mol at its maximum for the OH channel. A consistent comparison would treat both branches of the reaction using variational transition state theory; however, if this is done, the value of the adiabatic barrier maximum will increase for the HONO channel making it even more dynamically unfavorable. Since the rates for the OH channel are already higher, increasing the barrier for the HONO channel will only increase the difference. Therefore, we can predict that the OH channel is favored over that for HONO formation at all temperatures from 300 to 2400 K.

3.3 Thermochemical kinetic analysis

Appendix B gives a more indepth discussion of the results of the thermochemical analysis. In this section we review those results and present additional analysis for reaction (R4) and (R6). The new thermochemical kinetic analysis presented in detail in appendix B includes important dynamical effects that will allow reliable estimates of Arrhenius parameters. As a test of the importance of these dynamical effects and as a guide to estimating the nonsubstantial contributions the thermochemical kinetic analysis is performed on seven reactions. Five of the reactions have been treated earlier by variational transition state theory[10,11,13-15] and provide rate constants in good agreement with experiment,[14,41] and the other two reactions are reaction (R4) and (R6) already discussed in this report. The theoretical rate constants are analyzed to obtain values for $\Delta_n S^{\circ}_T$, $\Delta_n H^{\circ}_T$, $\Delta_s S^{\circ}_T$ and $\Delta_s H^{\circ}_T$. The five new reactions considered are

$$H + H_2 \rightarrow H_2 + H \qquad \text{(R8)}$$

$$D + H_2 \rightarrow HD + H \qquad \text{(R9)}$$

$$H + D_2 \rightarrow HD + D \qquad \text{(R10)}$$

$$O(^3P) + H_2 \rightarrow OH + H \qquad (R11)$$

and

$$OH + H_2 \rightarrow H_2O + H \qquad (R12)$$

For these five reactions global *ab initio* potential energy surfaces were used in contrast to the reaction path Hamiltonian information used for reactions (R4) and (R6).

The activation parameters for the seven reactions are present in table 9 and are given in terms of the entropy and enthalpy of activation at 300 K, and the heat capacity of activation from 200 to 1500 K. Some general trends are seen in table 9. First, using the terminology discussed in section 2.3, the substantial contributions are large than the nonsubstantial ones; thus, the analysis in terms of the structure of the transition state gives the majority of the contributions to the total enthalpy and entropy of activation. However, the nonsubstantial contributions to both the enthalpy and entropy of activation are quite large and need to be included for accurate predictions of the rate constants. The values of the substantial enthalpy of activation at 300 K correlate with the barrier heights for the reactions, that is, $OH + H_2$ has the smallest barrier and $H + NH_3$ has the largest. For the nondeuterated reactions the nonsubstantial contributions tend to be larger for the systems with the larger barriers, i.e., tunneling is more important for the reactions with the higher barriers. Compared to the hydrogen cases, the deuterated reactions have smaller nonsubstantial contributions due to the lesser importance of tunneling.

The substantial contributions to the heat capacities of activation are negative, in general, which implies that the substantial enthalpies and entropies decrease with increasing temperature. In the present example, the nonsubstantial contributions to the heat capacity of activation go to zero at high temperatures. They are all positive and at low temperatures are much larger than the substantial ones causing large changes in the enthalpies and entropies at low temperatures.

The substantial contributions to the activation parameters are obtained from information about the potential at a single point along the minimum energy path. This enables the substantial contributions to be estimated from existing bond additivity or group additivity relationships.[6] The

Table 9. Activation parameters for seven reactions. (Enthalpies in units of kcal mol^{-1}, entropies and heat capacities in units of cal $mol^{-1}K^{-1}$, standard state is 1 atm.)

reaction	contribution	ΔH^{o}_{T} T=300K	ΔS^{o}_{T} T=300K	T=	ΔC^{o}_{T} 200	300	400	600	1000	1500
$H+H_2$	substantial	7.8	-19.6		-4.9	-4.2	-3.4	-2.1	-1.1	-1.0
	nonsubstantial	-2.6	-4.4		20.8	9.4	5.3	2.1	0.6	0.3
$D+H_2$	substantial	7.4	-20.1		-4.8	-4.0	-3.2	-2.0	-1.1	-1.0
	nonsubstantial	-2.2	-3.9		18.7	8.5	4.7	1.9	0.5	0.1
$H+D_2$	substantial	8.7	-20.5		-4.6	-3.5	-2.7	-1.7	-1.1	-1.0
	nonsubstantial	-1.7	-3.2		23.2	9.5	3.9	1.3	0.3	0.1
$O+H_2$	substantial	9.4	-20.9		-3.5	-3.0	-2.5	-1.7	-1.0	0.6
	nonsubstantial	-4.2	-8.9		9.0	19.2	12.8	3.2	0.6	0.0
$OH+H_2$	substantial	4.8	-23.3		-5.4	-3.9	-2.8	-1.5	-0.3	0.5
	nonsubstantial	-3.2	-5.2		13.2	9.6	5.8	2.6	1.0	0.6
$H+NH_3$	substantial	14.2	-20.4		-4.3	-3.0	-1.9	-0.8	-0.2	-0.1
	nonsubstantial	-5.0	-9.0		30.1	20.5	10.3	3.5	1.3	0.7
$D+ND_3$	substantial	14.6	-22.0		-3.7	-2.1	-1.1	-0.2	-0.1	-0.2
	nonsubstantial	-2.9	-5.4		36.7	13.9	6.3	2.2	0.7	0.3

nonsubstantial contributions are obtained from more extended information about the potential energy surface and, therefore, are harder to estimate. All the reactions studied here are hydrogen (or deuterium) atom transfer reactions with fairly high barriers. For these reactions the nonsubstantial contributions are predominantly from quantum mechanical tunneling and the effect of variationally optimizing the location of the transition state dividing surface is small. For reactions with smaller barriers we expect the effect of quantum mechanical tunneling to be smaller, but for those reactions the effects of variationally locating the dividing surface will become more important especially at higher temperatures.[42] It is therefore expected that the nonsubstantial contributions will be significant for a wide range of gas-phase chemical reactions and new methods are needed for estimating these quantities.

4. Conclusions

The main objective of this six-month Phase I research program was to establish the feasibility of using theoretical methods for describing the kinetics of chemical reactions important in nitrocubane decomposition. The accuracy of the theoretical methods has been established by comparison of different levels of theory for two chemical reactions, $H + NH_3 \rightarrow H_2 + NH_2$ and $HONO \rightarrow HNO_2$ and in comparison of the theoretical rate constants with experimental ones for the $H + NH_3 \rightarrow H_2 + NH_2$ reaction. These calculations indicate that the underlying *ab initio* electronic structure calculations provide a good zeroth-order description of the potential energy surfaces. The empirical bond additivity correction compensates for known errors in these potentials and the comparisons with experiment indicate that these correction are of quantitative accuracy.

For these theoretical methods to be of practical use they must be capable of treating systems which are larger than those presented here. The only inherent limitation in these methods is the computational effort of the *ab initio* electronic structure calculations which increases with increasing size of the reaction system. A requirement for the utility of this method is that the size of the *ab initio* electronic structure calculations is kept manageable. Although this leads to known

errors in the potential energy surfaces, the bond additivity correction provides a computationally efficient method of compensating for these errors. The relatively small reaction systems studied here were treated with a very modest expenditure of computational power, e.g., the entire calculation of the rate constants from 200 to 2400 K for the $H + NH_3 \rightarrow H_2 + NH_2$ reaction were carried out in several hours of Cray 1s computer time. The prospects of treating much larger systems are excellent.

Looking beyond the Phase I objectives towards the goal of providing a comprehensive treatment of propellant decomposition, methods are needed for treating the kinetics of very large polyatomic systems. Accurate calculations of rates for reactions involving very large polyatomic molecules is beyond the current computational capabilities of the electronic structure methods even with the use of empirical corrections. However, the kinetics of these systems can still be addressed using approximate methods for estimating kinetic parameters based on bond additivity and group additivity relationships. This type of approach requires the development of a database of information about substituent effects on kinetic parameters. As a first step in this direction, a systematic study was carried out for hydrogen attack on simple nitro containing compounds. Three different reaction paths were considered and the results show that the rates for one of them are relatively insensitive to substituent effects, whereas the rates for the other two change by several orders of magnitude upon interchange of substituents.

Qualitative information about substituent effects is in itself valuable; however, to be of practical use for providing reliable estimates of kinetic parameters for large polyatomic systems, methods of quantifying this type of information are needed. Benson's[6] thermochemical kinetic analysis of chemical reactions provides such a quantification scheme. Rates are based upon activation parameters (the enthalpy and entropy of activation) which are obtained from structural properties of the saddle point. These can often be reliably estimated using bond or group additivity relationships. The main deficiency in this approach is that it neglects important variational and quantum tunneling effects. A new approach to thermochemical kinetic analysis has been presented in this report which shows the great importance of these effects and provides a prescription for

including them in the analysis. The results reported here are the beginning of a new database of kinetic parameters which includes all the important dynamical effects needed for accurate calculations of the rates. Calculations of activation parameters for smaller systems using the semiempirical methods validated in this report will be used to build up this database to allow treatment of systems involving very large polyatomic molecules.

5. Acknowledgements

This research was sponsored by SDIO/IST and managed by the Office of Naval Research under contract number N00014-87-C-0746. The assistance of the ONR scientific officer, Dr. Richard Miller, is greatfully acknowledged. The authors have also benefited greatly from collaboration with Dr. Carl Melius and Dr. Michael Koszykowski at Sandia National Laboratories, Livermore, California (SNLL). In addition, computer time was made available on the SNLL Cray 1s at no expense to this program. The expertise of Dr. Byron Lengsfield made possible the MCSCF calculations on the HONO rearrangement. The computer facilities for the MCSCF calculations were made available through the U.S. Army Ballistics Research Laboratory, Aberdeen Proving Ground, Maryland.

References

1. Eaton and Cole, J. Am. Chem. Soc. **86**, 3157 (1964).
2. R. A. Fifer and J. A. Lannon, Comb. and Flame **24**, 369 (1975); R. A. Fifer, Proc. Tenth International Shock Tube Symposium, Shock Tube Research Society, Japan, 1975, p. 613; R. A. Fifer, 17th Symposium (International) on Combustion, The Combustion Institute, 1979, p. 587; R. A. Fifer and H. E. Holmes, 16th JANNAF Combustion Meeting, CPIA Pub. 308, 1979, Vol. II, p. 35; C. U. Morgan and R. A. Beyer, 15th JANNAF Combustion Meeting, CPIA Pub. 297, 1979, Vol I, p. 359.
3. C. F. Melius, Proceedings of the 24th JANNAF Combustion Meeting, Monterey, CA, Oct. 1977.
4. Review of variational transition state theory include D. G. Truhlar and B. C. Garrett, Acct. Chem. Res. **13**, 440 (1980); R. B. Walker and J. C. Light, Ann. Rev. Phys. Chem. **31**, 401 (1980); P. Pechukas, Ann. Rev. Phys. Chem. **32**, 159 (1981); D. G. Truhlar, A. D. Isaacson, R. T. Skodje, and B. C. Garrett, J. Phys. Chem. **86**82252 (1982); **87**, 4554(E) (1983); D. G. Truhlar, W. L. Hase, and J. T. Hynes, J. Phys. Chem. **87**, 2664 (1983); D. G. Truhlar and B. C. Garrett, Ann. Rev. Phys. Chem. **35**, 159 (1984); D. G. Truhlar, A. D. Isaacson, and B. C. Garrett in *The Theory of Chemical Reaction Rates* , edited by M. Baer (CRC Press, Boca Raton, FL, 1985), Vol IV, p. 65.
5. C. F. Melius and J. S. Binkley, Paper WSS/CI 83-16, 1983 Fall Meeting of the Western States Section of the Combustion Institute, University of California, Los Angeles, Oct. 17-18 (1983); C. F. Melius and J. S. Binkley, in *The Chemistry of Combustion Processes* , edited by T. M. Sloane (American Chemical Society, Washington, D.C., 1984), ACS Symp. Ser. No. **249**, 103; C. F. Melius and J. S. Binkley, Symp. (Int.) Comb. [Proc.] **20**, 575 (1985); R. A. Perry and C. F. Melius, Symp. (Int.) Comb. [Proc.] **20**, 639 (1985); P. Ho, M. E. Coltrin, J. S. Binkley, and C. F. Melius, J. Phys. Chem. **89**, 4647 (1985); **90**, 3399 (1986).
6. S. W. Benson, *Thermochemical Kinetics* (Wiley, New York, 1976).

7. S. Glasstone, K.J. Laidler, and H. Eyring, *Theory of Rate Processes*, (McGraw-Hill, New York, 1941); H.S. Johnston, *Gas Phase Reaction Rate Theory*, (Ronald Press, New York, 1966); D.L. Bunker, *Theory of Gas Phase Reaction Rates*, (Pergamon Press, Oxford, 1966); K.J. Laidler, *Theories of Chemical Reaction Rates*, (McGraw-Hill, New York, 1969).

8. B. C. Garrett and D. G. Truhlar, J. Chem. Phys. **70**, 1593 (1979); J. Phys. Chem. **83**, 1052, 3058(E) , 1079 (1979); **84**, 682(E), 805 (1980).

9. B. C. Garrett and D. G. Truhlar, J. Phys. Chem. **83**, 1915, 2921 (1979); J. Chem. Phys. **72**, 3460 (1980).

10. D. G. Truhlar and B. C. Garrett, Proc. Nat'l. Acad. Sci. USA **76**, 4755 (1979).

11. B. C. Garrett and D. G. Truhlar, J. Chem. Phys. **72**, 3450 (1980).

12. B. C. Garrett, D. G. Truhlar, R. S. Grev, and A. W. Magnuson, J. Phys. Chem. **84**, 1730 (1980); **87**, 4554(E) (1983).

13. B. C. Garrett, D. G. Truhlar, R. S. Grev, and R. B. Walker, J. Chem. Phys. **73**, 235 (1980); B. C. Garrett, D. G. Truhlar, R. S. Grev, A. W. Magnuson, and J. N. L. Connor, J. Chem. Phys. **73**, 1721 (1980); B. C. Garrett, D. G. Truhlar, R. S. Grev, G. C. Schatz, and R. B. Walker, J. Phys. Chem. **85**, 3806 (1981); D. K. Bondi, D. C. Clary, J. N. L. Connor, B. C. Garrett, and D. G. Truhlar, J. Chem. Phys. **76**, 4986 (1982); D. C. Clary, B. C. Garrett, and D. G. Truhlar, J. Chem. Phys. **78**, 777 (1983); B. C. Garrett, D. G. Truhlar, A. F. Wagner, and T. H. Dunning, J. Chem. Phys. **78**, 4400 (1983); D. K. Bondi, J. N. L. Connor, B. C. Garrett, and D. G. Truhlar, J. Chem. Phys. **78**, 5981 (1983); B. C. Garrett and D. G. Truhlar, J. Chem. Phys. **79**, 4931 (1983); **81**, 309 (1984); D. G. Truhlar, B. C. Garrett, P. G. Hipes, and A. Kuppermann, J. Chem. Phys. **81**, 3542 (1984); B. C. Garrett, N. Abusalbi, D. J. Kouri, and D. G. Truhlar, J. Chem. Phys. **83**, 2252 (1985); B. C. Garrett, D. G. Truhlar, and G. C. Schatz, J. Am. Chem. Soc. **108**, 2876 (1986).

14. D. G. Truhlar, K. Runge, and B. C. Garrett, in Symp. (Int.) Comb. [Proc.] **20**, 585 (1984); B. C. Garrett and D. G. Truhlar, Int. J. Quantum Chem. **21**, 17 (1987).

15. B. C. Garrett, D. G. Truhlar, J. M. Bowman, A. F. Wagner, D. Robie, S. Arepathi, N. Presser, and R. J. Gordon, J. Am. Chem. Soc. **108**, 3515 (1986).

16. A. D. Isaacson and D. G. Truhlar, J. Chem. Phys. **76**, 1380 (1982); D. G. Truhlar, A. D. Isaacson, R. T. Skodje and B. C. Garrett, J. Chem. Phys. **77**, 3516 (1982); A. D. Isaacson, M. T. Sund, S. N. Rai, and D. G. Truhlar, J. Chem. Phys. **82**, 1338 (1985); B. C. Garrett, M. J. Redmon, R. Steckler, D. G. Truhlar, M. S. Gordon, K. K. Baldridge, and D. Bartol, J. Phys. Chem. **92**, 0000 (1988).

17. A. D. Isaacson, D. G. Truhlar, S. N. Rai, R. Steckler, G. C. Hancock, B. C. Garrett, and M. J. Redmon, Computer Phys. Comm. **47**, 91 (1987).

18. E. Wigner, Z. Phys. Chem. B **19**, 203 (1932).

19. R. A. Marcus, J. Chem. Phys. **45**, 4493, 4500 (1966); **46**, 959 (1967); **49**, 2610 (1968); D. G. Truhlar, J. Chem. Phys. **53**, 2041 (1970); R. T. Skodje, D. G. Truhlar, and B. C. Garrett, J. Chem. Phys. **77**, 5955 (1982).

20. R. T. Skodje, D. G. Truhlar, and B. C. Garrett, J. Phys. Chem. **85**, 3019 (1981).

21. M. Dupuis, J. Rys, and H. F. King, J. Chem. Phys. **5**, 111 (1976).; M. Dupuis and H. F. King, J. Chem. Phys. **8**, 3998 (1978); M. Dupuis, ibid. **4**, 5758 (1981); T. Takada, M. Dupuis, and H. F. King, J. Chem. Phys. **75**, 332 (1981); S. Kato and K. Morokuma, Chem. Phys. Lett. **65**, 19 (1979); J. A. Pople, R. Krishnan, H. B. Schlegel, and J. S. Binkley, Int. J. Quant. Chem. Symp. **13**, 225 (1979); R. Krishnan, H. B. Schlegel, and J. A. Pople, J. Chem. Phys. **72**, 4654 (1980); P. Pulay, in *The Force Concept in Chemistry*, edited by B. M. Deb (Van Nostrand, Princeton, 1981), p. 449; P. Pulay, J. Chem. Phys. **78**, 5043 (1983); Y. Osamua, Y. Yamaguchi, P. Saxe, M. A. Vincent, J. F. Gaw, and J. F. Scaefer, III, Chem. Phys. **72**, 131 (1982); R. N. Camp, H. F. King, J. W. McIver Jr., and D. Mullally, J. Chem. Phys. **79**, 1089 (1983); M. R. Hoffmann, D. J. Fox, J. F. Gaw, Y. Osamura, Y. Yamaguchi, R. S. Grev, G. Fitzgerald, H. F.

Schaefer III, P. J. Knowles, and N. C. Handy, J. Chem. Phys. **80**, 2660 (1984); T. J. Lee, N. C. Handy, J. E. Rice, A. C. Scheiner, and H. F. Schaefer III, J. Chem. Phys. **85**, 3930 (1986);J. F. Gaw, Y. Yamaguchi, H. F. Schaefer III, and N. C. Handy, J. Chem. Phys. **85**, 5132 (1986); M. Page, P. Saxe, G. F. Adams, and B. H. Lengsfield III, J. Chem. Phys. **81**, 434 (1984); M. Page, P. Saxe, G. F. Adams, and B. H. Lengsfield III, Chem. Phys. Lett. **104**, 587 (1984); G. Fitzgerald, R. J. Harrison, and R. J. Bartlett, J. Chem. Phys. **85**, 5143 (1986).

22. D. G. Truhlar, N. J. Kilpatrick, and B. C. Garrett, J. Chem. Phys. **78**, 2438 (1983).

23. J. C. Slater, Phys. Rev. **35**, 210 (1930), and *Quantum Theory of Matter*, (McGraw-Hill, New York, 1968); V. Fock, Z. Physik **61**, 126 (1930); D. R. Hartree, Proc. Cambridge Phil. Soc. **24**, 89 (1928), and *The Calculation of Atomic Structures*, (Wiley, New York, 1957); C. C. J. Roothan, Rev. Mod. Phys. **32**, 179 (1960).

24. P.-O. Lowdin, Adv. Chem. Phys. **2**, 207 (1959).

25. I. Shavitt, in *Methods of Electronic Structure Theory* (Modern Theoretical Chemistry, Vol. 3, ed. by H. F. Schaefer (Plenum, New York, 1977) p. 189; B. O. Roos and P. E. M. Siegbahn, *ibid.*, p. 277; R. F. Hausman, Jr. and J. Paldus, "The Unitary Group for the Evaluation of Electronic Energy Matrix Elements", (*Lecture Notes in Chemistry*, Vol. 22) ed. by J. Hinze (Springer-Verlag, New York, 1981) p. 1; I. Shavitt, *ibid.*, p. 51.

26. I. Shavitt, in *Advanced Theories and Computational Approaches to the Electronic Structure of Molecules*, C. E. Dykstra, ed. (D. Reidel, 1984) p. 185.

27. A. C. Wahl and G. Das, in *Applications of Electronic Structure Theory* (Modern Theoretical Chemistry, Vol. 3) ed. by H. F. Schaefer (Plenum, New York, (1977); "Recent Developments and Applications of Multi-Configuration Hartree-Fock Methods" (NRCC Proceedings, Vol. 10) ed. by M. Dupuis (Report LBL-12157, Lawrence Berkeley Laboratory, University of California, Berkeley, 1981); R. L. Shepard, I. Shavitt, and J. Simons, J. Chem. Phys. **76**, 543 (1982).

28. E. B. Brown, I. Shavitt, and R. Shepard, Chem. Phys. Lett. **105**, 363 (1984).

29. K. A. Breukner, Phys. Rev. **97**, 1353 (1955); *ibid.* **100**, 36 (1955); J. Goldstone, Proc. R. Soc. (London) Ser. A **239**, 267 (1957); H. P. Kelly, Adv. Chem. Phys. **14**, 129 (1969); R. J. Bartlett, Ann. Rev. Phys. Chem. **32**, 359 (1981); B. H. Brandow, Rev. Mod. Phys. **35**, 771 (1967).

30. J. A. Pople, J. S. Binkley, and R. Seeger, Int. J. Quantum Chem. Symp. **10**, 1 (1976); R. Krishnan and J. A. Pople, Int. J. Quantum Chem. **14**, 41 (1978); R. Krishnan, M. J. Frisch, and J. A. Pople, J. Chem. Phys. **72**, 4244 (1980).

31. R. J. Bartlett and I. Shavitt, Int. J. Quantum Chem. **S11**, 165 (1977).

32. W. J. Hehre, L. Random, P. v.R. Schleyer, and J. A. Pople, *Ab Initio Molecular Orbital Theory*, (Wiley and Sons, NY, 1986).

33. See, e.g., K. S. Pitzer, Quantum Chemistry (Prentice-Hall, Englewood Cliffs, NJ, 1953).

34. D. G. Truhlar and B. C. Garrett, submitted to J. Chem. Phys.

35. P. Marshall and A. Fontijn, J. Chem. Phys. **85**, 2637 (1986).

36. J. V. Michael, J. W. Sutherland, and R. B. Klemm, Int. J. Chem. Kinet. **17**, 315 (1985); J. Phys. Chem. **90**, 497 (1986).

37. W. Hack, P. Rouveirolles, and H. Gg. Wagner, J. Phys. Chem. **90**, 2505 (1986)

38. M. Demissy and R. Lesclaux, J. Am. Chem. Soc. **102**, 2897 (1980).

39. P. Marshall and A. Fontijn, J. Phys. Chem. **91**, 6297 (1987)

40. *JANAF Thermochemical Tables, Natl. Stand. Ref. Data Ser., Natl. Bur. Stand.* No. 37 (1971).

41. B. C. Garrett and D. G. Truhlar, J. Amer. Chem. Soc. **101**, 4534 (1979); B. C. Garrett, D. G. Truhlar, and R. S. Grev, in *Potential Energy Surfaces and Dynamics Calculations*, ed. by D. G. Truhlar (Plenum, New York, 1981), p. 587.

42. B. C. Garrett, D. G. Truhlar, and R. S. Grev, in *Potential Energy Surfaces and Dynamics Calculations*, edited by D. G. Truhlar (Plenum, New York, 1981), p. 587.

Appendices A.

Theoretical calculations of the thermal rate constants for the gas-phase chemical reactions $H + NH_3 \rightleftarrows H_2 + NH_2$ and $D + ND_3 \rightarrow D_2 + ND_2$

Theoretical calculations of the thermal rate constants for the gas-phase chemical reactions $H + NH_3 \rightleftarrows H_2 + NH_2$ and $D + ND_3 \rightleftarrows D_2 + ND_2$

Bruce C. Garrett

Chemical Dynamics Corporation

9560 Pennsylvania Avenue

Upper Marlboro, MD 20772

Michael L. Koszykowski and Carl F. Melius

Sandia National Laboratories

Livermore, CA 94550

Abstract. Rate constants for the title reactions are computed using variational transition state theory with semiclassical ground-state adiabatic transmission coefficients for the temperature range from 200 to 2400 K. The rates are computed from limited information about the potential energy surface along the minimum energy path as parameters of the reaction path Hamiltonian. The potential information is obtained from *ab initio* electronic structure calculations with an empirical bond additivity correction. The accuracy of this semiempirical technique for obtaining the potential information is tested by using increasingly higher quality *ab initio* electronic structure calculations before applying the bond additivity correction. For the reactions $H + NH_3 \rightleftarrows H_2 + NH_2$ and $D + ND_3 \rightarrow D_2 + ND_2$ the ultimate test is given by comparison with recent experimental results. The agreement is very good except for the very low temperature results for $H + NH_3 \rightarrow H_2 + NH_2$; the excellent agreement for the reverse reaction in the same temperature range indicates an inconsistency in these experimental results.

1. Introduction.

Hydrogen atoms abstraction reactions are ubiquitous in the combustion of hydrogen containing compounds. As an example, the gas-phase chemical reaction

$$H + NH_3 \rightarrow H_2 + NH_2 \qquad (R1)$$

is important in the thermal decomposition, pyrolysis, and combustion of ammonia. The rate of reaction (R1) has recently been measured using three different experimental techniques;[1-3] these experiments combine to yield rate data from 500 K – where the slowness of the reaction tests the limits of the sensitivity of the experimental apparatus – up to 1777 K. These experiments are in good agreement with each other in temperature regions where they overlap, but overall they disagree with older experiments[4,5] that indicated the reaction was much slower.

Compared to reaction (R1), its reverse

$$H_2 + NH_2 \rightarrow H + NH_3 \qquad (R2)$$

has been the subject of fewer direct measurements[3,6,7] although it is also important in ammonia combustion. The most recent measurement of the rate of reaction (R2) extends over the temperature range from 673 to 1003 K using a single experimental technique[3] and combined with the earlier study[6] provide reactions rates from 400 K up to 1003 K. By also studying (R1) in the same experimental apparatus, new estimates of the thermochemistry of the NH_2 radical have also been obtained. This type of information is useful in evaluating the equilibrium constant and in relating the rates of reactions (R1) and (R2) by detailed balance.

The deuterated analog of reaction (R1)

$$D + ND_3 \rightarrow D_2 + ND_2 \qquad (R3)$$

has also been studied using a single experimental technique over the temperature range from 590 to 1220 K.[8] The experimental rates of reactions (R1) and (R3) have been compared with theoretical ones based upon conventional transition state theory.[9] These calculations utilize information about the potential energy surface obtained from electronic structure calculations[1,2,8] using a bond additivity correction (the BAC-MP4 method).[10-14] The agreement of the theory and experiment indicates that the calculated barrier height of about 18 kcal/mol (or about 16 kcal/mol when

corrected for changes in zero point energy) is reasonable.[2] Curvature in the Arrhenius plot of the rate for reaction (R1) at low temperatures has been attributed to quantum mechanical tunneling, and attempts have been made to substantiate this claim using simple tunneling models.

The recent experimental work on the reactions (R1)-(R3) provides an excellent testing ground for theoretical methods for predicting gas-phase reaction rates since all three reactions involve the same potential energy surface. One of the purposes of the present paper is to provide a more rigorous treatment of the dynamics controlling rates of reactions (R1) and (R3) and to also provide the first theoretical estimates of the rate for reaction (R2) and predictions for its deuterated analog

$$D_2 + ND_2 \rightarrow D + ND_3 \qquad \text{(R4)}$$

Previous calculations on the reaction (R1) and (R3) employed conventional transition state theory in which the dynamical bottleneck is assumed to occur at the saddle point for the reaction. As will be shown later, because of the nature of the electronic structure information about the potential energy surface utilized in these calculations, the use of conventional transition state theory leads to inconsistencies in the treatment; but by basing the calculations upon variational transition state theory[15-22] these inconsistencies are no longer a problem. Another advantage of using variational transition state theory is that it allows for a consistent treatment of quantum tunneling effects which are important at low temperatures. A second goal of this work is to reexamine the importance of quantum mechanical tunneling in these reactions utilizing consistent semiclassical adiabatic transmission coefficients and extending the rate data to lower temperatures.

Compared to other dynamical methods for obtaining reaction rates, variational transition state theory has the practical advantage of not requiring a global representation of the potential energy surface. From knowledge of the potential in a region around the minimum energy path connecting reactants to products, accurate estimates of the reaction rate can be made. This type of potential information can be directly obtained from modern electronic structure methods as the

energy and derivatives of the energy. Previous conventional transition state theory calculations of the rates for reactions (R1) and (R2) have utilized potential information obtained by the BAC-MP4 method.[10-14] One of the most important purposes of this paper is to critically evaluate the method used to obtain this potential energy surface information.

2. Theory

2.1. Variational transition state theory

Variational transition state theory with semiclassical transmission coefficients have been extensively review in the literature.[15-22] In the present work we briefly review the method with an emphasis on the potential energy surface information needed for the calculations.

Conventional transition state theory[9] reduces the calculation of the rate constant to one of quasiequilibrium statistical mechanics; the equilibrium rate is approximated as the equilibrium flux headed towards reactants through a dividing surface located at the saddle point. With this approximation, the rate constant $k^{\ddagger}(T)$ for temperature T takes on the simple familiar form

$$k^{\ddagger}(T) = \frac{k_B T}{h} \frac{Q^{\ddagger}(T)}{\Phi^R(T)} \exp\left(V^{\ddagger} / k_B T \right) \qquad (1)$$

where k_B is Boltzmann's constant, h is Planck's constant, $Q^{\ddagger}(T)$ is the partition function for the bound degrees of freedom at the saddle point, $\Phi^R(T)$ is the reactants partition function, and $V^{\ddagger}$ is the value of the potential at the saddle point. Thus conventional transition state theory requires information about the potential energy surface only in the saddle point and reactant regions. If the partition functions are computed using a harmonic approximation then the matrix of second derivatives (the Hessian matrix) suffices.

In variational transition state theory the dividing surface is viewed as a tentative dynamical bottleneck to flux, and the best bottleneck (the dividing surface allowing the least flow of flux) is

located by a variational procedure. The generalized expression for the thermal rate constant is given as a function of the location s of the dynamical bottleneck along the reaction coordinate

$$k^{GT}(T, s) = \frac{k_B T}{h} \frac{Q^{GT}(T, s)}{\Phi^R(T)} \exp\left(V_{MEP}(s) / k_B T \right) \tag{2}$$

where $Q^{GT}(T,s)$ is the generalized partition function for the bound degrees of freedom orthogonal to the reaction path at s, and $V_{MEP}(s)$ is the value of the potential along the reaction path at s. One version of variational transition state theory, the canonical variational theory (CVT),[23] results from minimizing eq. (2) with respect to s

$$k^{CVT}(T) = \min_s k^{GT}(T, s) \tag{3}$$

The improved canonical variational theory (ICVT)[24] also variationally optimizes the location of the transition state dividing surface for a given temperature, but provides an improved treatment of threshold energies by using an ensemble which removes energies below the ground-state adiabatic threshold. To compute the rate constant using either the canonical or improved canonical variational theory more information about the potential energy surface is required than for a conventional transition state theory calculation; information about the potential in a region around the reaction path is required.

The reaction path is defined as the minimum energy path connecting the saddle point with both the reactant and product regions. The minimum energy path is located by following the path of steepest decents in both directions from the saddle point in a mass weighted coordinate system such that each degree of freedom has the same effective mass in the kinetic energy expression. The first step from the saddle point is taken along the eigenvector of the negative eigenvalue of the Hessian, and subsequent steps are taken in the direction of the negative of the gradient (the first derivative of the energy). For a harmonic treatment of the partition functions, the matrix of second

derivatives along the minimum energy path will suffice. In this case the potential information needed is the energy and its first and second derivatives along the minimum energy path.

In the above expressions for the rate constant the bound degrees of freedom are treated quantum mechanically (i.e., the partition functions are evaluated quantum mechanically) but the motion along the reaction coordinate (the degree of freedom corresponding to the negative eigenvalue of the Hessian at the saddle point) is treated classically. Quantum mechanical effects on the reaction coordinate motion (e.g., quantum mechanical tunneling) is included by a multiplicative factor – the transmission coefficient. The Wigner correction factor[25] has been very popular for estimating quantum mechanical tunneling effects because it requires knowledge of the shape of the classical barrier near the saddle point; this type of information can be obtained from the negative eigenvalue of the Hessian at the saddle point. Unfortunately, the approximations of this method are rarely valid for chemical reactions, i.e., when tunneling is important it occurs over distances much longer than that represented by a quadratic representation of the potential near the saddle point, and a more global description of tunneling is required.

A consistent route to including *quantum* mechanical effects on reaction coordinate motion is provided by the vibrationally and rotationally adiabatic theory of reactions.[26-28] When reaction coordinate motion is treated classically one form of variational transition state theory – the microcanonical variational theory – yields an expression for the thermal rate constant which is equivalent to that obtained from the adiabatic theory of reactions.[23,28] Thus it is consistent within variational transition state theory to treat tunneling as occurring through the one-mathematical-dimensional vibrationally-rotationally adiabatic potential

$$V_a(s,\alpha) = V_{MEP}(s) + \varepsilon_\alpha^{GT}(s) \tag{5}$$

where α is a collective index of the quantum numbers for the bound modes and $\varepsilon_\alpha^{GT}(s)$ is the generalized transition state level for state α at the generalized transition state located at s along the reaction path.

For thermal rate constants the tunneling is approximated using only the ground state adiabatic potential curve (α=0) which is denoted $V^A(s)$. The adiabatic approximation is made in a curvilinear coordinate system, and, although the potential term is very simple, the kinetic energy term is complicated by factors dependent upon the curvature of the reaction path. For systems in which the curvature of the reaction path is not too severe, the small-curvature semiclassical adiabatic ground state (SCSAG) method[30] includes the effect of the reaction-path curvature to induce the tunneling path to 'cut the corner' and shorten the tunneling length. Combining the SCSAG transmission coefficient with the improved canonical variational theory rate constant yields

$$k^{ICVT/SCSAG}(T) = \kappa^{SCSAG}(T)\, k^{ICVT}(T) \qquad (4)$$

To construct the adiabatic potential, the type of potential information required is identical to that needed for the variational transition state theory calculation. For the SCSAG calculation it is also necessary to know the curvature of the reaction path which can be obtained from the first and second derivatives of the potential along the reaction path. Thus, to provide a consistent and accurate estimate of the tunneling, no new information about the potential energy surface is required.

The information about the potential energy surface is used in the POLYRATE program in the form of parameters of the reaction path Hamiltonian[31] at a set of points along the reaction path. Because of the expense of the electronic structure calculations the information about the potential is often limited, and the parameters of the reaction path Hamiltonian are interpolated from a sparse grid and can be extrapolated out to the asymptotic reactant and product regions.[15,32]

2.1. Quantum chemistry

Despite the developments in quantum chemistry in the past decade, it remains a challenge to calculated accurate potential energy surfaces useful for determining rates of activated chemical reactions. This is largely due to the fact that small changes in the barrier height translate into large

changes in the reaction rate (e.g., a change of only 0.5 kcal/mol at room temperature leads to a change in the rate of over a factor of two). Currently, *ab initio* calculations of energetics to within chemical accuracy is affordable only for relatively small systems. Even so, progress has been made in developing methods for determining reaction energetics, but these have relied on empirical corrections to *ab initio* calculations.

The concept of a molecule as a collection of individual bonds between atoms is central to the chemist's view of molecular structure and its rearrangement during reactions. The order of a bond (e.g., single bonds between monovalent atoms, double bonds between divalent atoms, etc.) has been used in establishing empirical rules relating bond order to bond lengths[33] and bond strengths.[34] The empirical knowledge that the dissociation energy for a given bond with a given bond order is, in general, roughly the same in different molecules has lead to the chemist's intuition that bond strengths are approximately additive. This concept of bond additivity has been successfully applied to obtaining estimates of the thermochemistry of stable species.[35] Within the last several years, this concept has been used in a more quantitative approach (the BAC-MP4 method) in which corrections are made to *ab initio* calculations.[10-14] The BAC-MP4 method has been successfully applied to predicting the thermochemistry of a wide variety of stable species and transient radical species that occur in combustion environments. More recently, the method has been extended to the calculation of the energetics of transition states for chemical reactions.[1,8,36]

Inherent in the BAC-MP4 method is the assumption that geometries and frequencies can be obtained to a good approximation from a Hartree-Fock calculation using a moderate sized basis. Therefore, a BAC-MP4 calculation begins with a Hartree-Fock (HF) optimization to the equilibrium or transition state geometry (i.e., locating the geometry at which the gradient vanishes) with a contracted atomic orbital basis which for the present application is denoted 6-31G*.[37] The Hessian matrix is also computed at the HF level using the same basis. The absolute energy for a given geometry is much harder to accurately compute and requires including a large percentage of the electron correlation energy. As a first step in this direction, at the optimized HF geometry, the energy is computed by full fourth-order Moller-Plesset perturbation theory[38,39] (MP4-SDTQ),

including the effects of all single, double, triple, and quadruple excitations in the contracted atomic orbital basis denoted 6-31G**.[37] Although the MP4 method does include a large fraction of the electron correlation energy, there are still errors due to basis set and higher order correlation effects, so the bond additivity correction (BAC) is applied.

The BAC correction is given as the sum of contributions over all bonds in the molecule

$$E_{BAC} = \sum_i \left(\Delta_f H^0_{0i} - E_i^{MP4} \right) - \sum_i \sum_{j<i} A_{ij} \exp\left(- \alpha_{ij} R_{ij} \right) \prod_{k \neq i,j} f_{ijk} \qquad (6)$$

where $\Delta H^{(}_{0i}$ is experimental atomic heat of formation of atom i, E_i^{MP4} is the atomic energy computed at the MP4 level for atom i, A_{ij} and α_{ij} are parameters determining the strength and range of the correction, R_{ij} is the length of the bond between atoms i and j, and the terms f_{ijk} damp out the bond additivity correction when atom k is bonded to either atom i or j. This damping factor takes the form

$$f_{ijk} = \left\{ 1 - F_j F_k \exp\left[- 2\alpha_{ik} \left(R_{ik} - R_0 \right) \right] \right\} \left\{ 1 - F_i F_k \exp\left[- 2\alpha_{jk} \left(R_{jk} - R_0 \right) \right] \right\} \qquad (7)$$

where the parameters F_i are dependent only on the type of atom i. A bond is assumed to be formed between atoms i and j if the bond length is less than some cutoff value

$$R_{ij} \leq 1.3 \left(R_i^{at} + R_j^{at} \right) \qquad (8)$$

where the parameter R_i^{at} is a measure of the atomic radius of atom i.

The parameters of the BAC-MP4 method are fitted to a database of experimental heats of formation of atomic and molecular species in a least squares sense. First the parameters ΔE_i are fitted to reproduce atomic heats of formation, then the parameters A_{ij}, α_{ij}, and F_i are fitted to

reproduce diatomic and polyatomic heats of formation. Because the parameters are fitted to heats of formation of molecular species, the BAC contains corrections to the zero point vibrational energy of the molecules as well as to the absolute energies. The values of the parameters of the BAC are therefore dependent upon the fact that the geometry and Hessian matrix are computed at the HF level as well as the fact that the absolute energies are computed by the MP4 method. In addition, the values of the parameters also depend on the nature of the basis sets used in the *ab initio* calculations, but we do not study basis set behavior in the present work. In the present paper we denote this method HF/BAC-MP4 to distinguish it from other possibilities described below. The parameters for the HF/BAC-MP4 method used in this study are presented in Table I.

Using the HF/BAC-MP4 method, the saddle point for the reaction is located at the HF level but the energy at the saddle point is determined by a MP4 calculation followed by a BAC correction. Therefore, although the gradient and Hessian matrix correspond to the saddle point (i.e., the gradient vanishes and the Hessian has one negative eigenvalue) the energy along the minimum energy path is not necessarily at its maximum at the saddle point. This inconsistency of the potential information makes the use of conventional transition state theory questionable since it is based on a knowledge of the potential energy surface only near the saddle point, and the potential energy can increase appreciably upon moving off of the saddle point along the minimum energy path . The variational transition state theory utilizes information all along the minimum energy path and the saddle point is not singled out as a special location. The variations of both the potential and the frequencies of the bound modes normal to the reaction path are included in the VTST calculation and the fact that the gradient vector vanishes at one location along the minimum path is of no practical consequence in the calculations.

The HF/BAC-MP4 method provides a practical method for obtaining information about the potential and variational transition state theory provides for a consistent use of this information in calculating a rate constant. After the saddle point is located at the HF level, the minimum energy path is located by following the path of steepest decents into the reactant and product regions. The gradient vector and Hessian matrix are computed at the HF level using the 6-31G* basis and these

are used in determining the minimum energy path. At each geometry along the minimum energy path the energy is obtained by a MP4-SDTQ calculation using the 6-31G** basis followed by the BAC correction. To insure that the BAC correction is a continuous function of the reaction coordinate, the BAC correction is always computed for bonds which are being broken and made in the course of the reaction and the criteria given in eq. (8) is not used for these special 'bonds'..

A major concern in using the HF/BAC-MP4 method is the accuracy of the computed potential energy surface information. One test of this is the comparison of computed rates with experimental ones. Tests of this nature can sometimes be inconclusive because cancellations of errors can lead to fortuitous agreement. Another test is to improve the quality in the underlying *ab initio* calculation to decrease the magnitude of the empirical bond additivity correction and test the effect on the computed rate constant. As a first step in this direction, we have reevaluated the potential information using the MP2/BAC-MP4 method. In this method the geometry of the equilibrium structure or transition state is determined using a full second-order Møller-Plesset perturbation theory (MP2-SD) calculation including the effects of all single and double excitations in the contracted atomic orbital basis denoted 6-31G*. The matrix of second derivatives is also calculated at the MP2 level at the same geometry. The minimum energy path is located by following the path of steepest descents using the gradient vectors and Hessian matrices computed at the MP2 level. For each point along the minimum energy, the energy is computed by the MP4-SDTQ method using the 6-31G** basis followed by a BAC calculation. Because the geometries and vibrational frequencies are different at the HF and MP2 levels, the BAC correction is also different . The parameters are refitted to experimental heats of formation as in the HF/BAC-MP4 method and the parameters used in the MP2/BAC-MP4 calculations are shown in Table I.

2.3. Anharmonicity

In a variational transition state theory calculation based upon a global potential energy surface the effects of anharmonicity in the potential energy surface are included using the independent-normal-mode approximation by including the principal anharmonicities in each mode.

When the potential energy surface information is included as parameters of the reaction path Hamiltonian, anharmonic effects can still be incorporated by including third and fourth derivatives of the potential along the independent normal modes. The effects of anharmonicity are important and must be included to obtain accurate estimates of the rate constants.

The bond additivity correction is based upon information about the potential energy surface only through quadratic terms but is designed to fit the experimental heats of formation of bound molecules which include the effects of anharmonicity. Therefore, the BAC method has anharmonic effects built into it in an averaged sense, not on a mode-by-mode basis. The harmonic frequencies computed at the HF level are known to be systematically high and the BAC method corrects for this discrepancy as well as including the effects of anharmonicity. Anharmonic effects are most important for lowest frequency modes and for the reactions studied here the lowest frequency mode of the reaction complex is a bound vibrational motion in the interaction region but becomes a hindered rotor in the asymptotic regions. Previous calculations on this system[1] have found that at the HF saddle point the hindered rotor partition function and harmonic oscillator partition function differ by only 15%. This is encouraging for computing the canonical variational theory rate constants for which the dynamical bottleneck is located near the HF saddle point where the harmonic approximation is expected to be valid. However, the calculated tunneling correction factor will be subject to greater uncertainties for lower temperature where contributions to the tunneling factor come from lower energies which sample a more extensive range of the reaction coordinate. In the present study, all modes are treated within the harmonic approximation with anharmonic effects entering through the BAC. Limits on the range of the tunneling at different temperatures will be reported as a guide to the accuracy of the tunneling corrections.

3. Computational details

Several algorithms for determining the minimum energy path have been tested[39] and one of the most efficient methods when numerical accuracy of about 1% is required is the lowest order Euler one-step algorithm. This method uses only the information about the gradient at the current

geometry to predict the next geometry along the minimum energy path. In the present study the minimum energy path was located using a gradient following algorithm suggested by Page and McIver[40] which utilizes both the gradient vector and Hessian matrix in determining the new geometry along the reaction path. The initial step from the saddle point was taken along the eigenvector of the negative eigenvalue of the Hessian matrix. Tests were preformed of the convergence of the ICVT/SCSAG rate constant with respect to the step size taken in the gradient following algorithm and the step size at which the the energy and derivative information was stored for use in interpolation of the parameters of the reaction path Hamiltonian. Since the Hessian matrix is used in the gradient following algorithm, the two step sizes are the same. Decreasing the step size from 0.10 to 0.05 a_0 was found to change the computed rates at 300 K by less than 20% and a step size of 0.05 a_0 is used in this work.

The tunneling correction factor computed using the SCSAG method is sensitive to the extent of the reaction path. Extending the reaction path to 0.8 a_0 towards the H + NH_3 asymptote and 1.2 a_0 towards the H_2 + NH_2 asymptote was sufficient to converge the computed rates to within 10% at 300 K and about 25% at 200 K. For the D + ND_3 reactions and its reverse (R4), the reaction path was extended out to 0.36 a_0 towards the D + ND_3 asymptote and 0.88 a_0 towards the D_2 + ND_2 asymptote. This was sufficient to converge the ICVT/SCSAG rate to better than 15% at 300 K but uncertainty of about 50% in the 200 K rate remains.

4. Results and discussion

4.1. Thermochemistry of the reactants and products

As a guideline to the type of accuracy expected from the HF/BAC-MP4 method in computing thermochemical data for bound molecular species a comparison is presented of experimental[41] and computed heats of formation and free energy of formation of the reactant and product species of the reactions studied here. Note that by definition the heat of formation and free

energy of formation of H_2 and D_2 are zero at all temperatures. The thermochemical data for the remaining species are shown in Tables II.

The BAC-MP4 results are in excellent agreement with the JANAF tables for all species except NH_2 and ND_2. For NH_2 and ND_2 the results agree well at lower temperatures but the BAC-MP4 free energies of formation systematically underestimate those from the JANAF tables at higher temperatures. The room temperature heat of formation of NH_2 as reported in the JANAF tables is in good agreement with recent experimental results of Gibson *et. al.*[42] (45.8±0.3 kcal/mol) and Hack *et. al.*[3] (45.9 kcal/mol). Based on bond additivity relationships, Benson[35] has predicted the room temperature heat of formation of NH_2 to be 46 kcal/mol and from Benson's tables, the heat of formation of NH_2 can be estimated at higher temperature to be 52 and 58 kcal/mol at 1000 and 1500 K, respectively. These are consistently higher that the JANAF tables which report 44.3 and 44.0 kcal/mol at these same temperatures. The thermochemistry of NH_2 and ND_2 above room temperature remains uncertain and the BAC-MP4 method presents a consistent procedure for obtaining reliable estimates at these temperatures.

4.2. $H + NH_3 \rightarrow H_2 + NH_2$ and $H_2 + NH_2 \rightarrow H + NH_3$ reaction rates

A comparison of the potential energy curve $V_{MEP}(s)$ and the ground-state adiabatic potential curves $V^A(s)$ for the HF/BAC-MP4 and MP2/BAC-MP4 methods is given in Figure 1. Comparison of the rates for reaction (R1) computed by the ICVT/SCSAG method using the potential information obtained by the HF/BAC-MP4 and MP2/BAC-MP4 methods is given in Table 3 and Figure 2. The potential along the minimum energy path and the adiabatic potential curves show very similar shapes for the two methods, although the MP2/BAC-MP4 results are shifted slightly to the left. The classical barrier heights are very similar, 17.1 kcal/mol for HF/BAC-MP4 compared to 16.7 kcal/mol for MP2/BAC-MP4, and the adiabatic barriers are 15.5 and 15.7 kcal/mol above the reactant zero point energies for the HF/BAC-MP4 and MP2BAC-MP4 methods, respectively.

The rate constants computed using this potential information agree well for temperatures above 300 K. At 300 K and below tunneling is very important and the rates are sensitive to finer details of the adiabatic potential curves. At 300 K, the rates computed using the two sets of potential information differ by only 50% but at 200 K the difference increases to a factor of 3.1. These results are very encouraging for obtaining accurate rates for a modest computing effort at all temperatures except those where very deep tunneling is important.

In Table 4 a comparison is made between the different dynamical methods of computing the rate constants for reaction (R1) using the potential information obtained by the HF/BAC-MP4 method. The results of conventional transition state theory (denoted TST) and the improved canonical variational theory (ICVT) neglect quantum mechanical tunneling effects whereas the improved canonical variational theory with small-curvature semiclassical adiabatic ground-state transmission coefficient (ICVT/SCSAG) includes tunneling within the vibrationally and rotationally adiabatic approximation. As described earlier, the HF/BAC-MP4 energy along the minimum energy path is not a maximum at the HF saddle point; therefore, it is not surprising that the ICVT results are much smaller than the TST ones. At 1000 K the TST results are higher by about 70% and at 300 K they are higher by about a factor of 5.5. Tunneling is very important for this reaction contributing 99.86%, 91.3%, 47.2% and 25.6% to the thermal reaction rate at 200, 300, 600, and 1000 K, respectively, by the SCSAG method. A large enhancement in the rate is observed when tunneling is included - the ICVT/SCSAG rates are larger than the ICVT ones by factors of 44.5, 7.7, 2.4, and 1.4 at 300, 400, 600, and 1000 K, respectively.

The reaction rates computed by the the ICVT/SCSAG method with the HF/MP4-BAC potential information for reaction (R1) are compared with the experimental reaction rates[1-3] in Figure 3. The overall agreement is very good except at the lowest temperatures which is discussed in more detail below. Arrhenius fits to the experimental results give activation energies of 16.0±0.2 kcal/mol for the temperature range from 908 to 1777 K,[1] 17.2±0.8 kcal/mol for the temperature range from 500 to 1140 K,[2] and 14.6±1.0 kcal/mol for the temperature range from 673 to 1003 K.[3] Activation energies derived from the computed rates show an interesting behavior

of initially increasing with increasing temperature but turning around and decreasing at even higher temperature; e.g., the computed activation energies are 12.9, 14.7, 17.1, and 14.7 kcal/mol over the temperature ranges 400-600 K, 600-1000 K, 1000-1500 K, and 1500-2400 K respectively. In general the agreement between the experimental and computed activation energies is excellent; however, he theoretical results systematically underestimate the experimental reaction rate indicating a systematic overestimate in the free energy of activation. The underestimation of the rate may be attributed to a barrier height which is too large; however, lowering just the barrier will tend to decrease the activation energy which is inconsistent with the experiments. Another possibility is that the energetics are approximately correct (i.e., the ground-state adiabatic barrier is about right) and that the entropic factors controlled by the higher lying vibrational levels are not accurately described.

The theoretical rate constants fall within the experimental error bars of Marshall and Fontijn[2] for all temperatures above 660 K. Below this temperature the experimental results show much more curvature in the Arrhenius plot than the theoretical rates and at 500 K the experimental rates are higher than the theoretical ones by about a factor of 4. Such curvature in the Arrhenius plot is often attributed to quantum mechanical tunneling, but in the present calculations the large amount of tunneling necessary to reproduce the experimental curvature is inconsistent with the excellent agreement between theory and experiment for temperatures above 660 K. For example, at 660 K the SCSAG tunneling correction factor is about 2 and gives good agreement with experiment. At 500 K the SCSAG tunneling correction factor is 3.6 but would have to be about 15 to agree with experiment. To reproduce this sharp increase in tunneling over such a small change in temperature would require a radically different shape of the adiabatic potential which is inconsistent with the reliability established in previous tests and uses of the methods.

Table 5 presents the reaction rates computed by the the ICVT/SCSAG method with the HF/MP4-BAC potential information for reaction (R2) and these are compared with the experimental ones of Hack *et. al.*[3] and Demissy and Lesclaux[6] in Figure 4. The agreement with the low temperature results of Demissy and Lesclaux is excellent (differences of 18-40%) but at

higher temperatures the computed rates are factors of 2.2 to 2.7 lower than the results of Hack *et. al.* The discrepancy at the higher temperatures can be attributed to uncertainties in the heat of formation of NH_2. At lower temperatures the computed heat of formation of NH_2 agrees well with the experimental values and we expect less uncertainty in the computed rate constant.

The rates of reaction (R2) are related to those of reaction (R1) by detailed balance. Knowledge of the equilibrium constant as a function of temperature allows calculation of rates for one of the reactions from the other. At lower temperatures the heats of formation of all four species (two reactants and two products) are accurately known, thus the equilibrium constant can be accurately computed at these temperatures. Therefore, the good agreement between the computed rates and the experimental results of Demissy and Lesclaux for reaction (R3) is inconsistent with the poorer agreement observed between theory and the experimental results of Marshall and Fontijn[2] for temperatures below 660 K. This is further evidence of the inconsistency of the low temperature experimental results for reaction (R1).

4.3. $D + ND_3 \rightarrow D_2 + ND_2$ and $D_2 + ND_2 \rightarrow D + ND_3$ reaction rates

Table 5 also presents the reaction rates computed by the ICVT/SCSAG method using the HF/BAC-MP4 potential information for reaction (R3) and (R4). These computed rates for reaction (R3) are compared with experimental one of Marshall and Fontijn[8] in Figure 5. Once again the agreement is excellent, although the theoretical results systematically underestimate the reaction rates. This underestimate is consistent with our observations for the $H + NH_3 \rightarrow H_2 + NH_2$ reaction that some feature of the potential energy surface is giving rise to a free energy of activation which is too low. Compared to reaction (R1), tunneling is less important for the deuterated reaction. For example, at 300 K, the ICVT/SCSAG transmission coefficient is 44.5 for reaction (R1) and only 8.5 for (R2), and at 600 K these decrease to 2.4 and 1.6, respectively. As for reaction (R1), the good agreement between the computed and experimental activation energy indicates that the reaction energetics are approximately correct but the entropic factors controlled by higher lying vibrational levels leads to the underestimate of the rates.

At the lower end of the experimental temperature range, 580 K, the agreement between the theoretical and experimental rates for reaction (R3) is excellent. This is in contrast to the divergence of theory and experiment for reaction (R1) in this temperature range. At 600 K, the dominant contribution to the tunneling occurs at energies about 1.1 and 0.2 kcal/mol below the adiabatic barrier maximum for reactions (R1) and (R3), respectively. At these energies the range of the adiabatic potential important in the tunneling calculations is given by the classical turning points at s=-0.35 and 0.01 for reaction (R1), and s=-0.22 and -0.07 for reaction (R3). For reaction (R1) the tunneling is deeper (at lower energies) and extends over a wider range of the adiabatic potential curve. However, the range of tunneling for both reactions at this temperature is quite short. To enhance the tunneling in reaction (R1) to match experiment would require an adiabatic potential which drop off much more precipitously. This would enhance the tunneling in reaction (R3) as well and lead to an overestimate of the rate in this temperature range. Thus, the good agreement near 580 K seen for reaction (R3) is inconsistent with the large underestimate for reaction (R1) at the same temperature.

5. Conclusions

Rate constants have been computed for the gas-phase chemical reactions $H + NH_3 \rightleftarrows H_2 + NH_2$ and $D + ND_3 \rightleftarrows D_2 + ND_2$ over the temperature range from 200 K to 2400 K. The rates are computed by variational transition state theory with semiclassical adiabatic ground-state transmission coefficients[15-22] using limited information about the potential energy surface along the reaction path. This type of information about the potential can be obtained directly from *ab initio* electronic structure calculations of the energy and its first and second derivative with respect to coordinates. In the present calculations, *ab initio* information is empirically adjusted by the BAC-MP4 method[10-14] to yield more reliable predictions of the reaction energetics.

The use of variational transition state theory in these calculations is mandated for several reasons: (1) it includes the factors most important in controlling the rate of chemical reactions and is currently the most cost effective method for obtaining reliable predictions of rates for a variety of

gas-phase reaction; (2) it is capable of utilizing limited information about the potential along the minimum energy path without requiring a global potential energy surface; (3) because of the nature of the semiempirical potential information utilized in this work, the dynamical bottleneck for the reaction does not occur at the saddle point for the reaction and a variational procedure to locate the optimum dividing surface is needed; and (4) it provides a consistent method for incorporating quantum mechanical tunneling effects which are crucial for accurate predictions of the rates, especially at temperatures below 600 K.

The BAC-MP4 method is a cost effective means of obtaining reliable information about the potential energy surface that is needed as input into the variational transition state theory calculations. With current computational capabilities, it is unpractical to calculate the necessary potential information from *ab initio* electronic structure calculations, and the use of semiempirical methods is required. The accuracy of the semiempirical potential information has been critically tested in this paper. Improving the quality of the underlying *ab initio* calculation from a Hartree-Fock (HF) calculation to a full second-order Moller-Plesset perturbation theory (MP2-SD) calculation decreased the magnitude of the empirical bond additivity correction. Comparison of the rate constants computed using the potential information from the HF/BAC-MP4 and MP2/BAC-MP4 methods showed little difference except at temperatures below 300 K where tunneling is more sensitive to details of the potential information. The good agreement obtained here is encouraging for the applicability of the more practical HF/BAC-MP4 to generate potential information for a variety of chemical reactions.

As a further tests of the methods employed here, the computed rates were compared with experiment for the reactions $H + NH_3 \rightleftarrows H_2 + NH_2$ and $D + ND_3 \rightarrow D_2 + ND_2$. For the reaction $H + NH_3 \rightarrow H_2 + NH_2$ (R1), theory and experiment are in excellent agreement for temperature from 660 K to 1770 K. For temperatures below 660 K the experimental rates become larger than the theoretical ones with differences of about a factor of 4 at 500 K. The computed reaction rates for the reaction $H_2 + NH_2 \rightarrow H + NH_3$ (R2) are in excellent agreement with experimental ones but the agreement is not as good at higher temperatures. The larger discrepancies at larger temperature

are attributed to large uncertainties in the thermochemistry of the NH_2 radical. Reaction (R2) is the reverse of (R1) and the rates are related by detailed balance; therefore, the excellent agreement between theory and experiment for the latter reaction at the lower temperatures is inconsistent with the larger discrepancies seen for the reverse reaction. (R1) in the same temperature range. The computed and experimental rates for the deuterated reaction $D + ND_3 \rightarrow D_2 + ND_2$ are in excellent agreement over the entire experimental temperature range from 590 to 1220 K. Once again, the agreement at the lower temperatures for this reaction is inconsistent with the large discrepancies observed in the same temperature range for reaction (R1).

The overall good agreement of the computed rate constants using different levels of theory for the potential information and the good agreement between the computed and experimental rate constants have given more confidence in the theoretical methods utilized here. The larger difference between theory and experiment for reaction (R1) at low temperatures indicate that the experiments should be reevaluated in this range.

6. Acknowledgements

This research was sponsored by SDIO/IST and managed by the Office of Naval Research under contract number N00014-87-C-0746.

References

1. J. V. Michael, J. W. Sutherland, and R. B. Klemm, Int. J. Chem. Kinet. **17**, 315 (1985); J. Phys. Chem. **90**, 497 (1986).
2. P. Marshall and A. Fontijn, J. Chem. Phys. **85**, 2637 (1986).
3. W. Hack, P. Rouveirolles, and H. Gg. Wagner, J. Phys. Chem. **90**, 2505 (1986)
4. D. L. Baulch, D. D. Drysdale, and D. G. Horne, *Evaluated Kinetic Data for High Temperature Reactions* (Butterworths, London, 1973), Vol. 2.
5. R. K. Hanson and S. Salimian, in *Combustion Chemistry* , edited by W. C. Gardiner, Jr. (Springer, New York, 1984), Chap. 6.
6. M. Demissy and R. Lesclaux, J. Am. Chem. Soc. **102**, 2897 (1980).
7. K. Holzrichter and H. Gg. Wagner, Symp. (Int.) Comb. [Proc.] 18th, 769 (1980).
8. P. Marshall and A. Fontijn, J. Phys. Chem. **91**, 6297 (1987)
9. S. Glasstone, K. J. Laidler, and H. Eyring, *The Theory of Rate Processes* (McGraw-Hill, New York, 1941).
10. C. F. Melius and J. S. Binkley, Paper WSS/CI 83-16, 1983 Fall Meeting of the Western States Section of the Combustion Institute, University of California, Los Angeles, Oct. 17-18, 1983.
11. C. F. Melius and J. S. Binkley, in *The Chemistry of Combustion Processes* , edited by T. M. Sloane (American Chemical Society, Washington, D.C., 1984), ACS Symp. Ser. No. **249**, 103.
12. C. F. Melius and J. S. Binkley, Symp. (Int.) Comb. [Proc.] **20**, 575 (1985).
13. R. A. Perry and C. F. Melius, Symp. (Int.) Comb. [Proc.] **20**, 639 (1985).
14. P. Ho, M. E. Coltrin, J. S. Binkley, and C. F. Melius, J. Phys. Chem. **89**, 4647 (1985); **90**, 3399 (1986).
15. A. D. Isaacson, D. G. Truhlar, S. N. Rai, R. Steckler, G. C. Hancock, B. C. Garrett, and M. J. Redmon, Computer Phys. Comm. **47**, 91 (1987).

16. D. G. Truhlar and B. C. Garrett, Acct. Chem. Res. **13**, 440 (1980)

17. R. B. Walker and J. C. Light, Ann. Rev. Phys. Chem. **31**, 401 (1980).

18. P. Pechukas, Ann. Rev. Phys. Chem. **32**, 159 (1981).

19. D. G. Truhlar, A. D. Isaacson, R. T. Skodje, and B. C. Garrett, J. Phys. Chem. **86**, 2252 (1982); **87**, 4554(E) (1983).

20. D. G. Truhlar, W. L. Hase, and J. T. Hynes, J. Phys. Chem. **87**, 2664 (1983).

21. D. G. Truhlar and B. C. Garrett, Ann. Rev. Phys. Chem. **35**, 159 (1984)

22. D. G. Truhlar, A. D. Isaacson, and B. C. Garrett in *The Theory of Chemical Reaction Rates* , edited by M. Baer (CRC Press, Boca Raton, FL, 1985), Vol IV, p. 65.

23. B. C. Garrett and D. G. Truhlar, J. Phys. Chem. **83**, 1079 (1980); **87**, 4553(E) 1983).

24. B. C. Garrett, D. G. Truhlar, R. S. Grev, and A. W. Magnuson, J. Phys. Chem. **84**, 1730 (1980); **87**, 4553(E) 1983).

25. E. Wigner, Z. Phys. Chem. B **19**, 203 (1932).

26. R. A. Marcus, J. Chem. Phys. **45**, 4493, 4500 (1966); **46**, 959 (1967); **49**, 2610 (1968).

27. D. G. Truhlar, J. Chem. Phys. **53**, 2041 (1970)

28. R. T. Skodje, D. G. Truhlar, and B. C. Garrett, J. Chem. Phys. **77**, 5955 (1982).

29. B. C. Garrett and D. G. Truhlar, J. Phys. Chem. **83**, 1052 (1980); **87**, 4553(E) 1983).

30. R. T. Skodje, D. G. Truhlar, and B. C. Garrett, J. Phys. Chem. **85**, 3019 (1981).

31. W. H. Miller, N. C. Handy, and J. E. Adams, J. Chem. Phys. **72**, 99 (1980).

32. D. G. Truhlar, N. T. Kilpatrick, and B. C. Garrett, J. Chem. Phys. **78**, 2438 (1983).

33. L. Pauling, J. Am. Chem. Soc. **69**, 542 (1947).

34. H. S. Johnston, *Gas Phase Reaction Rate Theory* (Ronald Press, New York, 1966).

35. S. W. Benson, *Thermochemical Kinetics* (Wiley, New York, 1976).

36. P. Marshall, A. Fontijn, and C. F. Melius, J. Chem. Phys. **86**, 5540 (1987).

37. R. Krishnan, J. S. Binkley, R. Seeger, and J. A. Pople, J. Chem. Phys. **72**, 650 (1980).

38. J. A. Pople, J. S. Binkley, and R. Seeger, Int. J. Quantum Chem. Symp. **10**, 1 (1976); J. A. Pople, R. Krishnan, H. B. Schlegel, and J. S. Binkley, Int. J. Quantum Chem. Symp. **14**, 545 (1978).

39. B. C. Garrett, M. J. Redmon, R. Steckler, D. G. Truhlar, K. K. Baldridge, D. Bartol, M. W. Schmidt, and M. S. Gordon, J. Phys. Chem., in press.

40. M. Page and J. W. McIver, Jr., J. Chem. Phys., in press.

41. *JANAF Thermochemical Tables, Natl. Stand. Ref. Data Ser., Natl. Bur. Stand.* No. 37 (1971).

42. S. T. Gibson, J. P. Greene, and J. Berkowitz, J. Chem. Phys. **83**, 4319 (1985).

Table 1. BAC-MP4 parameters for the H + NH_3 reaction system.

	HF/BAC-MP4	MP2/BAC-MP4
$\Delta_f H^0_{0H}$(kcal/mol)	51.63	51.63
$\Delta_f H^0_{0N}$(kcal/mol)	112.53	112.53
E^{MP4}_N(Hartree)	-0.498232	-0.498232
E^{MP4}_N(Hartree)	-54.473256	-54.473256
F_H	0.000001	0.000001
F_N	0.2174	0.2174
R^{at}_H(Å)	0.36	0.36
R^{at}_N(Å)	0.71	0.71
A_{HH}(kcal/mol)	18.98	18.92
A_{NH}(kcal/mol)	69.66	68.06
α_{HH}(Å^{-1})	2.0	2.0
α_{NH}(Å^{-1})	2.0	2.0
R_0(Å)	1.4	1.4

Table 2. Thermochemistry for reactant and product species for the reactions $NH_3 + H \rightarrow NH_2 + H_2$ and $ND_3 + D \rightarrow ND_2 + D_2$. (Energies are in kcal/mol.)

	NH_3	H	NH_2	ND_3	D	ND_2
$\Delta_f H^0$(T=0K)	-9.3[a]	51.6	46.7	-15.5	51.6	41.3
	-9.3[b]	51.6	46.2	-12.3	52.5	45.0
$\Delta_f H^0$(T=300K)	-11.0	52.1	46.2	-17.2	52.1	38.5
	-11.0	52.1	45.5	-14.0	53.0	44.3
$\Delta_f G^0$(T=300K)	-4.0	48.5	49.1	-9.4	48.4	45.0
	-3.9	48.6	47.8	-6.2	49.3	46.9
$\Delta_f G^0$(T=600K)	3.7	44.8	55.3	-1.1	44.6	52.5
	3.8	44.8	50.3	2.1	45.5	49.8
$\Delta_f G^0$(T=1000K)	14.7	39.5	65.7	10.4	39.1	64.4
	14.8	39.6	54.1	13.7	40.1	53.8
$\Delta_f G^0$(T=1500K)	28.9	32.5	80.5	24.9	32.0	81.0
	28.8	32.6	59.1	28.1	33.1	59.0

[a] Top entry is from HF/BAC-MP4 calculations

[b] Lower entry is from JANAF tables (ref. 41).

Table 3. Comparison of ICVT/SCSAG reaction rates (in units of $cm^3molecule^{-1}s^{-1}$) computed using two different sets of information about the potential energy surface.

T,K	HF/BAC-MP4	MP2/BAC-MP4
200	9.9×10^{-24}	3.2×10^{-24}
300	1.8×10^{-20}	1.2×10^{-20}
400	2.0×10^{-18}	1.6×10^{-18}
600	4.5×10^{-16}	4.0×10^{-16}
1000	6.2×10^{-14}	6.2×10^{-14}
1500	1.1×10^{-12}	1.1×10^{-12}
2400	6.9×10^{-12}	8.1×10^{-12}

Table 4. Comparison of three levels of variational transition state theory rate constants (in units of $cm^3molecule^{-1}s^{-1}$) for reaction (R1) computed using HF/BAC-MP4 potential information.

T,K	TST	ICVT	ICVT/SCSAG
200	$1.4x10^{-26}$	$1.1x10^{-27}$	$9.9x10^{-24}$
300	$2.2x10^{-21}$	$4.1x10^{-22}$	$1.8x10^{-20}$
400	$9.2x10^{-19}$	$2.6.x10^{-19}$	$2.0x10^{-18}$
600	$4.2x10^{-16}$	$1.8x10^{-16}$	$4.5x10^{-16}$
1000	$7.7x10^{-14}$	$4.6x10^{-14}$	$6.2x10^{-14}$
1500	$1.4x10^{-12}$	$9.5x10^{-13}$	$1.1x10^{-12}$
2400	$1.7x10^{-11}$	$1.0x10^{-12}$	$6.9x10^{-12}$

Table 5. ICVT/SCSAG thermal rate constants for three reactions computed using HF/BAC-MP4 potential information.

T,K	$H_2 + NH_2$	$D + ND_3$	$D_2 + ND_2$
200	5.4×10^{-20}	4.9×10^{-26}	1.6×10^{-21}
300	2.3×10^{-18}	8.2×10^{-22}	2.8×10^{-19}
400	3.6×10^{-17}	2.3×10^{-19}	7.8×10^{-18}
600	1.0×10^{-15}	1.1×10^{-16}	3.5×10^{-16}
1000	2.8×10^{-14}	2.7×10^{-14}	1.3×10^{-14}
1500	2.2×10^{-13}	6.1×10^{-13}	1.3×10^{-13}
2400	8.7×10^{-13}	8.8×10^{-12}	1.1×10^{-12}

Figure Captions

Figure 1. Comparison of potential energy along the minimum energy path [$V_{MEP}(s)$] and ground-state adiabatic potential [$V^A(s)$] as a function of reaction coordinate s computed using the HF/BAC-MP4 method (solid curves) and the MP2/BAC-MP4 method (dashed curves) for the reaction $H + NH_3 \rightarrow H_2 + NH_2$.

Figure 2. Rate constants as a function of temperature for the reaction $H + NH_3 \rightarrow H_2 + NH_2$ computed using the improved canonical variational theory with small-curvature semiclassical adiabatic ground-state transmission coefficient from potential information obtained using the HF/BAC-MP4 method (solid curves) and the MP2/BAC-MP4 method (dashed curves).

Figure 3. Comparison of computed and experimental rate constants for the reaction $H + NH_3 \rightarrow H_2 + NH_2$. The experimental results are from P. Marshall and A. Fontijn, ref. (2), denoted MF (•); the Arrhenius fit of J. V. Michael, J. W. Sutherland, and R. B. Klemm, ref. (1), denoted MSK (short dashed curve); and the Arrhenius fit of W. Hack, P. Rouveirolles, and H. Gg. Wagner, ref. (3), denoted HRW (long dashed curve). The solid line is the result of the improved canonical variational theory with small-curvature semiclassical adiabatic ground-state transmission coefficient (ICVT/SCSAG) from potential information obtained using the HF/BAC-MP4 method.

Figure 4. Comparison of computed and experimental rate constants for the reaction $H_2 + NH_2 \rightarrow H + NH_3$. The experimental results are the Arrhenius fit of W. Hack, P. Rouveirolles, and H. Gg. Wagner, ref. (3), denoted HRW (short dashed curve) and the Arrhenius fit of M. Demissy and R. Lesclaux, ref. (6), denoted DL (long dashed curve). The solid line is the result of the improved canonical variational theory with small-curvature semiclassical adiabatic ground-state transmission

coefficient (ICVT/SCSAG) from potential information obtained using the HF/BAC-MP4 method.

Figure 5. Comparison of computed and experimental rate constants for the reaction $D + ND_3 \rightarrow D_2 + ND_2$. The experimental results are from P. Marshall and A. Fontijn, ref. (8), denoted MF (•). The solid line is the result of the improved canonical variational theory with small-curvature semiclassical adiabatic ground-state transmission coefficient (ICVT/SCSAG) from potential information obtained using the HF/BAC-MP4 method.

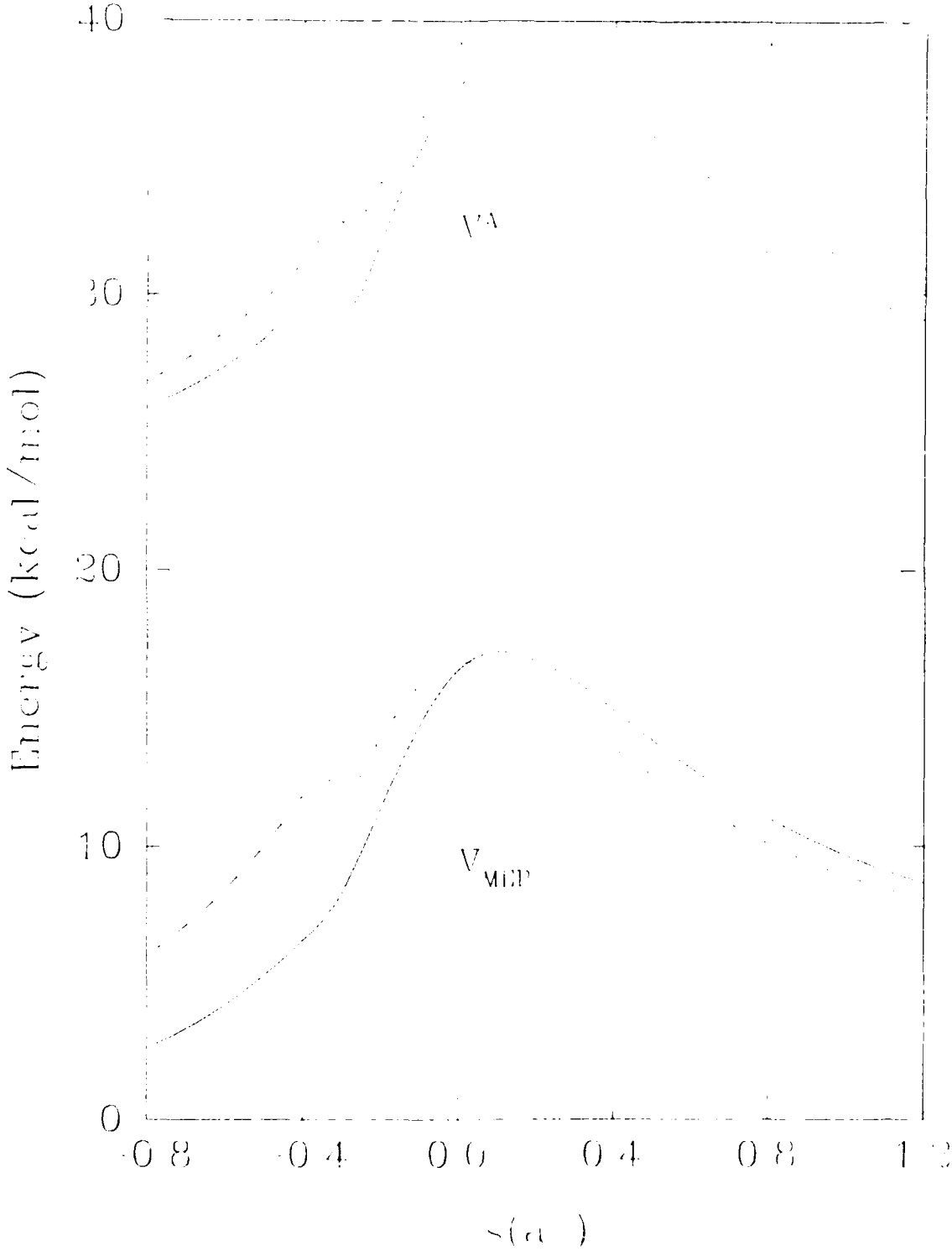
40
30
20
10
0
Energy (kcal/mol)
V_{MEP}
-0.8
-0.4
0.0
0.4
0.8

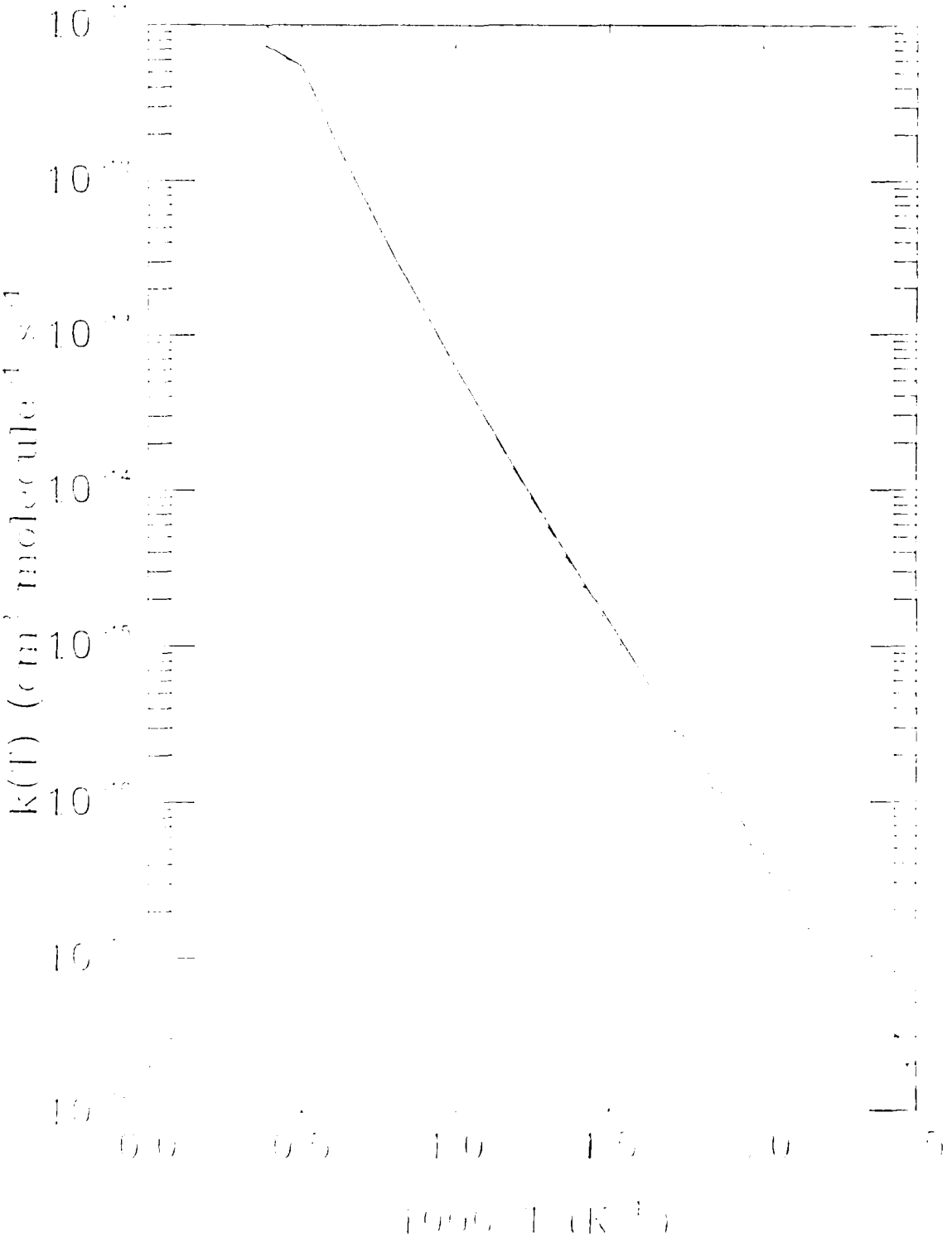
k(D) (cm³ molecule⁻¹ s⁻¹)
1000 T (K⁻¹)

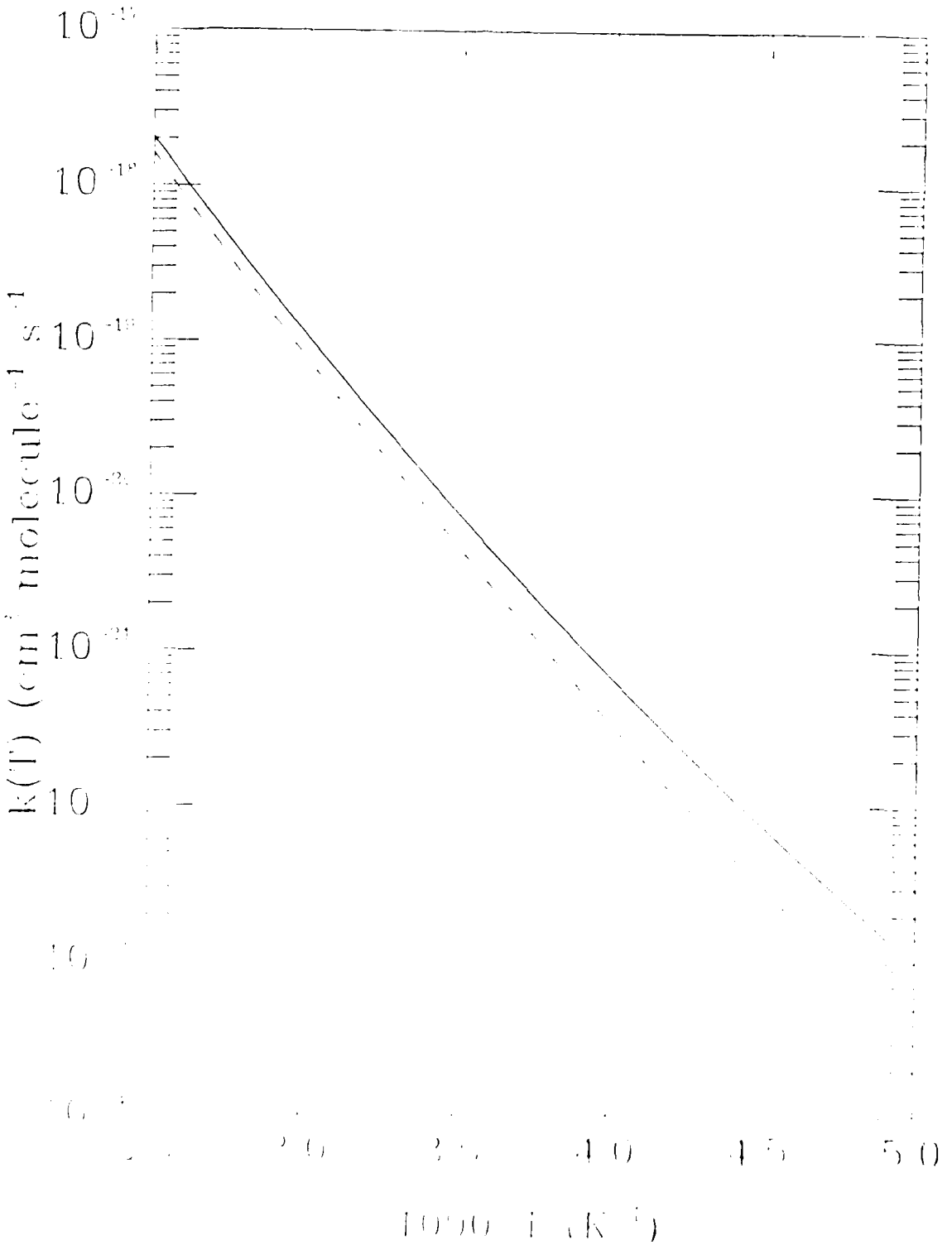
k(T) (cm³ molecule⁻¹ s⁻¹)
1000 / T (K⁻¹)

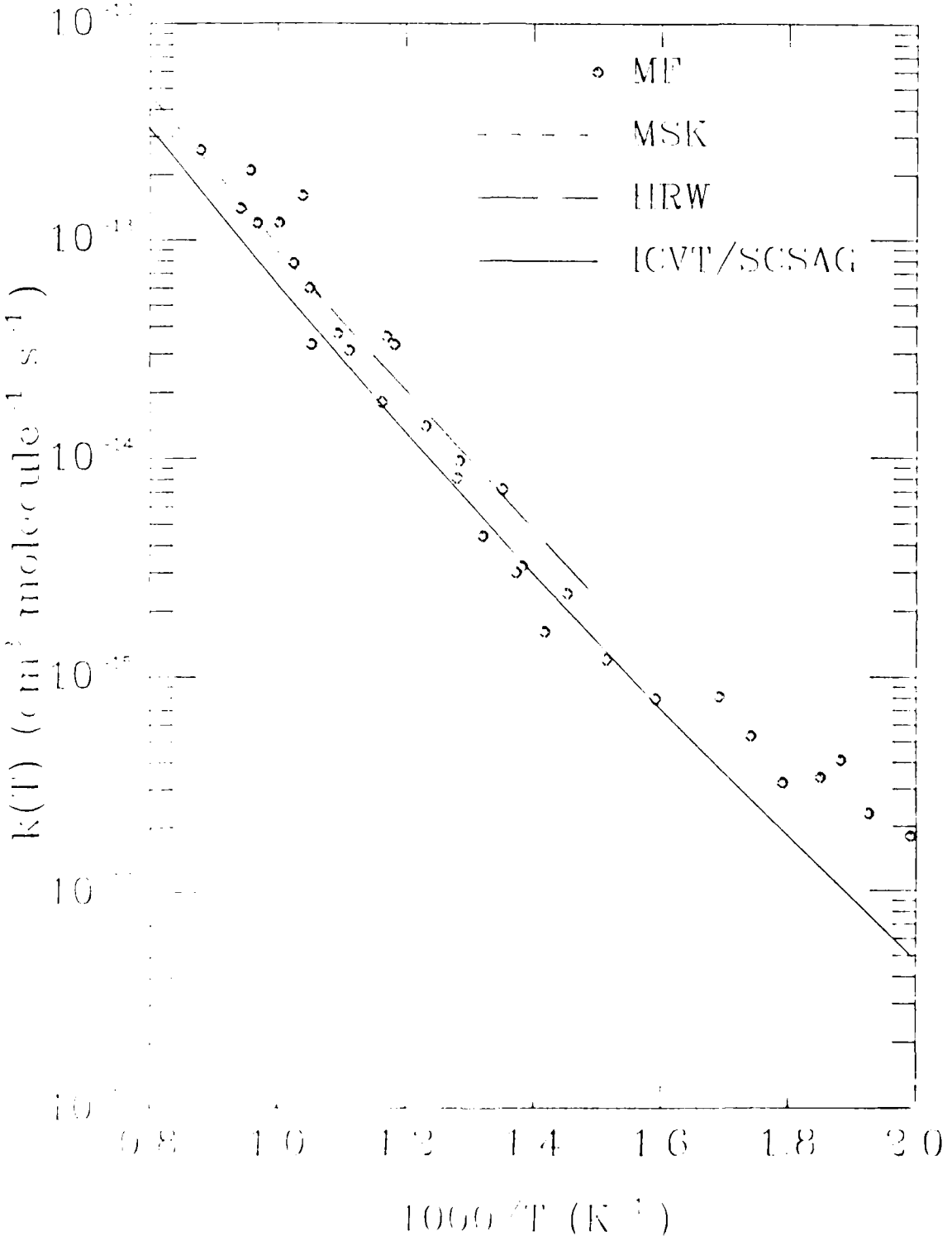
MP
MSK
HRW
ICVT/SCSAG
k(T) (cm³ molecule⁻¹ s⁻¹)
1000/T (K⁻¹)
0.8
1.0
1.2
1.4
1.6
1.8
2.0

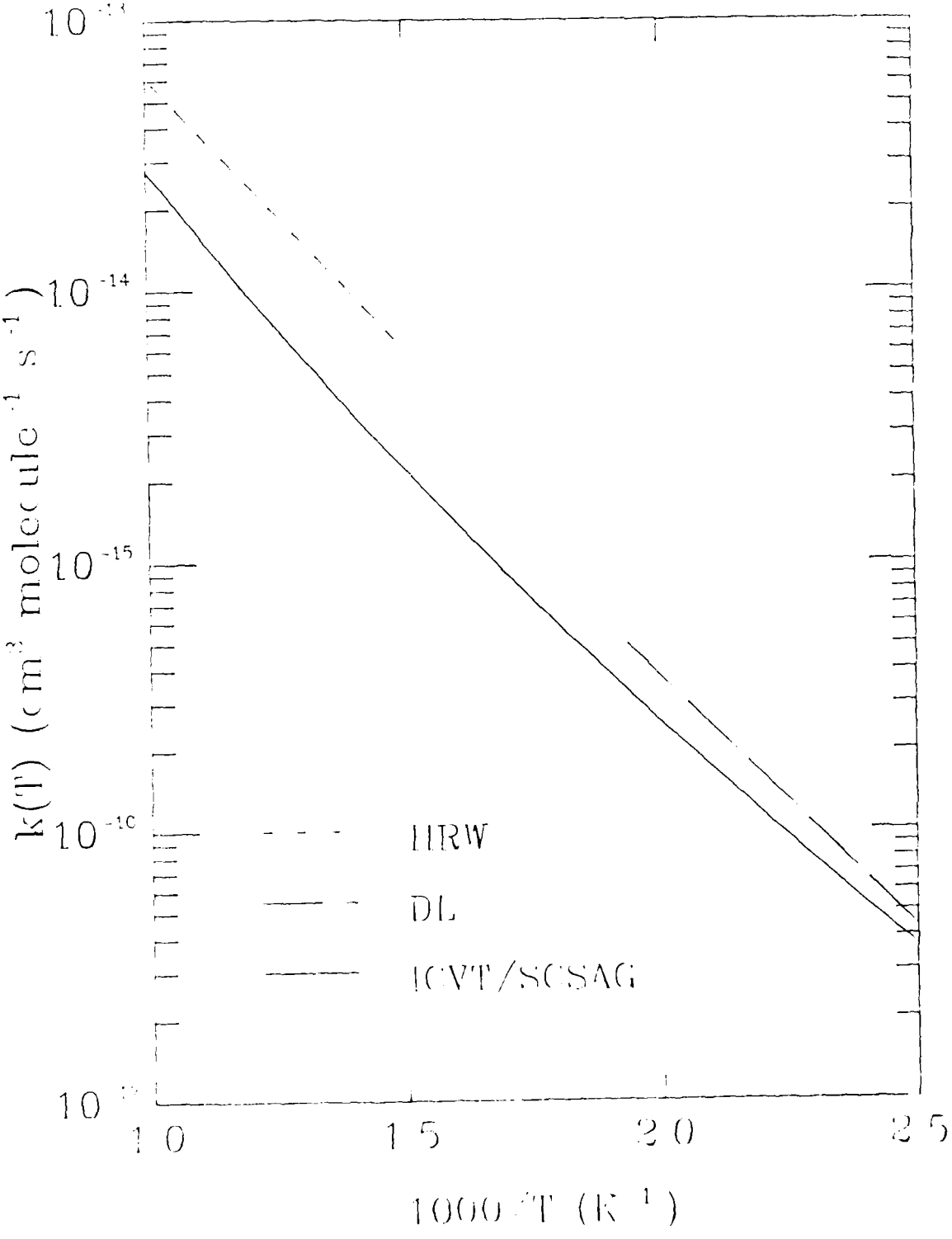
10^{-13}
10^{-14}
10^{-15}
10^{-16}
10^{-17}
k(T) (cm^3 molecule^{-1} s^{-1})
HRW
DL
ICVT/SCSAG
10
15
20
25
1000/T (K^{-1})

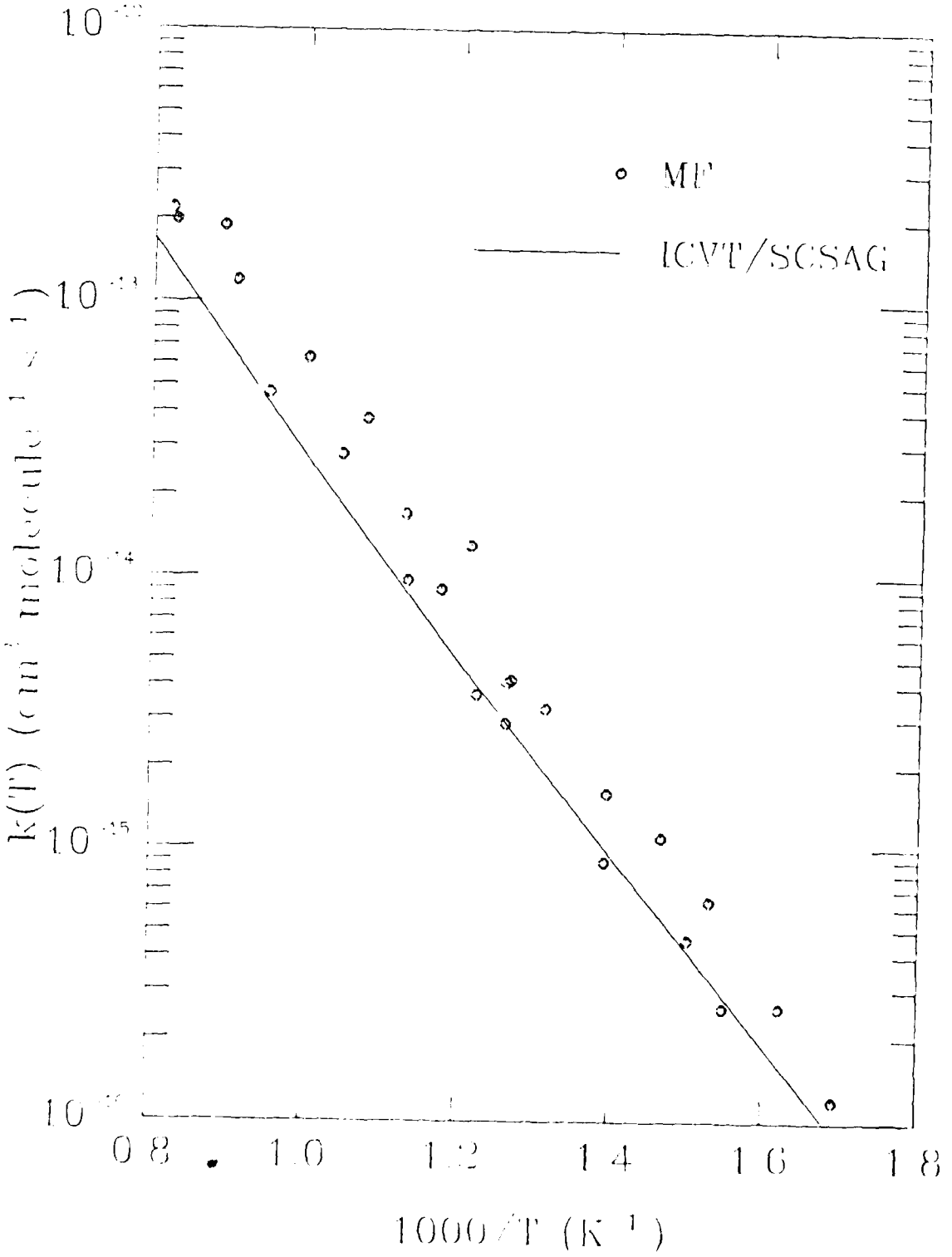
MP
ICVT/SCSAG
k(T) (cm³ molecule⁻¹ s⁻¹)
1000/T (K⁻¹)
0.8
1.0
1.2
1.4
1.6
1.8

Appendices B.

Thermochemical kinetic analysis of tunneling and the incorporation

of tunneling contributions in thermochemical kinetics

Thermochemical Kinetic Analysis of Tunneling and the Incorporation of Tunneling Contributions in Thermochemical Kinetics

Donald G. Truhlar
Department of Chemistry
University of Minnesota
Minneapolis, MN 55455

Bruce C. Garrett
Chemical Dynamics Corporation
9560 Pennsylvania Avenue
Upper Marlboro, MD 20772

(Received:)

Abstract. We partition the phenomenological enthalpy and entropy of activation for five hydrogen-atom transfer reactions, $H + H_2 \rightarrow H_2 + H$, $D + H_2 \rightarrow HD + H$, $H + D_2 \rightarrow HD + D$, $O(^3P) + H_2 \rightarrow OH + H$, and $OH + H_2 \rightarrow H_2O + H$ into quasithermodynamic and nonquasithermodynamic ("substantial" and "nonsubstantial") contributions. The latter, which are not considered explicitly in previous thermochemical kinetic models, are very significant. The present analysis could serve as the start of a semiempirical data base for the inclusion of variational and tunneling effects in future thermochemical kinetic models.

1. Introduction

From a knowledge of the structure and vibrational frequencies of bound chemical species, statistical mechanics provides the prescription for the direct calculation of thermochemical data such as heats of formation of stable compounds and heat release and equilibrium constants for chemical reactions.[1] The structural and energetic information can be reduced into thermodynamic quantities, the enthalpy and entropy, which can be accurately approximated using bond additivity and group additivity relationships. The quasithermodynamic formulation of conventional transition state theory[2,3] allows these ideas to be extended to the estimation of reaction rate constants.

In thermochemical kinetics a quasiequilibrium is postulated between reactants and a transition state complex and the conventional transition state theory rate constant $k^{\neq}(T)$ is expressed in terms of the associated quasiequilibrium constant $K_p^{\neq}(T)$ as

$$k^{\neq}(T) = \frac{k_B T}{h}(C^o)^{\Delta n^{\neq}} K_p^{\neq}(T) \qquad (1)$$

In equation (1), k_B is Boltzmann's constant, T is the temperature, h is Planck's constant, C^o is the concentration in the standard state, and $\Delta n^{\neq}$ is the stoichiometric change in the number of moles in passing from the reactants to the transition state. The equilibrium constant can be expressed in terms similar to the usual thermodynamic quantities

$$K_p^{\neq}(T) = \exp\left(-\Delta_r G_T^o / RT\right) \qquad (2)$$

where $\Delta_r G_T^o$ is the conventional transition state theory approximation to the standard state free energy of activation at temperature T and R is the gas constant. (The standard state for all equations and tables in this paper is the ideal gas state at 1 atm.) The free energy of activation can be further factored

$$\Delta_r G^o_T = - T\Delta_r S^o_T + \Delta_r H^o_T \qquad (3)$$

where $\Delta_r H^o_T$ and $\Delta_r S^o_T$ are the enthalpy and entropy of activation, respectively, at temperature T, and are related to the equilibrium constant by the standard thermodynamic relationship

$$\Delta_r H^o_T = RT^2 \frac{d \ln K^{\neq}_p}{dT} \qquad (4)$$

$$\Delta_r S^o_T = RT \frac{d \ln K^{\neq}_p}{dT} + R \ln K^{\neq}_p(T) \qquad (5)$$

For an ideal gas at a standard state of P^o = 1 atm, the concentration of the standard state is given by P^o/RT, and, using eq. (1), $\Delta_r S^o_T$ and $\Delta_r H^o_T$ can be expressed in terms of the reaction rate constant. For a bimolecular reaction ($\Delta n^{\neq} = -1$) we obtain

$$\Delta_r H^o_T = RT^2 \frac{d \ln k^{\neq}}{dT} - 2RT \qquad (6)$$

$$\Delta_r S^o_T = \frac{\Delta_r H^o_T}{T} + R \ln \left[\frac{k^{\neq}(T) h P^o}{(k_B T)^2 N_A^u} \right] \qquad (7)$$

where N_A is Avogadro's number, and u is 1 for $k^{\neq}(T)$ in molar units and 0 for $k^{\neq}(T)$ in molecular units.

In many cases useful practical accuracy can be obtained by estimating $\Delta_r S^o_T$ and $\Delta_r H^o_T$ by group additivity and computing the rate constant from eqs (1) - (3).[3] This is particularly appealing when conventional transition state theory,[2,3] or variational transition state theory with a temperature-independent transition state, is accurate. In this case, the quasi-

AD-A198 498 THEORETICAL INVESTIGATIONS OF NITROCUBANE DECOMPOSITION 2/2
(U) CHEMICAL DYNAMICS CORP UPPER MARLBORO MD
B C GARRETT ET AL 29 FEB 88 N00014-87-C-0746
UNCLASSIFIED F/G 7/4 NL

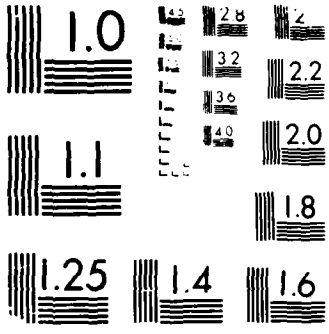

MICROCOPY RESOLUTION TEST CHART

activation parameters may be interpreted in terms of the free energy (or enthalpy and entropy) change on passing to a single transition state complex. For this interpretation the transition state is treated just like a bound, stable molecule except that one degree of freedom is missing, corresponding to the reaction coordinate; all the bound internal degrees of freedom can be analyzed in terms of the structure and vibrational frequencies. In many cases, however, this simple picture breaks down because the variational transition state depends on temperature or is not a good dynamical bottleneck, because of nonequilibrium effects, or because of quantal effects on reaction-coordinate motion.[4-7] In such cases, if the rate constant is still represented by eqs. (1) and (2), $\Delta_r G^o_T$ cannot be calculated by statistical mechanics from the properties of a single transition state complex. In the spirit of group additivity though, an attempt can be made to represent these effects by additional "group" contributions. We will call such contributions "nonsubstantial" contributions.

The rate constant can be expressed in terms of a transmission coefficient $\kappa(T)$ which includes the nonsubstantial contributions and a rate constant $k^{GTST}(T,s)$ based on a single temperature-independent location s of the generalized transition state:

$$k(T) = \kappa(T)\, k^{GTST}(T,s) \tag{8}$$

We introduce the factorizations

$$k^{GTST}(T,s) = \frac{k_B T}{h}(C^o)^{\Delta n^{\neq}} \exp\left(\Delta_s S^o_T / R\right) \exp\left(-\Delta_s H^o_T / RT\right) \tag{9}$$

and

$$\kappa(T) = \exp\left(\Delta_n S^o_T / R\right) \exp\left(-\Delta_n H^o_T / RT\right) \tag{10}$$

where $\Delta_s S^o_T$ and $\Delta_s H^o_T$ are substantial activation parameters obtained from the properties of a generalized transition state, "a substance", by expressions analogous to eqs. (4) and (5), and $\Delta_n S^o_T$ and $\Delta_n H^o_T$ are nonsubstantial activation parameters obtained from

$$\Delta_n H^o_T = RT^2 \frac{d \ln \kappa}{dT} \tag{11}$$

$$\Delta_n S^o_T = RT \frac{d \ln \kappa}{dT} + R \ln \kappa(T) \tag{12}$$

The nonsubstantial activation parameters $\Delta_n S^o_T$ and $\Delta_n H^o_T$ parametrize contributions from temperature-independent and temperature-dependent factors in the transmission coefficient, respectively. Since $\Delta_n S^o_T$ and $\Delta_n H^o_T$ are quasithermodynamic parameters, their temperature dependences are given by the usual formulas

$$\Delta_s S^o_T = \Delta_s S^o_{T_o} + \int_{T_o}^{T} \left(\Delta_s C^o_P / T \right) dT \tag{13}$$

and

$$\Delta_s H^o_T = \Delta_s H^o_{T_o} + \int_{T_o}^{T} \Delta_s C^o_P \, dT \tag{14}$$

where $\Delta_s C^o_P$ is the temperature-dependent substantial heat capacity of activation. The parameters $\Delta_n S^o_T$ and $\Delta_n H^o_T$ are purely phenomenological; however, because of their definition in eqs. (11) and (12), their temperature dependences can also be obtained from a single heat capacity analog $\Delta_n C^o_P$ given by expressions analogous to eqs. (13) and (14). In this case the nonsubstantial heat capacity cannot be given the physical interpretation of the change in heat capacity of the molecular complex as it proceeds from reactants to the transition state, but it will be useful for providing a compact representation of the temperature dependence of both $\Delta_n S^o_T$ and $\Delta_n H^o_T$.

Estimates of the nonsubstantial activation parameters can be combined with estimates of the quasithermodynamic activation parameters to yield more accurate rate constants. In order to estimate the nonsubstantial contributions in the general case it is useful to have some experience with their magnitude. In the present article we consider five reactions for which variational

transition state theory calculations[8-15] with transmission coefficients to account for quantal effects on the reaction coordinate motion provide rate constants in good agreement with experiment,[13,16-27] and we analyze the theoretical rate constants to obtain values for $\Delta_n S^o_T$, $\Delta_n H^o_T$, $\Delta_s S^o_T$ and $\Delta_s H^o_T$. The reactions considered are

$$H + H_2 \rightarrow H_2 + H \qquad (R1)$$

$$D + H_2 \rightarrow HD + H \qquad (R2)$$

$$H + D_2 \rightarrow HD + D \qquad (R3)$$

$$O(^3P) + H_2 \rightarrow OH + H \qquad (R4)$$

and

$$OH + H_2 \rightarrow H_2O + H \qquad (R5)$$

In these cases the largest contributions to the nonsubstantial activation parameters are due to tunneling.

2. Theory

We consider two factorizations of the total variational transition state theory rate constant. The first allows a quantitative assessment of the improvement over conventional transition state theory obtained by including the effects of variationally locating the transition state and the effects of quantum mechanical tunneling. This factorization is based upon the improved canonical variational theory[10] (ICVT) rate constant $k^{ICVT}(T)$ with a semiclassical transmission coefficient[10,14,28-31] $\kappa_{tun}(T)$ that accounts for quantal effects (tunneling and nonclassical reflection) on reaction coordinate motion

$$k(T) = \kappa_{tun}(T)\, k^{ICVT}(T) \qquad (15)$$

$$= \kappa_{tun}(T)\, \kappa_{var}(T)\, k^{\neq}(T) \tag{16}$$

where $\kappa_{var}(T)$ is defined by

$$\kappa_{var}(T) = k^{ICVT}(T)/k^{\neq}(T) \tag{17}$$

Both $\kappa_{var}(T)$ and $\kappa_{tun}(T)$ are parametrized as in eq. (10) leading to

$$\Delta_a S^o_T = \Delta_{tun} S^o_T + \Delta_{var} S^o_T + \Delta_{\neq} S^o_T \tag{18}$$

$$\Delta_a H^o_T = \Delta_{tun} H^o_T + \Delta_{var} H^o_T + \Delta_{\neq} H^o_T \tag{19}$$

where $\Delta_{\neq} S^o_T$ and $\Delta_{\neq} H^o_T$ are given by eqs. (6) and (7) and represent the substantial contributions and $\Delta_{tun} S^o_T$, $\Delta_{tun} H^o_T$, $\Delta_{var} S^o_T$, and $\Delta_{var} H^o_T$ represent nonsubstantial contributions.

The second factorization attempts to maximize the substantial contributions to the enthalpy and entropy while minimizing the nonsubstantial contributions by basing the substantial part on a single temperature-independent transition state located at the maximum of the adiabatic ground-state potential curve[10] s^{AG}_* (the variational transition state at 0K) instead of the conventional transition state at the saddle point. We write

$$k^{ICVT}(T) = \kappa_{therm}(T)\, k^{GTST}(T, s^{AG}_*) \tag{20}$$

where $\kappa_{therm}(T)$ accounts for finite-temperature deviations due to the temperature dependence of the improved canonical variational transition state. Analysis of $k^{GTST}(T, s^{AG}_*)$ by eq. (9) yields $\Delta_s S^o_T$ and $\Delta_s H^o_T$ and analysis of eqs. (15) and (20) yields

$$\Delta_n S^o_T = \Delta_{tun} S^o_T + \Delta_{therm} S^o_T \tag{21}$$

$$\Delta_n H_T^o = \Delta_{tun} H_T^o + \Delta_{therm} H_T^o \qquad (22)$$

In all cases we used *ab initio* potential energy surfaces, namely the surface of Liu, Siegbahn, one of the authors, and Horowitz[32-34] for reactions (R1)-(R3), a surface called M2,[12] based on the modified[35] polarization configuration interaction calculations of Walch *et. al.*[36-38] for reaction (R4), and the Walch-Dunning-Schatz-Elgersma surface[39,40] for reaction (R5).

For reaction (R1)-(R4), $\kappa_{tun}(T)$ is approximated by the least-action ground-state (LAG) method.[31] In these cases all geometries along the minimum energy paths are collinear, stretching anharmonicity is included by the WKB approximation[41] for the ground state and the Morse I approximation[42] for excited states, and bending anharmonicity is included by a quadratic-quartic approximation.[43,44] For reaction (R5), $\kappa_{tun}(T)$ is approximated by the small-curvature semiclassical adiabatic ground-state (SCSAG) approximation.[14,28-31] For this reaction all geometries along the minimum energy path are coplanar, anharmonicity is included by the independent-normal-mode approximation[6,14] by the Morse III approximation[14] for in-plane vibrations and by a quadratic-quartic approximation for out-of-plane bends.

3. Results and Discussion

Tables I-V show results of the factorization of the activation parameters into contributions from conventional TST, variational effects, and tunneling effects for the five reactions over a range of temperatures from 200 to 1500K. Table VI summarizes the results of the factorization into substantial and nonsubstantial contributions at four selected temperatures for all five reactions. The finite-temperature deviations of the VTST contributions from their substantial part are also shown for reference. Table VII provides a compact presentation of the substantial and nonsubstantial contribution to the activation parameters for the five reactions in terms of the heat capacities of activation.

The nonsubstantial contributions (primarily from tunneling) to both the enthalpy and entropy of activation are seen to be quite large. For the systems studied here the classical barriers are fairly high (9.8 kcal/mol for H + H_2 and isotopic analogs, 12.6 kcal/mol for O + H_2, and 6.1 kcal/mol for OH + H_2) which favors locating the variational dividing surface close to the saddle point. Therefore, the variational contributions to the enthalpy and entropy of activation are in general small; they are largest for the reaction with the smallest barrier, OH + H_2, where they contribute up to 0.5 kcal/mol to $\Delta_{var}H^o_T$ and 3 cal $mol^{-1}K^{-1}$ to $\Delta_{var}S^o_T$. The high barriers also lead to considerable tunneling at low temperatures. This is reflected in the large contributions to the enthalpies and entropies of activation at temperatures from about 600K and below. Tunneling effectively lowers the threshold for reaction below the classical threshold, and thereby makes a negative contribution to the enthalpy of activation. Thus, since tunneling decreases with increasing temperature, $\Delta_{tun}H^o_T$ also increases (becomes less negative). We see a similar trend for the entropy of activation; $\Delta_{tun}S^o_T$ is consistently less than zero but decreases in magnitude for increasing temperature.

Table VI shows that most of the effect of variationally optimizing the location of the transition state dividing surface at each temperature can be obtained by placing the transition state dividing surface at a single temperature-independent location – the maximum of the ground state adiabatic curve ($s=s^{AG}_*$). A measure of the importance of placing the dividing surface at a location different than s^{AG}_* is provided by $\Delta_{therm}S^o_T$ and $\Delta_{therm}H^o_T$ which are both small – these quantities vary from -0.1 to 0.0 cal $mol^{-1}K^{-1}$ and from -0.1 to 0.1 kcal/mol, respectively, for all five reactions from 200 to 1500K. The effect of the variational contributions in Tables I-V are approximately combined with the TST contributions to give the substantial contributions in Table VI (e.g., $\Delta_sH^o_T \approx \Delta_{\neq}H^o_T + \Delta_{var}H^o_T$) and the nonsubstantial contributions are dominated by the tunneling contributions.

Another interesting trend seen in Tables I-V is that $\Delta_{\neq}H^o_T$ monotonically decreases with increasing temperature for all reactions. From eq. (6) we see that if $\ln k^{\neq}(T)$ varies linearly with 1/T then $\Delta_{\neq}H^o_T$ will decrease with temperature from the -2RT term. At the low temperature the

decrease is approximately equal to -2RT but at higher temperatures the curvature of $\ln k^{\neq}(T)$ becomes larger and $\Delta_{\neq}H^{o}_{T}$ decreases less rapidly. Because the variational contribution are small this trend is also reflected in the substantial enthalpy of activation seen in Table VI. Also, as noted above, the nonsubstantial contributions have the same trends as the tunneling contributions. Because tunneling is so important at the lower temperatures, the total enthalpy of activation (substantial plus nonsubstantial) increases with increasing temperature for all five reactions at the lowest few temperatures. For all systems except $OH + H_2$ this trend reverses at higher T so that the total enthalpy of activation does not have a monotonic dependence on the temperature.

These trends are also exhibited in the heat capacities shown in Table VII. We see that for all five reactions the substantial contributions to the heat capacity of activation are negative and the nonsubstantial contributions are positive. At low temperatures ($T \leq 400$ K) the magnitude of the nonsubstantial contributions to ΔC^{o}_{P} are larger than those of the substantial contributions, leading to a net increase in both $\Delta_a S^{o}_{T}$ and $\Delta_a H^{o}_{T}$ for increasing temperature. For all reactions except the $OH + H_2$ reaction the magnitude of the substantial contributions to ΔC^{o}_{P} becomes larger at temperatures above 600 K, and both $\Delta_a S^{o}_{T}$ and $\Delta_a H^{o}_{T}$ decrease with further increases in T.

It is typical to write the rate constant in Arrhenius form

$$k(T) = A_T \exp\left[- E_a(T) / k_B T \right] \tag{23}$$

and express the Arrhenius parameters in terms of the enthalpy and entropy of activation. From the Tolman definition[45-47] of the activation energy we obtain

$$E_{act}(T) = \Delta_s H^{o}_{T} + \Delta_n H^{o}_{T} + 2RT \tag{24}$$

and using eqs. (8)-(10), (23), and (24) we obtain

$$\ln A_T = \ln\left[\frac{(k_B T)^2 N^{u}_{A}}{hP^{o}} \right] + \frac{\Delta_s S^{o}_{T} + \Delta_n S^{o}_{T}}{R} + 2 \tag{25}$$

For all five reactions studied here, the substantial contributions to the activation energy are nearly constant at low temperature, changing by less than 0.2 kcal/mol from 200 to 400 K. However, because of the importance of tunneling at low temperature the total activation energies are greatly decreased at these lower temperature – by as much as 5.7 kcal/mol at 200 K for the $O + H_2$

reaction -- and the activation energy changes significantly over the entire temperature range. For example, the activation energy for the O + H_2 reaction is 4.8, 6.4, 8.2, 9.9, 11.6, and 13.3 kcal/mol at 200, 300, 400, 600, 100, and 1500 K. Similarly, the change in the entropy of activation with temperature and the explicit temperature dependence in eq. (25) lead to a change in A_T for this reaction of 4 orders of magnitude from 200 to 1500 K.

Using estimates of the contributions to the conventional TST entropy of activation based on group additivity relationships, Benson[3] has approximated the Arrhenius A factor for the H + D_2 reaction; an estimate for $\Delta_{\neq}S^{o}_{300}$ of -18.7 cal $mol^{-1}K^{-1}$ yielded $A_{300} = 10^{-9.8}cm^3molecule^{-1}s^{-1}$. The estimate of $\Delta_{\neq}S^{o}_{300}$ is slightly higher than our computed value of -20.6 cal $mol^{-1}K^{-1}$ but neglects the contribution of -3.2 cal $mol^{-1}K^{-1}$ from tunneling. Combining the substantial and nonsubstantial contributions yields our computed value of $A_T = 10^{-10.9}cm^3molecule^{-1}s^{-1}$. Our results show that tunneling contributions can change the Arrhenius A factor by over an order of magnitude at low temperatures. Benson's estimate of the Arrhenius A factor at 300K is in better agreement with our computed value at 1000K ($10^{-9.6}cm^3molecule^{-1}s^{-1}$), where tunneling contributions are less than 30%.

4. Conclusions

A new partitioning of the phenomenological enthalpy and entropy of activation into quasithermodynamic and nonquasithermodynamic contributions has been presented. The former are obtained from the properties of a single temperature-independent transition state (a "substance") and are called substantial contributions. The nonquasithermodynamic contributions are obtained from more global properties of the potential energy surface (including the dependence of the variational transition state on temperature and quantum mechanical tunneling effects) and are called nonsubstantial contributions. An analysis of these contributions has been performed on five reactions for which the potential energy surface is known to give computed rate constants in excellent agreement with experiment. This analysis shows that the nonsubstantial contributions

can be very significant; for example, for the OH + H_2 reaction the substantial and nonsubstantial contributions to the enthalpy of activation at 300 K are 4.8 and -3.8 kcal/mol, respectively, and for the O + H_2 reaction the substantial and nonsubstantial contributions to the entropy of activation at 300 K are -20.9 and -8.9 cal $mol^{-1}K^{-1}$, respectively, for a standard state of 1 atm.

All the reactions studied here are hydrogen (or deuterium) atom transfer reactions with fairly high barriers. For these reactions the nonsubstantial contributions are predominantly from quantum mechanical tunneling and the effect of variationally optimizing the location of the transition state dividing surface is small. For reactions with smaller barriers we expect the effect of quantum mechanical tunneling to be smaller, but for those reactions the effects of variationally locating the dividing surface will become more important especially at higher temperatures.[48,49] It is therefore expected that the nonsubstantial contributions will be significant for a wide range of gas-phase chemical reactions.

The temperature dependence of the quasithermodynamic (substantial) contributions to both the enthalpy and entropy of activation can be expressed in terms of a single temperature-dependent substantial heat capacity of activation. Because of the definitions of the nonquasithermodynamic (nonsubstantial) contributions they can also be expressed in terms of a single temperature-dependent nonsubstantial heat capacity of activation. This allows the enthalpy and entropy of activation to be compactly tabulated in terms of their values at a single temperature (e.g., room temperature) and the temperature dependence given by the heat capacity of activation at several temperatures. This provides the basis for establishing a semiempirical data base with includes important variational and tunneling effects in a thermochemical kinetic model.

5. Acknowledgements

This research was sponsored by SDIO/IST and managed by the Office of Naval Research under contract number N00014-87-C-0746 and was also supported in part by the US Department of Energy, Office of Basic Energy Sciences, under grant no. DE-FG02-86ER13579.

6. References

1. See, e.g., K. S. Pitzer, Quantum Chemistry (Prentice-Hall, Englewood Cliffs, NJ, 1953).
2. S. Glasstone, K. J. Laidler, and H. Eyring, The Theory of Rate Processes (McGraw-Hill, New York, 1941).
3. S. W. Benson, Thermochemical Kinetics, 2nd. ed. (John Wiley and Sons, New York, 1976).
4. D. G. Truhlar and B. C. Garrett, Acc. Chem. Res. **13**, 440 (1980).
5. D. G. Truhlar and B. C. Garrett, Annu. Rev. Phys. Chem. **35**, 159 (1984).
6. D. G. Truhlar, A. D. Isaacson, and B. C. Garrett, in Theory of Chemical Reaction Dynamics, edited by M. Baer (CRC Press, Boca Raton, Fl, 1985), Vol. 4, p. 65.
7. M. M. Kreevoy and D. G. Truhlar, in Investigation of Rates and Mechanisms of Reactions, Part 1, edited by C. F. Bernasconi (John Wiley and Sons, New York, 1986), p. 13.
8. B. C. Garrett and D. G. Truhlar, Proc. Natl. Acad. Sci. USA **76**, 4755 (1979).
9. B. C. Garrett and D. G. Truhlar, J. Chem. Phys. **72**, 3460 (1980).
10. B. C. Garrett, D. G. Truhlar, R. S. Grev, and A. W. Magnuson, J. Phys. Chem. **84**, 1730 (1980); **87**, 4554(E) (1983).
11. D. G. Truhlar, K. Runge, and B. C. Garrett, in Twentieth Symposium (International) on Combustion (Combustion Institute, Pittsburgh, 1984), p. 585.
12. B. C. Garrett and D. G. Truhlar, Int. J. Quantum Chem. **21**, 17 (1987).
13. B. C. Garrett, D. G. Truhlar, J. M. Bowman, A. F. Wagner, D. Robie, S. Arepalli, N. Presser, and R. J. Gordon, J. Amer. Chem. Soc. **108**, 3515 (1986).
14. A. D. Isaacson and D. G. Truhlar, J. Chem. Phys. **76**, 1380 (1982).
15. A. D. Isaacson, M. T. Sund, S. N. Rai, and D. G. Truhlar, J. Chem. Phys. **82**, 1338 (1985).
16. W. R. Schulz and D. J. LeRoy, J. Chem. Phys. **42**, 3869 (1965).

17. A. A. Westenberg and N. deHaas, J. Chem. Phys. **47**, 1393 (1967).

18. D. L. Baulch, D. D. Drysdale, D. G. Horne, and A. C. Lloyd, Evaluated Kinetic Data for High-Temperature Reactions, Vol. 1 (Butterworths, London, 1972).

19. D. N. Mitchell and D. J. LeRoy, J. Chem. Phys. **58**, 3449 (1973).

20. G. L. Schott, R. W. Getzinger, and W. A. Seitz, Int. J. Chem. Kinet. **6**, 921 (1974).

21. R. N. Dubinsky and J. D. McKenney, Can. J. Chem. **53**, 3531 (1975).

22. I. M. Campbell and B. J. Handy, J. Chem. Soc. Faraday Trans. I **74**, 316 (1978).

23. G. C. Light and J. H. Matsumoto, Int. J. Chem. Kinet. **12**, 451 (1980).

24. K. M. Pamidimukkala and G. B. Skinner, J. Chem. Phys. **76**, 311 (1982).

25. A. R. Ravishankara, J. M. Nicovich, R. L Thompson, and F. P. Tully, J. Phys. Chem. **85**, 2498 (1981).

26. N. Cohen and K. Westberg, J. Phys. Chem. Ref. Data **12**, 531 (1983).

27. N. Presser and R. J. Gordon, J. Chem. Phys. **82**, 1291 (1985).

28. R. T. Skodje, D. G. Truhlar, and B. C. Garrett, J. Phys. Chem. **85**, 3019 (1981).

29. D. G. Truhlar, A. D. Isaacson, R. T. Skodje, and B. C. Garrett, J. Phys. Chem. **86**, 2252 (1982); **87**, 4554(E) (1983).

30. R. T. Skodje, D. G. Truhlar, and B. C. Garrett, J. Chem. Phys. **77**, 5955 (1982).

31. B. C. Garrett and D. G. Truhlar, J. Chem. Phys. **79**, 4931 (1983).

32. B. Liu, J. Chem. Phys. **58**, 1925 (1973).

33. P. Siegbahn and B. Liu, J. Chem. Phys. **68**, 2457 (1978).

34. D. G. Truhlar and C. J. Horowitz, J. Chem. Phys. **68**, 2466 (1978), **71**, 1514(E) (1979).

35. K. T. Lee, J. M. Bowman, A. F. Wagner, and G. C. Schatz, J. Chem. Phys. **76**, 3583 (1982).

36. S. P. Walch, T. H. Dunning, Jr., F. W. Bobrowicz, and R. Raffenetti, J. Chem. Phys. **72**, 406 (1980).

37. S. P. Walch, T. H. Dunning, Jr., F. W. Bobrowicz, and R. Raffenetti, J. Chem. Phys. **72**, 2894 (1980).

38. J. M. Bowman, A. F. Wagner, S. P. Walch, and T. H. Dunning, Jr., J. Chem. Phys. **81**, 1739 (1984).

39. S. P. Walch and T. H. Dunning, Jr., J. Chem. Phys. **72**, 1303 (1980).

40. G. C. Schatz and H. H. Elgersma, Chem. Phys. Lett. **73**, 21 (1980).

41. B. C. Garrett and D. G. Truhlar, J. Chem. Phys. **81**, 309 (1984).

42. B. C. Garrett and D. G. Truhlar, J. Phys. Chem. **83**, 1709 (1979); **87**, 4553(E) (1983).

43. D. G. Truhlar, J. Mol. Spectrosc. **38**, 415 (1971).

44. B. C. Garrett and D. G. Truhlar, J. Phys. Chem. **83**, 1915 (1979).

45. D. G. Truhlar, J. Chem. Educ. **55**, 309 (1978).

46. N. C. Blais, D. G. Truhlar, and B. C. Garrett, J. Phys. Chem. **85**, 1094 (1981).

47. N. C. Blais, D. G. Truhlar, and B. C. Garrett, J. Chem. Phys. **76**, 2768 (1982).

48. B. C. Garrett and D. G. Truhlar, J. Amer. Chem. Soc. **101**, 4534 (1979).

49. B. C. Garrett, D. G. Truhlar, and R. S. Grev, in Potential Energy Surfaces and Dynamics Calculations, edited by D. G. Truhlar (Plenum, New York, 1981), p. 587.

Table I. Activation parameters for the reaction $H + H_2 \rightarrow H_2 + H$ on the LSTH potential energy surface. (Enthalpies in units of kcal mol^{-1}, entropies in units of cal $mol^{-1}K^{-1}$, standard state is 1 atm.)

T,K	$\Delta_{\neq}H^{o}_{T}$	$\Delta_{var}H^{o}_{T}$	$\Delta_{tun}H^{o}_{T}$	$\Delta_{\neq}S^{o}_{T}$	$\Delta_{var}S^{o}_{T}$	$\Delta_{tun}S^{o}_{T}$
200	8.3	0.0	-4.0	-17.8	0.0	-10.2
300	7.8	0.0	-2.6	-19.6	0.0	-4.4
400	7.5	0.0	-1.9	-20.7	0.0	-2.3
600	6.9	0.0	-1.2	-21.8	0.0	-0.9
1000	6.3	0.0	-0.7	-22.6	0.0	-0.3
1500	6.0	0.0	-0.5	-22.9	0.0	-0.1

Table II. Activation parameters for the reaction $D + H_2 \rightarrow DH + H$ on the LSTH potential energy surface. (Enthalpies in units of kcal mol^{-1}, entropies in units of cal mol^{-1} K^{-1}, standard state is 1 atm.)

T,K	$\Delta_{\neq}H^{o}_{T}$	$\Delta_{var}H^{o}_{T}$	$\Delta_{tun}H^{o}_{T}$	$\Delta_{\neq}S^{o}_{T}$	$\Delta_{var}S^{o}_{T}$	$\Delta_{tun}S^{o}_{T}$
200	7.8	0.1	-3.5	-18.3	0.0	-9.1
300	7.3	0.1	-2.2	-20.1	0.0	-3.9
400	7.0	0.1	-1.6	-21.2	0.0	-2.1
600	6.5	0.1	-1.0	-22.2	0.0	-0.8
1000	6.0	0.0	-0.6	-22.8	-0.1	-0.2
1500	5.7	-0.1	-0.4	-23.1	-0.2	-0.1

Table III. Activation parameters for the reaction $H + D_2 \rightarrow HD + D$ on the LSTH potential energy surface. (Enthalpies in units of kcal mol^{-1}, entropies in units of cal mol^{-1} K^{-1}, standard state is 1 atm.)

T,K	$\Delta_{\neq}H^{o}_{T}$	$\Delta_{var}H^{o}_{T}$	$\Delta_{tun}H^{o}_{T}$	$\Delta_{\neq}S^{o}_{T}$	$\Delta_{var}S^{o}_{T}$	$\Delta_{tun}S^{o}_{T}$
200	9.0	0.1	-3.2	-18.9	0.0	-9.7
300	8.6	0.1	-1.7	-20.5	0.0	-3.2
400	8.3	0.1	-1.0	-21.4	0.0	-1.4
600	7.9	0.1	-0.6	-22.2	0.0	-0.5
1000	7.5	0.0	-0.3	-22.8	-0.1	-0.2
1500	7.0	-0.1	-0.2	-23.2	-0.1	-0.1

Table IV. Activation parameters for the reaction $O(^3P) + H_2 \rightarrow OH + H$ on the M2 potential energy surface. (Enthalpies in units of kcal mol^{-1}, entropies in units of cal mol^{-1} K^{-1}, standard state is 1 atm.)

T,K	$\Delta_{\neq}H^{o}_{T}$	$\Delta_{var}H^{o}_{T}$	$\Delta_{tun}H^{o}_{T}$	$\Delta_{\neq}S^{o}_{T}$	$\Delta_{var}S^{o}_{T}$	$\Delta_{tun}S^{o}_{T}$
200	9.5	0.2	-5.7	-19.6	0.0	-14.8
300	9.2	0.2	-4.2	-20.9	0.0	-8.9
400	8.9	0.2	-2.5	-21.7	0.0	-3.9
600	8.6	0.1	-1.1	-22.4	-0.1	-1.1
1000	8.2	0.0	-0.6	-22.9	-0.3	-0.3
1500	7.9	-0.3	-0.3	-23.1	-0.5	-0.1

Table V. Activation parameters for the reaction $OH + H_2 \rightarrow H_2O + H$ on the LSTH potential energy surface. (Enthalpies in units of kcal mol^{-1}, entropies in units of cal mol^{-1} K^{-1}, standard state is 1 atm.)

T,K	$\Delta_r H^o_T$	$\Delta_{var} H^o_T$	$\Delta_{tun} H^o_T$	$\Delta_{\neq} S^o_T$	$\Delta_{var} S^o_T$	$\Delta_{tun} S^o_T$
200	3.9	0.4	-4.4	-21.6	0.1	-10.1
300	4.3	0.4	-3.2	-23.5	0.2	-5.2
400	4.0	0.5	-2.5	-24.5	0.3	-3.0
600	3.6	0.4	-1.7	-25.4	0.2	-1.4
1000	3.4	0.3	-1.0	-25.6	0.0	-0.5
1500	3.6	0.1	-0.7	-25.5	-0.1	-0.2

Table VI. Activation parameters for five reactions. (Enthalpies in units of kcal mol^{-1}, entropies in units of cal mol^{-1} K^{-1}, standard state is 1 atm.)

		Reactions				
	T,K	$H+H_2$	$D+H_2$	$H+D_2$	$O+H_2$	$OH+H_2$
$\Delta_s H^o_T$	200	8.3	7.8	9.1	9.7	5.3
	300	7.8	7.4	8.7	9.4	4.8
	400	7.5	7.0	8.4	9.1	4.4
	1500	6.0	5.6	7.0	7.8	3.8
$\Delta_n H^o_T$	200	-4.0	-3.5	-3.2	-5.7	-4.4
	300	-2.6	-2.2	-1.7	-4.2	-3.2
	400	-1.9	-1.6	-1.0	-2.5	-2.5
	1500	-0.5	-0.5	-0.2	-0.5	-0.7
$\Delta_{therm} H^o_T$	200	0.0	0.0	0.0	0.0	0.0
	300	0.0	0.0	0.0	0.0	0.0
	400	0.0	0.0	0.0	0.0	0.0
	1500	0.0	0.0	0.1	-0.1	0.0
$\Delta_s S^o_T$	200	-17.8	-18.3	-18.9	-19.6	-21.4
	300	-19.6	-20.1	-20.5	-20.9	-23.3
	400	-20.7	-21.1	-21.4	-21.7	-24.2
	1500	-22.9	-23.2	-23.3	-23.6	-25.5
$\Delta_n S^o_T$	200	-10.2	-9.1	-9.7	-14.8	-10.1
	300	-4.4	-3.9	-3.2	-8.9	-5.2
	400	-2.3	-2.0	-1.4	-3.9	-3.1
	1500	-0.1	-0.1	-0.1	-0.2	-0.3
$\Delta_{therm} S^o_T$	200	0.0	0.0	0.0	0.0	0.0
	300	0.0	0.0	0.0	0.0	0.0
	400	0.0	0.0	0.0	0.0	0.0
	1500	0.0	0.0	0.0	-0.1	-0.1

Table VII. Activation parameters for five reactions. (Enthalpies in units of kcal mol^{-1}, entropies and heat capacities in units of cal $mol^{-1}K^{-1}$, standard state is 1 atm.)

reaction	contribution	ΔH^{o}_{T} T=300K	ΔS^{o}_{T} T=300K	T=	ΔC^{o}_{T} 200	300	400	600	1000	1500
$H+H_2$	substantial	7.8	-19.6		-4.9	-4.2	-3.4	-2.1	-1.1	-1.0
	nonsubstantial	-2.6	-4.4		20.8	9.4	5.3	2.1	0.6	0.3
$D+H_2$	substantial	7.4	-20.1		-4.8	-4.0	-3.2	-2.0	-1.1	-1.0
	nonsubstantial	-2.2	-3.9		18.7	8.5	4.7	1.9	0.5	0.1
$H+D_2$	substantial	8.7	-20.5		-4.6	-3.5	-2.7	-1.7	-1.1	-1.0
	nonsubstantial	-1.7	-3.2		23.2	9.5	3.9	1.3	0.3	0.1
$O+H_2$	substantial	9.4	-20.9		-3.5	-3.0	-2.5	-1.7	-1.0	-0.6
	nonsubstantial	-4.2	-8.9		9.0	19.2	12.8	3.2	0.6	0.0
$OH+H_2$	substantial	4.8	-23.3		-5.4	-3.9	-2.8	-1.5	-0.3	0.5
	nonsubstantial	-3.2	-5.2		13.2	9.6	5.8	2.6	1.0	0.6

END
DATE
FILMED
5-88
DTIC